Journal of
Nonlinear
Science

Check for
updates

A Homogenized Bending Theory for Prestrained Plates

Klaus Böhnlein[1] · **Stefan Neukamm**[1] ⬤ · **David Padilla-Garza**[1] ·
Oliver Sander[1] ⬤

Abstract

The presence of prestrain can have a tremendous effect on the mechanical behavior of slender structures. Prestrained elastic plates show spontaneous bending in equilibrium—a property that makes such objects relevant for the fabrication of active and functional materials. In this paper we study microheterogeneous, prestrained plates that feature non-flat equilibrium shapes. Our goal is to understand the relation between the properties of the prestrained microstructure and the global shape of the plate in mechanical equilibrium. To this end, we consider a three-dimensional, nonlinear elasticity model that describes a periodic material that occupies a domain with small thickness. We consider a spatially periodic prestrain described in the form of a multiplicative decomposition of the deformation gradient. By simultaneous homogenization and dimension reduction, we rigorously derive an effective plate model as a Γ-limit for vanishing thickness and period. That limit has the form of a nonlinear bending energy with an emergent spontaneous curvature term. The homogenized properties of the bending model (bending stiffness and spontaneous curvature) are characterized by corrector problems. For a model composite—a prestrained laminate composed of isotropic materials—we investigate the dependence of the homogenized properties on the parameters of the model composite. Secondly, we investigate the relation between the parameters of the model composite and the set of shapes with minimal bending energy. Our study reveals a rather complex dependence of these shapes on the com-

Communicated by Eliot Fried.

✉ Stefan Neukamm
stefan.neukamm@tu-dresden.de

Klaus Böhnlein
klaus.boehnlein@tu-dresden.de

David Padilla-Garza
david.padilla-garza@tu-dresden.de

Oliver Sander
oliver.sander@tu-dresden.de

[1] Faculty of Mathematics, Technische Universität Dresden, 01062 Dresden, Germany

⚛ Springer

posite parameters. For instance, the curvature and principal directions of these shapes depend on the parameters in a nonlinear and discontinuous way; for certain parameter regions we observe uniqueness and non-uniqueness of the shapes. We also observe size effects: The geometries of the shapes depend on the aspect ratio between the plate thickness and the composite period. As a second application of our theory, we study a problem of shape programming: We prove that any target shape (parametrized by a bending deformation) can be obtained (up to a small tolerance) as an energy minimizer of a composite plate, which is simple in the sense that the plate consists of only finitely many grains that are filled with a parametrized composite with a single degree of freedom.

Contents

Fig. 1 Design and experimentally observed cylindrical, equilibrium shapes of 3d-printed composite bilayer plates. Reproduced from Ge et al. (2013), with the permission of AIP Publishing

1 Introduction

General motivation. Natural and synthetic elastic materials often are prestrained. For slender structures, the presence of prestrain may have a huge impact on the mechanical behavior: Plates and films with prestrain often exhibit a complex equilibrium shape due to spontaneous bending, wrinkling and symmetry breaking (Klein et al. 2007; Ware et al. 2015; van Manen et al. 2018). Prestrain can be the result of different physical mechanisms, e.g., swelling or de-swelling of gels (Ionov 2013; Tanaka and Fillmore 1979), thermal expansion (Sigmund and Torquato 1997; Gibiansky and Torquato 1997), or the nematic-elastic coupling in liquid crystal elastomers (Warner and Terentjev 2007), and can be triggered by different stimuli—a property that makes such materials interesting for the fabrication of functional materials with a controlled shape change; see (van Manen et al. 2018) for a review. New manufacturing techniques such as additive manufacturing even enable the design of microstructured, prestrained materials whose functionality results from a complex interplay between the geometry, the material properties, and the prestrain distribution on a small length scale. An example is a self-assembling cube shown in Ge et al. (2013), whose functionality is due to a sandwich-type prestrained composite plate designed with a fibred microstructure, see Fig. 1.

The development of reliable models and simulation methods that are able to predict the macroscopic behavior based on the specification of the material on the small scale is an important part of understanding such materials and subject of ongoing research. **Scope and main results of the paper.** In this paper we are interested in the effective elastic behavior of prestrained composite plates. In particular, we seek to understand the *microstructure–shape relation*, i.e., the relation between the mechanical properties and prestrain distribution of the plate on the small length scale, and the emergent macroscopic equilibrium shape. The starting point of the analysis is the following energy functional of three-dimensional, nonlinear elasticity:

$$\mathcal{E}^{\varepsilon,h}(v) := \frac{1}{h} \int_{\Omega_h} W_\varepsilon\big(x, \nabla v(x) A_{\varepsilon,h}^{-1}(x)\big)\, dx, \qquad \Omega_h := S \times \left(-\tfrac{h}{2}, \tfrac{h}{2}\right). \tag{1}$$

Here, Ω_h denotes the reference configuration of the three-dimensional plate, $S \subset \mathbb{R}^2$ is the midsurface, $0 < h \ll 1$ denotes the plate thickness, and $v : \Omega_h \to \mathbb{R}^3$ is the deformation of the plate. The stored energy density function $W_\varepsilon(x, F)$ is assumed to be frame indifferent with a single, non-degenerate energy well at SO(3) for almost all $x \in \Omega_h$. It describes a heterogeneous composite with a microstructure that oscillates locally periodically in in-plane directions on a length scale $0 < \varepsilon \ll 1$ (see

Sect. 2.1 for details). In addition, (1) models a microheterogeneous prestrain based on a multiplicative decomposition of the deformation gradient ∇v with the matrix field $A_{\varepsilon,h} : \Omega_h \to \mathbb{R}^{3\times3}$ as in, e.g., (Bauer et al. 2020, Section 2.1). Like the stored energy function W_ε itself, we assume that $A_{\varepsilon,h}$ oscillates in in-plane directions.

As explained in (van Manen et al. 2018), there are two different mechanisms for prestrain-induced shape changes of plates, namely, the "buckling strategy" and the "bending strategy". In this paper, we are interested in the latter. As is well known, bending of plates can be driven by gradients of the prestrain along the thickness of the plate with a magnitude comparable to the thickness. Therefore, we assume that $A_{\varepsilon,h} = I_{3\times3} + h B_{\varepsilon,h}$ with $\|B_{\varepsilon,h}\|_{L^\infty(\Omega_h)} \lesssim 1$ uniformly in ε and h.

The first mathematical problem that we address is the rigorous derivation of a homogenized, nonlinear plate model with an effective prestrain as a Γ-limit of $\mathcal{E}^{\varepsilon,h}$ when both parameters ε and h tend to 0 simultaneously (Theorem 2.8). In the special case of a globally periodic microstructure, the derived model is given by a bending energy with an effective prestrain:

$$\mathcal{I}^\gamma_{\text{hom}} : H^2_{\text{iso}}(S; \mathbb{R}^3) \to \mathbb{R}, \qquad \mathcal{I}^\gamma_{\text{hom}}(v) = \int_S Q^\gamma_{\text{hom}}\big(\mathbb{I}_v(x') - B^\gamma_{\text{eff}}\big)\, dx', \qquad x' := (x_1, x_2). \quad (2)$$

Here, $H^2_{\text{iso}}(S; \mathbb{R}^3)$ is the nonlinear space of bending deformations, i.e., the set of all $v \in H^2(S; \mathbb{R}^3)$ satisfying the isometry constraint $(\nabla'v)^\top \nabla'v = I_{2\times2}$ where $\nabla' := (\partial_1, \partial_2)$. We denote by $\mathbb{I}_v := \nabla'v^\top \nabla'(\partial_1 v \wedge \partial_2 v)$ the second fundamental form associated with v and note that it captures the curvature of the deformed plate. The effective bending moduli are described by means of a positive-definite quadratic form $Q^\gamma_{\text{hom}} : \mathbb{R}^{2\times2}_{\text{sym}} \to [0, \infty)$, and the effective prestrain of the two-dimensional plate is described by a matrix $B^\gamma_{\text{eff}} \in \mathbb{R}^{2\times2}_{\text{sym}}$. Both Q^γ_{hom} and B^γ_{eff} can be derived from W_ε and $A_{\varepsilon,h}$ by homogenization formulas that require to solve certain corrector problems. These corrector problems are the equilibrium equations of linear elasticity posed on a representative volume with periodic boundary conditions, see Proposition 2.25.

It turns out that the precise form of the limiting energy $\mathcal{I}^\gamma_{\text{hom}}$ is sensitive to the relative scaling of the plate thickness h and the size ε of the microstructure: In order to capture this size effect we introduce the parameter $\gamma \in (0, \infty)$ and we shall assume that $\frac{h}{\varepsilon} \to \gamma$ as $(\varepsilon, h) \to 0$. As indicated by the notation, γ enters the formulas for the effective quantities Q^γ_{hom} and B^γ_{eff}. We remark that our result, Theorem 2.8, includes the more general case of a *locally periodic composite* (defined in Assumption 2.5 below), which leads to a x'-dependence of Q^γ_{hom} and B^γ_{eff}. Furthermore, we discuss displacement boundary conditions in Theorem 2.13.

The standard theory of Γ-convergence implies that (almost) minimizers of the scaled global energy $\frac{1}{h^2}\mathcal{E}^{\varepsilon,h}$ converge (up to subsequences) to minimizers of the plate energy $\mathcal{I}^\gamma_{\text{hom}}$. The minimizers of the latter thus capture the effective equilibrium shapes of the three-dimensional plate for $0 < \varepsilon, h \ll 1$. In Sect. 5 we investigate the minimizers of $\mathcal{I}^\gamma_{\text{hom}}$ and their dependence on the three-dimensional composite, i.e., on W_ε and $B_{\varepsilon,h}$. Understanding this relation can be seen as two steps:

(a) (Microstructure–properties relation). In Sect. 4 we first investigate the map $(W_\varepsilon, B_{\varepsilon,h}) \mapsto (Q^\gamma_{\text{hom}}, B^\gamma_{\text{eff}})$, which for each composite requires to solve a set
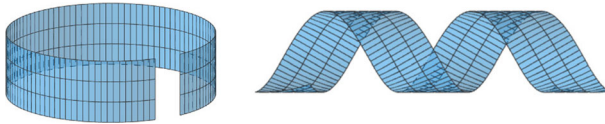
Fig. 2 Shapes with minimal energy predicted by our theory. A composite plate with prestrained fibres in one of the layers is considered. The design parameters are the volume fraction of the fibres and the angle that they form with the longitudinal axis of the strip. See Sect. 6.1 for details.

of three corrector problems of the type (20). While this can be done numerically (as we plan to do in a forthcoming paper), here we focus mostly on analytic results: In Lemma 4.2 we prove that isotropic composites with isotropic prestrain and a reflection symmetric geometry lead to orthotropic Q_{hom}^{γ} and diagonal B_{eff}^{γ}. Moreover, in Lemma 4.5 we obtain explicit formulas for Q_{hom}^{γ} and B_{eff}^{γ} in the case of a parametrized, isotropic laminate, see Fig. 4 for a schematic visualization.

(b) (Properties–shape relation). Once the effective coefficients of Q_{hom}^{γ} and B_{eff}^{γ} are known, minimizing the energy functional (2) determines the equilibrium shape of the plate. In the general case, there is no hope for explicit formulas for the minimizers. However, when Q_{hom}^{γ} and B_{eff}^{γ} are independent of $x' \in S$, then free minimizers correspond to cylindrical shapes with constant fundamental form. In this case, the minimization of the functional $\mathcal{I}_{\text{hom}}^{\gamma}$ simplifies to an algebraic minimization problem (53), which can be solved without the need for solving a nonlinear partial differential equation. Lemma 4.3 establishes a trichotomy result for the set of minimizers in the case when Q_{hom}^{γ} is orthotropic and yields a way to evaluate minimizers algorithmically.

By combining both steps we recover the desired *microstructure–shape relation*. In Sects. 4 and 5 we illustrate this procedure on the level of a parametrized, isotropic, two-component laminate. In Sect. 4 we focus on the microstructure–properties relation. We obtain explicit formulas that relate the parameters of the composite (in particular, the volume fractions of the components, the stiffness contrast, and the strength of the prestrain) to the effective quantities (Q_{hom}^{γ}, B_{eff}^{γ}). Based on this, in Sect. 5, we explore the parameter dependence of the geometry of shapes with minimal bending energy; see Fig. 2 for an example.

Our detailed parameter study shows that the geometries of shapes with minimal bending energy depend on the parameters in a rather complex, and partially counter-intuitive way. In particular, we observe a discontinuous dependence of the geometry on the parameters: E.g., the bending direction and the sign of the curvature may jump when perturbing the volume fraction of the components of the composite. We also observe a size effect: Qualitative and quantitative properties of the set of shapes with minimal energy depend on the scale ratio γ. Furthermore, we observe a break of symmetry: By changing the volume fraction we may transition from a situation where the set of shapes with minimal energy are a rotationally symmetric one-parameter family to a situation where the set consists of a unique shape.

In Sect. 6 we turn to the problem of shape programming: In Theorem 6.6 we prove that, in a nutshell, any shape that can be parametrized by a bending deformation $v \in H_{\text{iso}}^{2}(S; \mathbb{R}^{3})$ can be approximated by low energy deformations of a prestrained,

three-dimensional composite plate with a simple design. Here, simple means that the plate is partitioned into finitely many grains and each grain is filled by realizations of a prescribed, one-parameter family of a periodic, prestrained composite.

A brief survey of the methods and previous results. Our Γ-convergence result, Theorem 2.8, is concerned with simultaneous dimension reduction and homogenization in nonlinear elasticity. The asymptotics $h \to 0$ correspond to the derivation of a bending plate energy in the spirit of the seminal papers (Friesecke et al. 2002, 2006). Our analysis heavily relies on the geometric rigidity estimate of Friesecke et al. (2002) and the corresponding method to prove compactness for sequences of 3d-deformations with finite bending energy. On the other hand, the limit $\varepsilon \to 0$ describes the homogenization of microstructure. For the analysis of the simultaneous Γ-limit $(\varepsilon, h) \to 0$ we follow the general strategy introduced by the second author in the case of rods (Neukamm 2010, 2012). It relies on the fact that to leading order, the nonlinear energy can be written as a convex, quadratic functional of the scaled nonlinear strain. This allows using methods from convex homogenization, in particular, the notion of two-scale convergence (Nguetseng 1989; Allaire 1992; Visintin 2007), and a representation of effective quantities with the help of corrector problems. Results on simultaneous homogenization and dimension reduction for plates in the von-Kármán and bending regimes have been obtained by the second author together with Velčić and Hornung in Neukamm and Velčić (2013); Hornung et al. (2014), see also (Neukamm and Olbermann 2015; Cherdantsev and Cherednichenko 2015; Bukal and Velčić 2017; Hornung et al. 2018) for related works.

Extending these ideas, in the present paper we consider materials with a microheterogeneous prestrain, whose magnitude scales with the thickness h of the plate. The derivation of bending theories for prestrained plates (without homogenization) has first been studied by Schmidt (2007a, b); for related results in the context of nematic plates see (Agostiniani et al. 2017; Agostiniani and DeSimone 2017, 2020). In these works (as in our paper) the prestrain is modeled by a multiplicative decomposition $F_{el}A^{-1}$ of the deformation gradient F_{el} with a factor A that is close to identity, i.e., $A = I + hB$. As a consequence, admissible plate deformations of the limiting model are isometries for the Euclidean metric, and the multiplicative prestrain turns into a linearized, additive one. While the prestrain in Schmidt (2007b) is a macroscopic quantity, in the present paper we consider a microheterogeneous prestrain leading to an effective, homogenized prestrain in the limit model. A similar extension has been considered by the second author in Bauer et al. (2020) for the case of nonlinear rods. In contrast to previous results on dimension reduction for plates, our derivation, which invokes homogenization, requires a precise characterization of two-scale limits of the scaled nonlinear strain along sequences with finite bending energy. This is achieved in Proposition 3.2, which, in particular, affirmatively identifies the two-scale limits of the nonlinear strain in flat regions—a problem that remained open in Hornung et al. (2014). The proof of Proposition 3.2 is based on a wrinkling ansatz introduced by the third author in Padilla-Garza (2022).

Minimizers of bending energies for plates with prestrain have been studied first in the spatially homogeneous case with 2d-prestrains that are multiples of the identity matrix (Schmidt 2007a). In particular, Schmidt (2007a, Lemma 3.1) contains the convenient observation that in the homogenous case, free minimizers are cylindrical. As

usual in homogenization, non-isotropy of effective quantities typically emerges even for composites consisting of isotropic constituents materials. For the model (2) this means that the quadratic form Q_{hom}^{γ} is typically not isotropic, and that B_{eff}^{γ} is not a multiple of the identity. Therefore, compared to Schmidt (2007a), in our case the structure of minimizers is considerably richer. In particular, with Lemma 5.3 we classify the sets of minimizers into three families. In the spatially heterogeneous case or in the case of prescribed displacement boundary conditions, bending deformations with minimal energy are not necessarily cylindrical and explicit formulas are not available.

The numerical minimization of the energy (2) is highly nontrivial. Most works in the literature consider only the case without prestrain, i.e., $B_{\text{eff}}^{\gamma} = 0$. The first difficulty is the discretization of the space $H_{\text{iso}}^2(S; \mathbb{R}^3)$ of bending isometries, i.e., of deformations v in H^2 satisfying $(\nabla' v)^\top \nabla' v = I_{2 \times 2}$. No fully conforming discretizations seem to exist in the literature. Nonconforming discretizations based on the MINI- and Crouzeix–Raviart elements have been proposed in Bartels (2013b). Alternative discretizations using discrete Kirchhoff triangles or Discontinuous Galerkin (DG) finite elements appear in Bartels (2013a); Rumpf et al. (2021) and Bonito et al. (2021b), respectively. An approach using spline functions (which are in $H^2(S; \mathbb{R}^3)$, but are not pointwise isometries) appears in Mohan et al. (2022). Convergence results are given, e.g., in Bartels et al. (2017).

Prestrain is included in a few models, but the attention has been restricted so far only to the isotropic case, where $Q_{\text{hom}}^{\gamma}(G) = |G|^2$ and $B_{\text{eff}}^{\gamma} = \rho I$ for some $\rho \in \mathbb{R}$, see (Bonito et al. 2021a, 2022; Bartels et al. 2017). In Bartels et al. (2022), a model with a more general effective prestrain has been considered in the context of liquid crystal elastomer plates.

The second difficulty is the minimization of the non-convex energy functional (2), which is a challenge even without the prestrain. The works of Bartels use different numerical gradient flows together with linearizations of the isometry constraint (Bartels 2013a, b; Bartels et al. 2017; Bonito et al. 2021b). This leads to a (controllable) algebraic violation of the constraints beyond the one introduced by the discretization. Rumpf et al. (2021) use a Lagrange multiplier formulation and a Newton method instead, and preserve the exact isometry constraints at the grid vertices. Note that we do not numerically minimize (2) in the present manuscript. Situations requiring such approaches will be the subject of a later paper.

Finally, we remark that prestrained plates have also been intensively studied from the perspective of non-Euclidean elasticity, see (Bhattacharya et al. 2016; Lewicka and Pakzad 2011; Lewicka and Lučić 2020; Lewicka et al. 2010a, b, 2011, 2017; Lewicka 2020). In this context, the reference configuration is assumed to be a Riemannian manifold and the factor A in the decomposition $F_{\text{el}} A^{-1}$ is viewed as the square root of the metric. As observed in Bhattacharya et al. (2016) there is an interesting interplay between the critical scaling of the energy with respect to the thickness of the plate h and the curvature of the metric $\sqrt{A}$. More specifically, the minimum energy (per volume) is of order at most h^2 (as in our case) if and only if there exists an isometric immersion with finite bending energy of the metric $\sqrt{A}$. Recent works have also considered scaling regimes different from the bending one. For instance, scaling by h^4 leads to von-Kármán plate models, see (de Benito Delgado and Schmidt 2021, 2020). We note that the condition that the minimum energy scales at most like h^4 is

intimately linked to the structure of the Riemann curvature tensor of the metric $\sqrt{A}$. Moreover, the membrane scaling has been considered in Plucinsky et al. (2018a) and Plucinsky et al. (2018b) with applications to nematic liquid crystal elastomer plates and nonisometric origami.

Organization of the paper. In Sect. 2.1 we introduce the three-dimensional model. In Sect. 2.2 we present the limit plate model and state the Γ-convergence result. Section 2.3 contains the definition of the effective quantities via homogenization formulas and their characterization with the help of correctors. Section 3 establishes a characterization of the two-scale structure of limits of the nonlinear strain and establishes strong two-scale convergence for the nonlinear strain for minimizing sequences. Section 4 is devoted to the study of the microstructure–properties relation, and Sect. 5 to the properties–shape and microstructure-shape relations. In Sect. 6 we present our result on shape programming. All proofs are presented in Sect. 7. In the appendix, in Appendix 8.1 and 8.2 we discuss various properties of two-scale convergence for grained microstructures—a variant of two-scale convergence that we introduce in this paper.

2 Setup of the Model and Derivation of the Prestrained Plate Model

We derive the plate model by simultaneous homogenization and dimension reduction of a three-dimensional model. The proofs for all results stated in this section are collected in Sect. 7.

2.1 The Three-Dimensional Model and Assumptions on the Material Law and Microstructure

We denote by $\Omega_h := S \times (-\frac{h}{2}, \frac{h}{2})$ the reference configuration of a three-dimensional plate with thickness $h > 0$, where $S \subset \mathbb{R}^2$ is an open, bounded and connected Lipschitz domain. We call $\Omega := S \times (-\frac{1}{2}, \frac{1}{2})$ the corresponding domain of unit thickness. We use the shorthand notation $x = (x', x_3)$ with $x' := (x_1, x_2)$ and denote the *scaled deformation gradient* by $\nabla_h := (\nabla', \frac{1}{h}\partial_3)$ where $\nabla' := (\partial_1, \partial_2)$. Moreover, we write $I_{d \times d}$ to denote the unit matrix in $\mathbb{R}^{d \times d}$.

By rescaling (1) and specializing to the case

$$A_{\varepsilon,h}^{-1}(x', hx_3) = I_{3\times3} - h B_{\varepsilon,h}(x)$$

(i.e., $A_{\varepsilon,h} \approx I + h B_{\varepsilon,h}$) we obtain the energy functional $\mathcal{I}^{\varepsilon,h} : L^2(\Omega; \mathbb{R}^3) \to [0, +\infty]$,

$$\mathcal{I}^{\varepsilon,h}(v) := \begin{cases} \dfrac{1}{h^2} \displaystyle\int_\Omega W_\varepsilon\Big(x, \nabla_h v(x)(I_{3\times3} - h B_{\varepsilon,h}(x))\Big) \mathrm{d}x & \text{if } v \in H^1(\Omega; \mathbb{R}^3), \\ +\infty & \text{otherwise.} \end{cases} \tag{3}$$

We shall study the Γ-limit of $\mathcal{I}^{\varepsilon,h}$ as both small parameters ε and h converge to 0 simultaneously, and as already mentioned in the introduction, it turns out that the

obtained Γ-limit will depend on the limit of the ratio h/ε. To capture this size effect, we make the following assumption:

Assumption 2.1 (*Relative scaling of h and ε*) There exists a number $\gamma \in (0, \infty)$ and a monotone function $\varepsilon : (0, \infty) \to (0, \infty)$ such that $\lim_{h \downarrow 0} \varepsilon(h) = 0$ and $\lim_{h \downarrow 0} \frac{h}{\varepsilon(h)} = \gamma$.

The case $\gamma \ll 1$ corresponds to the situation of a plate that is thin compared to the typical size of the microstructure, while $\gamma \gg 1$ corresponds to the case of a microstructure that is very fine not only compared to the macroscopic dimensions of the problem, but also to the small thickness of the plate. Note that Assumption 2.1 excludes the extreme cases $\gamma = 0$ (i.e., $h \ll \varepsilon \ll 1$) and $\gamma = \infty$ (i.e., $\varepsilon \ll h \ll 1$). We comment on these cases in Remark 2.10.

Next, we state our assumptions on the material law, the microstructure of the composite, and the microstructure of the prestrain. Following (Bauer et al. 2020) we describe prestrained elastic materials by combining

- a geometrically nonlinear, stored energy function that describes a non-prestrained, elastic material with a *stress-free, nondegenerate* reference state at SO(3),

with

- a *multiplicative decomposition* of the deformation into an elastic part and a pre-strain that is of the order of the plate's thickness h and locally periodic (in in-plane directions) on the scale ε.

In Eckart (1940); Lee (1969); Kröner (1959), such a multiplicative decomposition of the deformation has been introduced in the context of finite strain elastoplasticity.

The stored energy functions we consider have to have certain standard properties. We collect appropriate functions and their linearizations in so-called *material classes*:

Definition 2.2 (*Nonlinear material class*) Let $0 < \alpha \leq \beta, \rho > 0$, and let $r : [0, \infty) \to [0, \infty]$ denote a monotone function satisfying $\lim_{\delta \to 0} r(\delta) = 0$.

- The class $\mathcal{W}(\alpha, \beta, \rho, r)$ consists of all measurable functions $W : \mathbb{R}^{3 \times 3} \to [0, +\infty]$ that

(W1) are frame indifferent: $W(RF) = W(F)$ for all $F \in \mathbb{R}^{3 \times 3}$, $R \in \mathrm{SO}(3)$;

(W2) are non-degenerate:

$$W(F) \geq \alpha \, \mathrm{dist}^2(F, \mathrm{SO}(3)) \quad \text{for all } F \in \mathbb{R}^{3 \times 3},$$
$$W(F) \leq \beta \, \mathrm{dist}^2(F, \mathrm{SO}(3)) \quad \text{for all } F \in \mathbb{R}^{3 \times 3} \text{ with } \mathrm{dist}^2(F, \mathrm{SO}(3)) \leq \rho;$$

(W3) are minimal at $I_{3 \times 3}$: $W(I_{3 \times 3}) = 0$;

(W4) admit a quadratic expansion at $I_{3 \times 3}$: For each W there exists a quadratic form $Q : \mathbb{R}^{3 \times 3} \to \mathbb{R}$ such that

$$|W(I_{3 \times 3} + G) - Q(G)| \leq |G|^2 r(|G|) \quad \text{for all } G \in \mathbb{R}^{3 \times 3}.$$

- The class $\mathcal{Q}(\alpha, \beta)$ consists of all quadratic forms Q on $\mathbb{R}^{3\times3}$ such that

$$\alpha|\operatorname{sym} G|^2 \leq Q(G) \leq \beta|\operatorname{sym} G|^2 \quad \text{for all } G \in \mathbb{R}^{3\times3},$$

where $\operatorname{sym} G := \frac{1}{2}(G + G^\top)$ is the symmetric part of G. We associate with each $Q \in \mathcal{Q}(\alpha, \beta)$ the fourth-order tensor $\mathbb{L} \in \operatorname{Lin}(\mathbb{R}^{3\times3}, \mathbb{R}^{3\times3})$ defined by the polarization identity

$$\mathbb{L}F : G := \frac{1}{2}\big(Q(F + G) - Q(F) - Q(G)\big), \tag{4}$$

where : denotes the standard scalar product in $\mathbb{R}^{3\times3}$.

Properties (W1)–(W4) are standard assumptions in the context of dimension reduction. In particular, stored energy functions of class $\mathcal{W}(\alpha, \beta, \rho, r)$ can be linearized at the identity (see, e.g., Padilla-Garza 2022; Müller and Neukamm 2011; Gloria and Neukamm 2011; Neukamm 2010) and the elastic moduli of the linearized model are given by the quadratic form Q of (W4). Furthermore, for any stored energy function W we have by (Neukamm 2012, Lemma 2.7)

$$W \in \mathcal{W}(\alpha, \beta, \rho, r) \quad \Longrightarrow \quad Q \in \mathcal{Q}(\alpha, \beta),$$

(which motivates the definition of the class $\mathcal{Q}(\alpha, \beta)$), and thus Q is a bounded and positive definite quadratic form on symmetric matrices in $\mathbb{R}^{3\times3}$.

For the plate model we consider particular stored energy functions that are elements of $\mathcal{W}$.

Assumption 2.3 (*Nonlinear material*) For all $\varepsilon > 0$ and α, β, ρ, r as in Definition 2.2, the elastic energy density $W_\varepsilon : \Omega \to [0, +\infty]$ of (3) is a Borel function such that $W_\varepsilon(x, \cdot) \in \mathcal{W}(\alpha, \beta, \rho, r)$ for almost every $x \in \Omega$.

Additionally, we shall assume that the microstructure of the composite is locally periodic, that is, we consider countably many open subsets S_j, called "grains" that partition S up to a null set, and assume that on each $S_j \times (-\frac{1}{2}, \frac{1}{2}) \subset \Omega$ the composite features a laterally periodic microstructure, possibly with a different reference lattice in each grain (Fig. 3). This leads to the following definition:

Definition 2.4 (Λ-*periodicity, grain structure, local periodicity*)

(i) Let $\Lambda \in \mathbb{R}^{2\times2}$ be invertible. A measurable function $\varphi : \mathbb{R}^2 \to \mathbb{R}$ is called Λ-*periodic* if $\varphi(\cdot + \tau) = \varphi(\cdot)$ for all $\tau \in \Lambda\mathbb{Z}^2$.
(ii) A *grain structure* is a finite or countable family $\{S_j, \Lambda_j\}_{j\in J}$ consisting of open, disjoint subsets S_j of S and matrices $\Lambda_j \in \mathbb{R}^{2\times2}$ such that $S \setminus (\bigcup_{j\in J} S_j)$ is a null set and

$$\frac{1}{C_J} \leq \Lambda_j^\top \Lambda_j \leq C_J \quad \text{in the sense of quadratic forms,} \tag{5}$$

for all $j \in J$ with a constant $C_J > 0$ independent of $j \in J$.
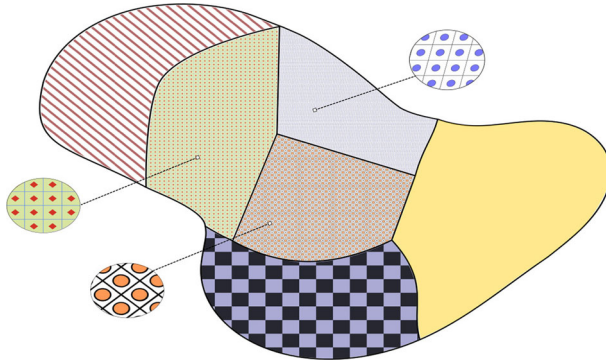
Fig. 3 Schematic picture of a microstructure with a different reference lattice and composite in each grain

(iii) A measurable function $\varphi : \Omega \times \mathbb{R}^2 \to \mathbb{R}$ is called *locally periodic (subordinate to the grain structure $\{S_j, \Lambda_j\}_{j \in J}$)*, if

$$\forall j \in J : \quad \varphi(x, \cdot) \text{ is } \Lambda_j\text{-periodic for a.e. } x \in S_j \times (-\tfrac{1}{2}, \tfrac{1}{2}). \tag{6}$$

Note that by (5) the geometry of the local lattices of periodicity is uniformly controlled. Our core assumption on the composite's microstructure is now that W_ε describes a composite that is locally periodic on scale $\varepsilon > 0$. Likewise, we shall assume that the prestrain is locally periodic and satisfies a smallness condition.

Assumption 2.5 (*Local periodicity of the composite and prestrain*) Let $\{S_j, \Lambda_j\}_{j \in J}$ be a grain structure as in Definition 2.4. Let Assumption 2.3 be satisfied and suppose that there exists $Q : \Omega \times \mathbb{R}^2 \times \mathbb{R}^{3 \times 3} \to \mathbb{R}$ with $Q(x, y, \cdot) \in \mathcal{Q}(\alpha, \beta)$ for a.e. $x \in \Omega$, $y \in \mathbb{R}^2$, such that the following properties hold:

(i) (Local periodicity of Q). The map $\mathbb{L}$ associated with Q via (4) is locally periodic subordinate to $\{S_j, \Lambda_j\}_{j \in J}$, and for each grain S_j, $j \in J$, the map $S_j \ni x' \mapsto \mathbb{L}(x', \cdot) \in L^\infty\big((-\tfrac{1}{2}, \tfrac{1}{2}) \times \mathbb{R}^2; \mathbb{R}^{3 \times 3 \times 3 \times 3}\big)$ is continuous.

(ii) (Strong two-scale approximation of Q_ε). The quadratic term $Q_\varepsilon(x, \cdot)$ in the expansion of $W_\varepsilon(x, \cdot)$ (cf. (W4) of Definition 2.2) satisfies

$$\limsup_{\varepsilon \to 0} \ \operatorname*{ess\,sup}_{x \in S_j \times (-\frac{1}{2}, \frac{1}{2})} \ \max_{\substack{G \in \mathbb{R}^{3 \times 3} \\ |G| = 1}} \big| Q_\varepsilon(x, G) - Q(x, \tfrac{x'}{\varepsilon}, G) \big| = 0 \quad \text{for all } j \in J.$$

Furthermore, we suppose that for all $\varepsilon, h > 0$ the prestrain $B_{\varepsilon,h} : \Omega \to \mathbb{R}^{3 \times 3}_{\text{sym}}$ of (3) is measurable and we suppose that there exists a Borel function $B : \Omega \times \mathbb{R}^2 \to \mathbb{R}^{3 \times 3}_{\text{sym}}$ such that:

(iii) (Local periodicity of B). The function B is locally periodic subordinate to $\{S_j, \Lambda_j\}_{j \in J}$, and

$$\sum_{j \in J} \int_{S_j} \fint_{\square_{\Lambda_j}} |B(x', x_3, y)|^2 \mathrm{d}(x_3, y) \mathrm{d}x' < \infty,$$

where $\Box_{\Lambda_j} := (-\frac{1}{2}, \frac{1}{2}) \times Y_{\Lambda_j}$ and $Y_{\Lambda_j} := \Lambda_j[-\frac{1}{2}, \frac{1}{2})^2$. Moreover, we write $\fint_{\Box_{\Lambda_j}} := \frac{1}{|\Box_{\Lambda_j}|} \int_{\Box_{\Lambda_j}}$ for the integral mean.

(iv) (Strong two-scale approximation and boundedness of $B_{\varepsilon(h),h}$). We have

$$\limsup_{h \to 0} \int_\Omega \left| B_{\varepsilon(h),h}(x) - B\left(x, \frac{x'}{\varepsilon(h)}\right) \right|^2 dx = 0 \quad \text{and} \quad \limsup_{h \to 0} \sqrt{h} \|B_{\varepsilon(h),h}\|_{L^\infty(\Omega)} < \infty,$$

where $\varepsilon(\cdot)$ is as in Assumption 2.1.

The main reason for considering not only the $\mathbb{Z}^2$-periodic case but the more general and flexible structure of Assumption 2.5 is our application to shape programming presented in Sect. 6. Note that by Assumption 2.5 we do not assume that W_ε is itself locally periodic. We only suppose that the quadratic term Q_ε in the expansion of W_ε is close to a locally periodic quadratic form (scaled by ε).

Remark 2.6 (*Examples for locally periodic composites*)

(a) ($\mathbb{Z}^2$-periodic case). A special case of a locally periodic composite in the sense of Assumption 2.5 is the $\mathbb{Z}^2$-*periodic case*, where the partition consists of the single grain S and the lattice of periodicity is everywhere the same and given by $\Lambda = I_{2\times2}$. More explicitly, in this case, we may consider a Borel function $W : (-\frac{1}{2}, \frac{1}{2}) \times \mathbb{R}^2 \times \mathbb{R}^{3\times3} \to [0, \infty]$ such that $W(x_3, y, \cdot) \in \mathcal{W}(\alpha, \beta, \rho, r)$ for a.e. $y \in \mathbb{R}^2$, $x_3 \in (-\frac{1}{2}, \frac{1}{2})$, and $\mathbb{R}^2 \ni y \to W(x_3, y, F)$ is $\mathbb{Z}^2$-periodic for a.e. $x_3 \in (-\frac{1}{2}, \frac{1}{2})$ and all $F \in \mathbb{R}^{3\times3}$. Then the family of scaled stored energy functions $W_\varepsilon(x', x_3, F) := W(x_3, \frac{x'}{\varepsilon}, F)$ satisfies Assumption 2.5. Note that in this example $W_\varepsilon(x', x_3, F)$ is itself $\varepsilon\mathbb{Z}^2$-periodic w.r.t. $x' \in \mathbb{R}^2$.

(b) A simple example of a composite that is locally periodic subordinate to a grain structure $\{S_j, \Lambda_j\}_{j \in J}$ is given by $W_\varepsilon(x', x_3, F) := \sum_{j \in J} 1_{S_j}(x') W(x_3, \Lambda_j^{-1} \frac{x'}{\varepsilon}, F)$ where W is as above. Then the family W_ε satisfies Assumption 2.5.

Remark 2.7 (*Examples of prestrains*)

(a) Under reasonable assumptions, polymer hydrogels, i.e., networks of hydrophilic rubber molecules, can be modeled by considering a prestrain of the form $B = \frac{\lambda-1}{h} I_{3\times3}$, where λ is a material parameter depending on the free swelling factor (Flory and Rehner Jr 1943).

(b) Nematic liquid crystal elastomers are materials consisting of a polymer network inscribed with liquid crystals. These materials feature a coupling between the liquid crystal orientation and elastic properties that can be modeled by considering a prestrain of the form $B = \bar{r}(\frac{1}{3} I_{3\times3} - n \otimes n)$, where $n : S \to \mathbb{R}^3$ is a unit vector field describing the local orientation of the liquid crystals, and $\bar{r}$ is a material parameter (see Warner and Terentjev 2007).

(c) In finite-strain thermoelasticity (see Vujošević and Lubarda 2002), prestrains of the form $B = (\bar{\beta} - \bar{\alpha})n_0 \otimes n_0 - \bar{\beta} I_{3\times3}$ are considered to describe materials that (after a change of temperature) stretch in a direction $n_0 : S \to \mathcal{S}^2$ with factor $\bar{\alpha}$, and contract in directions orthogonal to n_0 with factor $\bar{\beta}$.

2.2 The Limit Model and Convergence Results

We now discuss the model that results from letting $(\varepsilon, h) \to 0$ simultaneously. The limit energy can be written as the sum of two contributions. The first one is a homogenized bending energy $\mathcal{I}_{\text{hom}}^{\gamma} : L^2(S; \mathbb{R}^3) \to [0, \infty]$ that includes an effective prestrain $B_{\text{eff}}^{\gamma} \in L^2(S; \mathbb{R}_{\text{sym}}^{2 \times 2})$ that captures the impact of the prestrain B on the macroscale:

$$\mathcal{I}_{\text{hom}}^{\gamma}(v) := \begin{cases} \int_S Q_{\text{hom}}^{\gamma}(x', \mathbb{I}_v - B_{\text{eff}}^{\gamma}(x')) dx' & \text{if } v \in H_{\text{iso}}^2(S; \mathbb{R}^3), \\ +\infty & \text{else,} \end{cases} \tag{7}$$

where

$$\mathbb{I}_v := \nabla' v^{\top} \nabla' b_v \quad \text{and} \quad b_v := (\partial_1 v \wedge \partial_2 v)$$

denote the second fundamental form (expressed in local coordinates) of the surface parametrized by v and the surface normal, respectively. Above, the quadratic form Q_{hom}^{γ} describes the homogenized elastic moduli of the composite. The second contribution $\mathcal{I}_{\text{res}}^{\gamma}$ (defined in Definition 2.22 below) is a residual energy that is independent of the deformation u, and is quadratic in the prestrain B. Both effective quantities—the quadratic form Q_{hom}^{γ} describing the homogenized elastic moduli of the composite, and the effective prestrain B_{eff}^{γ}—only depend on the linearized material law Q, the prestrain B, and the scale ratio γ. More specifically,

- $Q_{\text{hom}}^{\gamma}(x', \cdot) : \mathbb{R}_{\text{sym}}^{2 \times 2} \to \mathbb{R}$ is a positive definite quadratic form given by the homogenization formula of Definition 2.17 below,
- $B_{\text{eff}}^{\gamma}(x') \in \mathbb{R}_{\text{sym}}^{2 \times 2}$ is given by the averaging formula of Definition 2.22 below,
- $\mathcal{I}_{\text{res}}^{\gamma}(B) \geq 0$ is defined in Definition 2.22.

Both Q_{hom}^{γ} and B_{eff}^{γ} can be evaluated for any $x' \in S$ by solving linear corrector problems. In Sect. 2.3 we present an algorithm to evaluate these quantities, and we show numerical experiments in Sect. 4.

Our first result establishes Γ-convergence for $(h, \varepsilon) \to 0$:

Theorem 2.8 (Γ-convergence) *Let* Assumptions 2.1 *and* 2.5 *be satisfied. Then the following statements hold:*

(a) (Compactness). Let $(v_h) \subset L^2(\Omega; \mathbb{R}^3)$ be a sequence with equibounded energy, i.e.,

$$\limsup_{h \to 0} \mathcal{I}^{\varepsilon(h), h}(v_h) < \infty. \tag{8}$$

Then

$$\limsup_{h \to 0} \frac{1}{h^2} \int_{\Omega} \text{dist}^2 \left(\nabla_h v_h(x), \text{SO}(3) \right) dx < \infty, \tag{9}$$

and there exists $v \in H_{\text{iso}}^2(S; \mathbb{R}^3)$ and a subsequence (not relabeled) such that

$$v_h - \fint_{\Omega} v_h dx \to v \qquad\qquad in \ L^2(\Omega), \tag{10a}$$

and

$$\nabla_h v_h \to (\nabla' v, b_v) \qquad\qquad in \ L^2(\Omega). \qquad (10b)$$

Here and below, $b_v := \partial_1 v \wedge \partial_2 v$ is the surface normal vector, and $\wedge$ denotes the vector product.

(b) *(Lower bound). If $(v_h) \subset L^2(\Omega; \mathbb{R}^3)$ is a sequence with $v_h - \fint_\Omega v_h \mathrm{d}x \to v$ in $L^2(\Omega)$, then*

$$\liminf_{h \to 0} \mathcal{I}^{\varepsilon(h),h}(v_h) \geq \mathcal{I}^\gamma_{\mathrm{hom}}(v) + \mathcal{I}^\gamma_{\mathrm{res}}(B).$$

(c) *(Recovery sequence). For any $v \in H^2_{\mathrm{iso}}(S; \mathbb{R}^3)$ there exists a sequence $(v_h) \subset W^{1,\infty}(\Omega; \mathbb{R}^3)$ with $v_h \to v$ strongly in $H^1(\Omega; \mathbb{R}^3)$ such that*

$$\lim_{h \to 0} \mathcal{I}^{\varepsilon(h),h}(v_h) = \mathcal{I}^\gamma_{\mathrm{hom}}(v) + \mathcal{I}^\gamma_{\mathrm{res}}(B), \qquad (11)$$

and, in addition,

$$\limsup_{h \to 0} h^{\frac{1}{2}} \|\nabla_h v_h - (\nabla' v, b_v)\|_{L^\infty(\Omega)} = 0. \qquad (12)$$

(See Sects. 7.2, 7.3, and 7.4 for the proof of (a),(b), and (c), respectively.)

Remark 2.9 (*Identification of functions defined on S with their canonical extension to Ω*) In the paper we tacitly identify functions defined on S, say $v : S \to \mathbb{R}^3$, with their canonical extension to Ω, namely, $\Omega \ni (x', x_3) \mapsto v(x')$. This clarifies the meaning of statements such as (10).

The main points of Theorem 2.8 are the parts (b) and (c). The implication (9) $\implies$ (10), which is the main point of Part (a), has already been proven by Friesecke et al. (2002) using their celebrated geometric rigidity estimate.

Remark 2.10 (*The cases $\gamma = \infty$ and $\gamma = 0$*) In Theorem 2.8 we assume that $\gamma \in (0, \infty)$, which means that h and $\varepsilon(h)$ converge to 0 with the same order. The result changes for $\gamma = \infty$ and $\gamma = 0$, respectively. We note that Theorem 2.8 can be extended to the case $\gamma = \infty$ (i.e. when $\varepsilon \ll h$) based on the methods developed in this paper and Hornung et al. (2014). In contrast, the case $\gamma = 0$, which corresponds to $h \ll \varepsilon$, is more subtle. Even in the case without prestrain (i.e., $B = 0$) it is not fully understood, and the resulting Γ-limit can be qualitatively different depending on the relative scaling between h^2 and ε: The cases $h^2 \ll \varepsilon \ll h$ and $\varepsilon \ll h^2$ are treated in Cherdantsev and Cherednichenko (2015) and Velčić (2015), respectively. The sequential limit $\varepsilon \to 0$ after $h \to 0$ is discussed in Neukamm and Olbermann (2015).

We also establish a variant of the theorem for plates with displacement boundary conditions on straight parts of the boundary. For the precise formulation of the resulting two-dimensional model we introduce a set $\mathcal{A}_{BC}$ of bending deformations with the appropriate boundary conditions. Note that the following definition introduces additional assumptions on the geometry of S:

Definition 2.11 (*Two-dimensional displacement boundary conditions*) Let S be a convex and bounded Lipschitz domain with piece-wise C^1-boundary. We consider $k_{BC} \in \mathbb{N}$ relatively open, non-empty lines segments $\mathcal{L}_i \subset \partial S$ and a reference isometry $v_{BC} \in H^2_{\mathrm{iso}}(S; \mathbb{R}^3)$ such that for $i = 1, \dots, k_{BC}$ (the trace of) $\nabla' v_{BC}$ is constant on $\mathcal{L}_i \cap \partial S$. We introduce a space of bending deformations that satisfy the following displacement boundary conditions on the line-segments:

$$\mathcal{A}_{BC} := \left\{ v \in H^2_{\mathrm{iso}}(S; \mathbb{R}^3) \,:\, v = v_{BC} \text{ and } \nabla' v = \nabla' v_{BC} \text{ on } \mathcal{L}_1 \cup \dots \cup \mathcal{L}_{k_{BC}} \right\}.$$

We shall see that the boundary conditions of Definition 2.11 emerge from sequences of 3d-deformations (v_h) with finite bending energy that satisfy boundary conditions of the form

$$v_h = (1 - h\delta)v_{BC} + hx_3 b_{v_{BC}} \quad \text{on } (\mathcal{L}_1 \cup \dots \cup \mathcal{L}_{k_{BC}}) \times \left(-\frac{1}{2}, \frac{1}{2} \right), \qquad (13)$$

where $\delta \in \mathbb{R}$ denotes a fixed parameter. More precisely, we recall the following extension of the compactness part (a) of Theorem 2.8, proved in (Bartels et al. 2022, Theorem 2.9 (a)):

Lemma 2.12 (Emergence of two-dimensional boundary conditions) *Let S and $\mathcal{A}_{BC}$ be as in Definition 2.11. Consider a sequence $(v_h) \subset H^1(\Omega; \mathbb{R}^3)$ satisfying (9) and (13) for some fixed $\delta \in \mathbb{R}$. Then there exists a subsequence (not relabeled) and $v \in \mathcal{A}_{BC}$ such that $v_h \to v$ in $L^2(\Omega)$ and $\nabla_h v_h \to (\nabla' v, b_v)$ in $L^2(\Omega)$.*

We finally show that we can construct recovery sequences that feature the boundary conditions (13):

Theorem 2.13 (Recovery sequences subject to displacement boundary conditions) *Consider the setting of* Theorem 2.8 *and assume boundary conditions as in* Definition 2.11. *If additionally*

$$C_B := \sup_{j \in J} \operatorname{ess\,sup}_{x' \in S_j} \fint_{\square_{\Lambda_j}} |B(x', x_3, y)|^2 \mathrm{d}(x_3, y) < \infty, \qquad (14)$$

then there exists $\delta > 0$ (only depending on C_B) such that for any $v \in H^2_{\mathrm{iso}}(S; \mathbb{R}^3)$ there exists a sequence $(v_h) \subset H^1(\Omega; \mathbb{R}^3)$ with $v_h \to v$ strongly in $H^1(\Omega; \mathbb{R}^3)$ satisfying (11), (12), and the displacement boundary conditions (13).

(See Sect. 7.4 for the proof.)

The argument for Theorem 2.13 is based on recent results obtained by us together with Bartels et al. (2022). In particular, there we prove for S and $\mathcal{A}_{BC}$ as in Definition 2.11 the approximation property

$$\mathcal{A}_{BC} \cap C^\infty(\bar{S}; \mathbb{R}^3) \text{ is dense in } (\mathcal{A}_{BC}, \| \cdot \|_{H^2(S; \mathbb{R}^3)}), \qquad (15)$$

see (Bartels et al. 2022, Proposition 2.11). It extends previous results by Pakzad (2004) and Hornung (2011) on the approximation of isometries by smooth isometries to the case of affine boundary conditions on line segments.

Remark 2.14 (*Convergence of almost minimizers*) Theorem 2.8 together with Theorem 2.13 and Lemma 2.12 implies that the sequence of functionals

$$\mathcal{I}_h : L^2(\Omega; \mathbb{R}^3) \to [0, \infty], \qquad \mathcal{I}_h(v) := \begin{cases} \mathcal{I}^{\varepsilon(h),h}(v) & \text{if } v \text{ satisfies}(13), \\ +\infty & \text{else,} \end{cases}$$

Γ-converges in $L^2(\Omega)$ for $h \to 0$ to the functional

$$\mathcal{I} : L^2(\Omega; \mathbb{R}^3) \to [0, \infty], \qquad \mathcal{I}(v) := \begin{cases} \mathcal{I}^\gamma_{\text{hom}}(v) + \mathcal{I}^\gamma_{\text{res}}(B) & \text{if } v \in \mathcal{A}_{BC}, \\ +\infty & \text{else.} \end{cases}$$

Thanks to the boundary condition and strict convexity of (7) viewed as a function of $\mathbb{I}_v$, the limit functional admits a minimizer in the set $\mathcal{A}_{BC}$. Furthermore, by the imposed boundary conditions, the sequence $(\mathcal{I}_h)$ is equicoercive in $L^2(\Omega; \mathbb{R}^3)$, and thus standard arguments from the theory of Γ-convergence imply that any sequence of almost minimizers (v_h), i.e., functions for which

$$\mathcal{I}_h(v_h) \leq \inf \mathcal{I}_h + h,$$

converges (modulo a sub-sequence, not relabeled) to v_*, a minimizer of $\mathcal{I}^\gamma_{\text{hom}}$ in the set $\mathcal{A}_{BC}$. In view of the compactness part (a) of Theorem 2.8 we even get

$$\nabla_h v_h \to (\nabla' v_*, b_{v_*}) \qquad \text{strongly in } L^2(\Omega).$$

Furthermore, in Sect. 3.2 below we shall also see that the associated sequence of nonlinear strains strongly two-scale converges to a limit that is completely determined by v_*, cf. Remark 3.5 in connection with Proposition 3.4.

2.3 The Homogenization Formula and Corrector Problems

This section presents the definitions of the homogenized quadratic form Q^γ_{hom}, the effective prestrain B^γ_{eff}, and the residual energy $\mathcal{I}^\gamma_{\text{res}}$. The definition of $Q^\gamma_{\text{hom}}(x', \cdot)$ and $B^\gamma_{\text{eff}}(x')$ for a fixed material point $x' \in S$, only depends on the quadratic energy density

$$\left(-\frac{1}{2}, \frac{1}{2}\right) \times \mathbb{R}^2 \times \mathbb{R}^{3\times3} \ni (x_3, y, G) \mapsto Q(x', x_3, y, G)$$

and the prestrain tensor

$$\left(-\frac{1}{2}, \frac{1}{2}\right) \times \mathbb{R}^2 \ni (x_3, y) \mapsto B(x', x_3, y)$$

of Assumption 2.5—both only at the position x'. In view of this, we first present a *local* definition of the effective quantities for $x' \in S$ fixed, and discuss their continuity

properties. Secondly, we present the global definition of the effective quantities and of the residual energy $\mathcal{I}_{\text{res}}^{\gamma}$, see Definition 2.27 below.

Local definition of the effective quantities. For the local definition it is useful to introduce the following terminology:

Definition 2.15 (Λ-*periodic, admissible quadratic form and prestrain*) Let $\Lambda \in \mathbb{R}^{2\times 2}$ be invertible and $0 < \alpha \leq \beta < \infty$.

(i) A Borel function $Q : (-\frac{1}{2}, \frac{1}{2}) \times \mathbb{R}^2 \times \mathbb{R}^{3\times 3} \to \mathbb{R}$ is called a Λ-*periodic, admissible quadratic form*, if $Q(x_3, y, \cdot)$ is a quadratic form of class $\mathcal{Q}(\alpha, \beta)$ for a.e. $(x_3, y) \in (-\frac{1}{2}, \frac{1}{2}) \times \mathbb{R}^2$, and $Q(x_3, \cdot, G)$ is Λ-periodic for all $G \in \mathbb{R}^{3\times 3}$ and a.e. x_3.

(ii) A Borel function $B : (-\frac{1}{2}, \frac{1}{2}) \times \mathbb{R}^2 \to \mathbb{R}_{\text{sym}}^{3\times 3}$ is called a Λ-*periodic, admissible prestrain*, if B is square integrable and $B(x_3, \cdot)$ is Λ-periodic for a.e. x_3.

Note that in this definition, the variable y lives in the space $\mathbb{R}^2$ where the periodic microstructure is defined, and not in the macroscopic space $S \subset \mathbb{R}^2$. In the following we frequently use the notation $\square_\Lambda = (-\frac{1}{2}, \frac{1}{2}) \times Y_\Lambda$ and $Y_\Lambda = \Lambda[-\frac{1}{2}, \frac{1}{2})^2$ that we introduced in Assumption 2.5 (iii). By Λ-periodicity, Q and B can be restricted to $\square_\Lambda$ without loss of information.

Remark 2.16 (*Reference cell of periodicity and representative volume element*) If we consider $Q : \Omega \times \mathbb{R}^2 \times \mathbb{R}^{3\times 3} \to \mathbb{R}$ and $B : \Omega \times \mathbb{R}^2 \to \mathbb{R}_{\text{sym}}^{3\times 3}$ from Assumption 2.5, then the functions $Q(x', \cdot)$ and $B(x', \cdot)$ are Λ-periodic and admissible in the sense of Definition 2.15. (More precisely, we have to choose $\Lambda = \Lambda_j$ if $x_j \in S_j$ for some $j \in J$). The set Y_Λ is the reference cell of periodicity, see Appendix 8.1. From the perspective of homogenization, the set $\square_\Lambda$ can be viewed as a three-dimensional *representative volume element* that is attached to a (macroscopic) position x' in the midsurface S—the restriction of $Q(x', \cdot, G)$ and $B(x', \cdot)$ to $\square_\Lambda$ represents the microstructure of the composite at position x'.

We start by presenting a variational definition for the effective quantities Q_{hom}^{γ} and B_{eff}^{γ} of Theorem 2.8 associated to a general Λ-periodic and admissible quadratic form Q and prestrain B. After that, we shall establish a representation of these quantities based on correctors. This yields a convenient computational scheme for evaluating Q_{hom}^{γ} and B_{eff}^{γ}, see Proposition 2.25 below. We then show that the effective quantities Q_{hom}^{γ} and B_{eff}^{γ} continuously depend on Q and B.

The definition of the homogenized quadratic form involves the function space $H_\gamma^1(\square_\Lambda; \mathbb{R}^3)$, which consists of all local H^1-functions $\varphi : (-\frac{1}{2}, \frac{1}{2}) \times \mathbb{R}^2 \to \mathbb{R}^3$ that are Λ-periodic in the second argument (the y-variable); see (130) for the precise definition.

Definition 2.17 (*Homogenized quadratic form*) Given a Λ-periodic, admissible quadratic form Q, we define the associated homogenized quadratic form $Q_{\text{hom}}^{\gamma} : \mathbb{R}_{\text{sym}}^{2\times 2} \to [0, \infty)$ as

$$Q_{\text{hom}}^{\gamma}(G) := \inf_{M, \varphi} \fint_{\square_\Lambda} Q\big(x_3, y, \iota(x_3 G + M) + \text{sym} \nabla_\gamma \varphi\big) \mathrm{d}(x_3, y), \qquad (16)$$

where the infimum is taken over all $M \in \mathbb{R}^{2\times 2}_{\text{sym}}$ and $\varphi \in H^1_\gamma(\square_\Lambda; \mathbb{R}^3)$, and where $\nabla_\gamma := (\nabla_y, \frac{1}{\gamma}\partial_3)$. Above, we denote by $\iota(G)$ the unique 3×3-matrix whose upper-left 2×2-block is equal to $G \in \mathbb{R}^{2\times 2}$ and whose third column and row are zero.

Remark 2.18 (*Special cases*) For $\Lambda = I_{2\times 2}$ we recover the known case of a $\mathbb{Z}^2$-periodic composite. In that situation, $Q^\gamma_{\text{hom}}(G)$ coincides with the formula derived in Hornung et al. (2014). In the spatially homogeneous case where Q is independent of x_3 and y, we recover the formula of Friesecke et al. (2002),

$$Q^\gamma_{\text{hom}}(G) = \frac{1}{12} \min_{d \in \mathbb{R}^3} Q(\iota(G) + d \otimes e_3).$$

Next, we turn to the definition of the effective prestrain B^γ_{eff}. We adapt the scheme in Bauer et al. (2020), which is based on orthogonal projections in the Hilbert space of functions $G : (-\frac{1}{2}, \frac{1}{2}) \times \mathbb{R}^2 \to \mathbb{R}^{3\times 3}_{\text{sym}}$, $(x_3, y) \mapsto G(x_3, y)$ that are Λ-periodic in y and square integrable on $\square_\Lambda$. Specifically, let $L^2(\Lambda; \mathbb{R}^{3\times 3}_{\text{sym}})$ be the space of Λ-periodic functions in $L^2_{\text{loc}}(\mathbb{R}^2; \mathbb{R}^{3\times 3}_{\text{sym}})$, see Appendix 8.2, and consider the Hilbert space

$$\mathbf{H}_\Lambda := L^2\big((-\tfrac{1}{2}, \tfrac{1}{2}); L^2(\Lambda; \mathbb{R}^{3\times 3}_{\text{sym}})\big), \qquad \big(G, G'\big)_\Lambda := \fint_{\square_\Lambda} \mathbb{L}G : G' \mathrm{d}(x_3, y).$$

Note that the induced norm satisfies

$$\|G\|^2_\Lambda = \fint_{\square_\Lambda} Q(x_3, y, G)\mathrm{d}(x_3, y). \tag{17}$$

We further consider the subspaces

$$\mathbf{H}^\gamma_{\text{rel}, \Lambda} := \Big\{\iota(M) + \text{sym}\,\nabla_\gamma\varphi \,:\, M \in \mathbb{R}^{2\times 2}_{\text{sym}}, \; \varphi \in H^1_\gamma(\square_\Lambda; \mathbb{R}^3)\Big\}$$

and

$$\mathbf{H}^\gamma_\Lambda := \Big\{\iota(x_3 G) + \chi \,:\, G \in \mathbb{R}^{2\times 2}_{\text{sym}}, \; \chi \in \mathbf{H}^\gamma_{\text{rel}, \Lambda}\Big\}$$

and note that they are closed subspaces of $\mathbf{H}_\Lambda$. Here and below, we understand $\iota(x_3 G)$ as the map in $\mathbf{H}_\Lambda$ defined by $(x_3, y) \mapsto \iota(x_3 G)$. The closedness of the subspaces can be seen by using Korn's inequality in form of Lemma 8.5 in combination with Poincaré's inequality. We denote by $\mathbf{H}^{\gamma, \perp}_{\text{rel}, \Lambda}$ the orthogonal complement of $\mathbf{H}^\gamma_{\text{rel}, \Lambda}$ in $\mathbf{H}^\gamma_\Lambda$, and write $P^{\gamma, \perp}_{\text{rel}, \Lambda}$ for the orthogonal projection from $\mathbf{H}_\Lambda$ onto $\mathbf{H}^{\gamma, \perp}_{\text{rel}, \Lambda}$. Similarly, we write P^γ_Λ for the orthogonal projection from $\mathbf{H}_\Lambda$ onto $\mathbf{H}^\gamma_\Lambda$.

Remark 2.19 (*Interpretation of* $\mathbf{H}^\gamma_{\text{rel}, \Lambda}$ *and* $\mathbf{H}^\gamma_\Lambda$) Note that we have the orthogonal decomposition

$$\mathbf{H}_\Lambda = \mathbf{H}^\gamma_\Lambda \oplus \big(\mathbf{H}^\gamma_\Lambda\big)^\perp = \mathbf{H}^\gamma_{\text{rel}, \Lambda} \oplus \mathbf{H}^{\gamma, \perp}_{\text{rel}, \Lambda} \oplus \big(\mathbf{H}^\gamma_\Lambda\big)^\perp$$

The spaces $\mathbf{H}^{\gamma}_{\mathrm{rel}, \Lambda}$ and $\mathbf{H}^{\gamma}_{\Lambda}$ naturally show up in the two-scale analysis of the nonlinear strain: Indeed, as we shall prove below in Proposition 3.2, when considering a sequence of deformations (v_h) in $H^1(S; \mathbb{R}^3)$ with finite bending energy and limit $v \in H^2_{\mathrm{iso}}(S; \mathbb{R}^3)$, the associated sequence of nonlinear strains $E_h(v_h) := \frac{\sqrt{\nabla_h v_h^{\top} \nabla_h v_h} - I_{3\times 3}}{h}$ weakly two-scale converges (up to a subsequence) to a limit E, and for a.e. $x' \in S$, the limiting strain takes the form $E(x', \cdot) = \iota(x_3 \mathbb{II}_v(x')) + \chi$ for some $\chi \in \mathbf{H}^{\gamma}_{\mathrm{rel}, \Lambda}$. The field χ can be interpreted as a corrector that captures the oscillations on the scale $\varepsilon(h)$ that emerge along the selected subsequence of $(E_h(y_h))$. Note that in the definition of the effective quadratic form $Q^{\gamma}_{\mathrm{hom}}$ we relax the local energy by infinimizing over all $\iota(M) + \mathrm{sym}\, \nabla_{\gamma} \varphi = \chi \in \mathbf{H}^{\gamma}_{\mathrm{rel}, \Lambda}$, see (16). With help of the scalar product $(\cdot, \cdot)_{\Lambda}$, the infimization can be rephrased as an orthogonal projection: $Q^{\gamma}_{\mathrm{hom}}(G) = \| P^{\gamma, \perp}_{\mathrm{rel}, \Lambda} \iota(x_3 G) \|^2_{\Lambda}$.

Next, we turn to the definition of the effective prestrain $B^{\gamma}_{\mathrm{eff}}$. We first note that B can be decomposed into two parts: $P^{\gamma}_{\Lambda} B$ (the orthogonal projection of B onto $\mathbf{H}^{\gamma}_{\Lambda}$), and the orthogonal complement, $(I - P^{\gamma}_{\Lambda})B$. The energy contribution of the latter is captured by the residual energy introduced below. As we shall see, only $P^{\gamma}_{\Lambda} B$ interacts with the deformation. We define $B^{\gamma}_{\mathrm{eff}}$ in such a way that we can express the energy contribution associated with $P^{\gamma}_{\Lambda} B$ in the form $Q^{\gamma}_{\mathrm{hom}}(B^{\gamma}_{\mathrm{eff}})$. For this purpose, in the following lemma, we introduce an operator $\mathbf{E}^{\gamma}_{\Lambda}$.

Lemma 2.20 *Let $\gamma \in (0, \infty)$, and let Q be Λ-periodic and admissible in the sense of Definition 2.15. Then the map*

$$\mathbf{E}^{\gamma}_{\Lambda} : \mathbb{R}^{2\times 2}_{\mathrm{sym}} \to \mathbf{H}^{\gamma, \perp}_{\mathrm{rel}, \Lambda}, \qquad \mathbf{E}^{\gamma}_{\Lambda}(G) := P^{\gamma, \perp}_{\mathrm{rel}, \Lambda}\big(\iota(x_3 G)\big)$$

is a linear isomorphism, and

$$\sqrt{\tfrac{\alpha}{12}} |G| \leq \left(\fint_{\square_{\Lambda}} |\mathbf{E}^{\gamma}_{\Lambda}(G)|^2 \right)^{\frac{1}{2}} \leq \sqrt{\tfrac{\beta}{12}} |G|,$$

for all $G \in \mathbb{R}^{2\times 2}_{\mathrm{sym}}$.

(See Sect. 7.1 for the proof.)

Remark 2.21 In view of the definition of $\mathbf{E}^{\gamma}_{\Lambda}$ and of $Q^{\gamma}_{\mathrm{hom}}$ in Definition 2.17, we have $Q^{\gamma}_{\mathrm{hom}}(G) = \fint_{\square_{\Lambda}} Q(x_3, y, \mathbf{E}^{\gamma}_{\Lambda}(G)) \mathrm{d}(x_3, y)$ for all $G \in \mathbb{R}^{2\times 2}_{\mathrm{sym}}$. Furthermore, the proof of Lemma 2.20 reveals that

$$\frac{\alpha}{12} |G|^2 \leq Q^{\gamma}_{\mathrm{hom}}(G) \leq \frac{\beta}{12} |G|^2 \qquad \text{for all } G \in \mathbb{R}^{2\times 2}_{\mathrm{sym}}. \tag{18}$$

Definition 2.22 (*Effective prestrain*) Let $\gamma \in (0, \infty)$, and let Q, B be Λ-periodic and admissible in the sense of Definition 2.15. We define the effective prestrain $B^{\gamma}_{\mathrm{eff}} \in \mathbb{R}^{2\times 2}_{\mathrm{sym}}$ associated with Q and B by

$$B^{\gamma}_{\mathrm{eff}} := (\mathbf{E}^{\gamma}_{\Lambda})^{-1}\Big(P^{\gamma, \perp}_{\mathrm{rel}, \Lambda}(\mathrm{sym}\, B) \Big). \tag{19}$$

Next, we represent Q_{hom}^γ and B_{eff}^γ by means of three corrector problems. These are linear Korn-elliptic partial differential equations with domain $\square_\Lambda$ subject to periodic boundary conditions in the y-variable. The weak formulation (20) (below) of these corrector problems can be phrased as a variational problem in the Hilbert space $H_\gamma^1(\square_\Lambda; \mathbb{R}^3)$ (defined in (130)), and the coefficients are given by $\mathbb{L}$, the symmetric fourth-order tensor obtained in (4) from Q via polarization.

Lemma 2.23 (Existence of a corrector) *Let Q and B be Λ-periodic and admissible in the sense of* Definition 2.15, *and assume that $\frac{1}{C_\Lambda} \leq \Lambda^\top \Lambda \leq C_\Lambda$. Let $G \in \mathbb{R}_{\mathrm{sym}}^{2\times 2}$. Then there exists a unique pair*

$$M_G \in \mathbb{R}_{\mathrm{sym}}^{2\times 2}, \qquad \varphi_G \in H_\gamma^1(\square_\Lambda; \mathbb{R}^3) \text{ with } \int_{\square_\Lambda} \varphi_G \mathrm{d}(x_3, y) = 0,$$

solving the corrector problem

$$\int_{\square_\Lambda} \mathbb{L}\big(\iota(x_3 G + M_G) + \mathrm{sym}(\nabla_\gamma \varphi_G)\big) : \big(\iota(M') + \mathrm{sym}(\nabla_\gamma \varphi')\big)\mathrm{d}(x_3, y) = 0 \quad (20)$$

for all $\varphi' \in H_\gamma^1(\square_\Lambda; \mathbb{R}^3)$ and $M' \in \mathbb{R}_{\mathrm{sym}}^{2\times 2}$. Moreover, there exists a constant $C = C(\alpha, \beta, \gamma, C_\Lambda)$ such that

$$|M_G|^2 + \fint_{\square_\Lambda} |\nabla_\gamma \varphi_G|^2 \mathrm{d}(x_3, y) \leq C|G|^2. \tag{21}$$

We call (M_G, φ_G) the corrector associated with G.

(See Sect. 7.1 for the proof.)

Remark 2.24 We note that (20) is the Euler–Lagrange equation of the minimization problem in the definition of $Q_{\mathrm{hom}}^\gamma(G)$ in (16). In particular, (M_G, φ_G) is the unique minimizer of (16) (modulo an additive constant for φ_G).

Proposition 2.25 (Representation via correctors) *Let Q and B be Λ-periodic and admissible in the sense of* Definition 2.15, *and assume that $\frac{1}{C_\Lambda} \leq \Lambda^\top \Lambda \leq C_\Lambda$. Let G_1, G_2, G_3 be an orthonormal basis of $\mathbb{R}_{\mathrm{sym}}^{2\times 2}$ and denote by (M_{G_i}, φ_{G_i}) the corrector associated with G_i in the sense of* Lemma 2.23.

(a) (Representation of Q_{hom}^γ). The matrix $\widehat{Q} \in \mathbb{R}^{3\times 3}$ defined by

$$\widehat{Q}_{ik} := \fint_{\square_\Lambda} \mathbb{L}\big(\iota(x_3 G_i + M_{G_i}) + \mathrm{sym}(\nabla_\gamma \varphi_{G_i})\big) : \iota(x_3 G_k)\mathrm{d}(x_3, y)$$

is symmetric and positive definite, and we have

$$\frac{\alpha}{12} I_{3\times 3} \leq \widehat{Q} \leq \frac{\beta}{12} I_{3\times 3}, \tag{22}$$

in the sense of quadratic forms. Moreover, for all $G \in \mathbb{R}^{2\times 2}_{\text{sym}}$ we have the representation

$$Q^{\gamma}_{\text{hom}}(G) = \sum_{i,j=1}^{3} \widehat{Q}_{ij} \widehat{G}_i \widehat{G}_j,$$

where $\widehat{G}_1$, $\widehat{G}_2$, $\widehat{G}_3$ are the coefficients of G with respect to the basis G_1, G_2, G_3.
(b) (Representation of B^{γ}_{eff}). Define $\widehat{B} \in \mathbb{R}^3$ by

$$\widehat{B}_i := \fint_{\square_\Lambda} \mathbb{L}\big(\iota(x_3 G_i + M_{G_i}) + \text{sym}(\nabla_\gamma \varphi_{G_i})\big) : B \, \mathrm{d}(x_3, y), \quad i = 1, 2, 3.$$

Then we have $B^{\gamma}_{\text{eff}} = \sum_{i=1}^{3} \big(\widehat{Q}^{-1} \widehat{B}\big)_i G_i$.

(See Sect. 7.1 for the proof.)

The following lemma shows that the correctors and the effective quantities associated with an admissible pair (Q, B) continuously depends on (Q, B):

Lemma 2.26 (Continuity) *Consider a sequence of Λ-periodic and admissible pairs (Q_n, B_n), $n \in \mathbb{N} \cup \{\infty\}$, and assume that for $n \to \infty$,*

$$\begin{aligned} Q_n(x_3, y, G) &\to Q_\infty(x_3, y, G) & \textit{for all } G \in \mathbb{R}^{3\times 3} \textit{ and a.e. } (x_3, y), \\ B_n &\to B_\infty & \textit{strongly in } L^2(\square_\Lambda). \end{aligned}$$

Denote by $Q^{\gamma}_{\text{hom},n}$, $B^{\gamma}_{\text{hom},n}$, and $(M_{n,i}, \varphi_{n,i})$ the effective quantities and correctors associated with (Q_n, B_n) in the sense of Proposition 2.25. *Then for $n \to \infty$,*

$$\begin{aligned} Q^{\gamma}_{\text{hom},n}(G) &\to Q^{\gamma}_{\text{hom},\infty}(G) & \textit{for all } G \in \mathbb{R}^{2\times 2}_{\text{sym}}, & \quad (23) \\ B^{\gamma}_{\text{eff},n} &\to B^{\gamma}_{\text{eff},\infty} & \textit{in } \mathbb{R}^{2\times 2}_{\text{sym}}, & \quad (24) \\ M_{n,i} &\to M_{\infty,i} & \textit{in } \mathbb{R}^{2\times 2}_{\text{sym}}, & \quad (25) \\ \varphi_{n,i} &\to \varphi_{\infty,i} & \textit{strongly in } H^1_\gamma(\square_\Lambda; \mathbb{R}^3). & \quad (26) \end{aligned}$$

(See Sect. 7.1 for the proof.)
Global definition of the effective quantities. We present the *global* definition of the effective quantities and introduce the residual energy associated with a *locally periodic composite*:

Definition 2.27 (*Homogenized coefficients, effective prestrain and residual energy*)
For (Q, B) as in Assumption 2.5 define the *homogenized quadratic form* Q^{γ}_{hom} : $S \times \mathbb{R}^{2\times 2}_{\text{sym}} \to [0, \infty)$ and *the effective prestrain* $B^{\gamma}_{\text{eff}} : S \to \mathbb{R}^{2\times 2}_{\text{sym}}$ as follows: For all $x' \in S_j$, $j \in J$, we define $Q^{\gamma}_{\text{hom}}(x', G)$ and $B^{\gamma}_{\text{eff}}(x')$ by (16) and (19) applied with $\Lambda = \Lambda_j$, $Q = Q(x', \cdot)$, and $B = B(x', \cdot)$. Furthermore, define the *residual energy* as

$$\mathcal{I}^{\gamma}_{\text{res}}(B) := \sum_{j \in J} \int_{S_j} \fint_{\square_{\Lambda_j}} Q\big(x', x_3, y, (I - P^{\gamma}_{\Lambda_j})(\text{sym } B(x', \cdot))\big) \mathrm{d}(x_3, y) \mathrm{d}x'. \quad (27)$$

Remark 2.28 (*Regularity in x'*) Assumption 2.5 (i) in connection with Lemma 2.26 implies that $Q_{\text{hom}}^{\gamma}(\cdot, G)$ is continuous in each of the grains S_j, $j \in J$, and that B_{eff}^{γ} is measurable. In particular, we deduce that the integral in $\mathcal{I}_{\text{hom}}^{\gamma}$ (which requires measurability of the integrand) is well-defined.

Let us anticipate that in the Γ-convergence proof, we shall first obtain as a Γ-limit the "abstract" functional $\widetilde{\mathcal{I}}^{\gamma} : H_{\text{iso}}^2(S; \mathbb{R}^3) \to \mathbb{R}$,

$$\widetilde{\mathcal{I}}^{\gamma}(v) := \min_{M, \varphi} \sum_{j \in J} \int_{S_j} \fint_{\square_{\Lambda_j}} Q\Big(x', x_3, y, \iota(x_3 \mathbb{I}_v + M) + \text{sym}\,\nabla_{\gamma}\varphi - B\Big) \mathrm{d}(x_3, y)\mathrm{d}x', \tag{28}$$

where the minimization is over all corrector pairs (M, φ) with $M \in L^2(S; \mathbb{R}_{\text{sym}}^{2 \times 2})$ and $\varphi \in L^2\big(S; H_{\gamma,\text{uloc}}^1\big)$ that are locally periodic in the sense of (6). The reason why the relaxation w.r.t. M and φ occurs can be explained by means of the two-scale structure of the limiting strain, which we analyze in Proposition 3.2 in the next section. The following lemma, whose proof is based on the projection scheme introduced above, shows that the abstract Γ-limit decomposes as claimed in Theorem 2.8:

Lemma 2.29 (Representation of the abstract Γ-limit) *Let* Assumption 2.5 *be satisfied and let* $\widetilde{\mathcal{I}}^{\gamma} : H_{\text{iso}}^2(S; \mathbb{R}^3) \to \mathbb{R}$ *be defined by* (28). *Then*

$$\widetilde{\mathcal{I}}^{\gamma}(v) = \mathcal{I}_{\text{hom}}^{\gamma}(v) + \mathcal{I}_{\text{res}}^{\gamma}(B),$$

with $\mathcal{I}_{\text{hom}}^{\gamma}$ *and* $\mathcal{I}_{\text{res}}^{\gamma}$ *defined in* (7) *and* (27), *respectively.*

(See Sect. 7.1 for the proof.)

3 Two-Scale Limits of Nonlinear Strain

As in previous works on simultaneous homogenization and dimension reduction (Neukamm 2010, 2012; Hornung et al. 2014), it is crucial to have a precise understanding of the oscillatory behavior of the nonlinear strain

$$E_h(v_h) := \frac{\sqrt{(\nabla_h v_h)^{\top} \nabla_h v_h} - I_{3 \times 3}}{h} \tag{29}$$

for sequences of deformations $(v_h) \subseteq H^1(\Omega; \mathbb{R}^3)$ with finite bending energy in the sense of (9). In this section, we give a precise characterization of weak two-scale limits of the nonlinear strain E_h along sequences of deformations with finite bending energy (Proposition 3.2). Furthermore, we prove that E_h strongly two-scale converges along sequences of deformations with converging energy (Proposition 3.4).

3.1 Characterization of Sequences with Finite Bending Energy

In Friesecke et al. (2002) it is shown that any sequence (v_h) satisfying (9) admits a subsequence (also called (v_h)) such that there is a bending deformation $v \in H_{\text{iso}}^2(S; \mathbb{R}^3)$

for which

$$v_h - \fint_\Omega v_h \to v \qquad\qquad \text{strongly in } L^2(\Omega), \qquad (30)$$

and vector fields $M \in L^2(S; \mathbb{R}^{2\times 2}_{\text{sym}})$ and $d \in L^2(\Omega; \mathbb{R}^3)$ such that

$$E_h(v_h) \rightharpoonup \iota(x_3 \mathbb{I}_v + M) + \text{sym}(d \otimes e_3) \qquad\qquad \text{weakly in } L^2(\Omega). \qquad (31)$$

When adding homogenization to the game, the identification of the weak limit of the nonlinear strain is not sufficient; we need to resolve the two-scale structure of (31). For this we appeal to the following variant of two-scale convergence. It is a rather straightforward extension of the notion introduced in Neukamm (2012, 2010) to the locally periodic setting that we consider here. In the following definition, $L^2_{\text{uloc}}(\mathbb{R}^2)$ denotes the space of uniform locally p-integrable functions, see (127). Likewise, $L^2(\Lambda_j)$ denotes the space Λ_j-periodic functions in $L^2_{\text{loc}}(\mathbb{R}^2)$, see Appendix 8.1. Also recall the notation $Y_{\Lambda_j} = \Lambda_j[-\frac{1}{2}, \frac{1}{2})^2$ and $\square_{\Lambda_j} = (-\frac{1}{2}, \frac{1}{2}) \times Y_{\Lambda_j}$.

Definition 3.1 (*Two-scale convergence for locally periodic functions*) Let $\{S_j, \Lambda_j\}_{j\in J}$ be a grain structure in the sense of Definition 2.4, and suppose that $h \mapsto \varepsilon(h)$ satisfies Assumption 2.1. We say that a sequence $(\varphi_h) \subset L^2(\Omega)$ weakly two-scale converges in L^2 as $h \to 0$ to a function $\varphi \in L^2(\Omega; L^2_{\text{uloc}}(\mathbb{R}^2))$ if (φ_h) is bounded in $L^2(\Omega)$, and

(i) φ is locally periodic in the sense of (6), and
(ii) for all $j \in J$ and $\psi \in C_c^\infty\big(S_j \times (-\frac{1}{2}, \frac{1}{2}); C(\Lambda_j)\big)$,

$$\lim_{h\to 0} \int_\Omega \varphi_h(x)\psi\big(x, \tfrac{x'}{\varepsilon(h)}\big)dx = \int_{S_j} \fint_{\square_{\Lambda_j}} \varphi(x', x_3, y)\psi(x', x_3, y)d(x_3, y)dx'.$$

Here the space of two-scale test-functions $C_c^\infty\big(S_j \times (-\frac{1}{2}, \frac{1}{2}); C(\Lambda_j)\big)$ consists of all smooth $C(\Lambda_j)$–valued functions with support compactly contained in $S_j \times (-\frac{1}{2}, \frac{1}{2})$ where $C(\Lambda_j)$ denotes the space of continuous, Λ_j-periodic functions, see Appendix 8.1.

We say that (φ_h) strongly two-scale converges to φ if additionally

$$\int_\Omega |\varphi_h|^2 dx \;\to\; \sum_{j\in J} \int_{S_j} \fint_{\square_{\Lambda_j}} |\varphi(x', x_3, y)|^2 d(x_3, y)dx'.$$

We write $\varphi_h \overset{2}{\rightharpoonup} \varphi$ and $\varphi_h \overset{2}{\longrightarrow} \varphi$ in L^2 for weak and strong two-scale convergence in L^2, respectively.

Appendix 8.2 lists some properties of this notion of two-scale convergence. In particular, Proposition 8.3 in Appendix 8.2 shows that two-scale limits of bounded sequences of scaled gradients $\nabla_h v_h$ can be written in the form $(\nabla' v(x'), 0) + \nabla_\gamma \varphi(x', x_3, y)$ where $\nabla_\gamma = (\partial_{y_1}, \partial_{y_2}, \frac{1}{\gamma}\partial_3)$ with a *macroscopic* function $v \in H^1(S; \mathbb{R}^3)$ and a correction

φ that is a locally periodic function in $L^2(S; H^1_{\gamma,\text{uloc}})$; see (129) for the definition of the space $H^1_{\gamma,\text{uloc}}$ (it contains all functions defined on $(-\frac{1}{2}, \frac{1}{2}) \times \mathbb{R}^2$ with values in $\mathbb{R}^3$ whose H^1-norm on cubes $(0, z) + (-\frac{1}{2}, \frac{1}{2})^3$ can be bounded uniformly in $z \in \mathbb{R}^2$). This and further two-scale convergence methods are used to establish the next result, which identifies the structure of two-scale limits of the nonlinear strain.

Proposition 3.2 (Characterization of the two-scale limiting strain) *Let* $\{S_j, \Lambda_j\}_{j \in J}$ *be a grain structure in the sense of* Definition 2.4, *and suppose that* $\varepsilon(h)$ *is as in* Assumption 2.1 *for some* $\gamma \in (0, \infty)$.

(a) *Let* $(v_h) \subseteq H^1(\Omega; \mathbb{R}^3)$ *be a sequence of finite bending energy, satisfying* (9), *with limit* $v \in H^2_{\text{iso}}(S; \mathbb{R}^3)$ *in the sense of* (30). *Then, up to a subsequence,*

$$E_h(v_h) \overset{2}{\rightharpoonup} \iota(x_3 \mathbb{I}_v + M) + \text{sym} \nabla_\gamma \varphi, \qquad (32)$$

for a matrix field $M \in L^2(S; \mathbb{R}^{2\times2}_{\text{sym}})$ *and a corrector* $\varphi \in L^2(S; H^1_{\gamma,\text{uloc}})$ *that is locally periodic in the sense of* (6).

(b) *For all* $v \in H^2_{\text{iso}}(S; \mathbb{R}^3)$, $M \in L^2(S; \mathbb{R}^{2\times2}_{\text{sym}})$, *and any corrector* $\varphi \in L^2(S; H^1_{\gamma,\text{uloc}})$ *satisfying* (6), *there exists a sequence* (v_h) *in* $H^1(\Omega; \mathbb{R}^3)$ *such that*

$$v_h \to v \qquad\qquad\qquad \text{strongly in } L^2(\Omega; \mathbb{R}^3)$$
$$E_h(v_h) \overset{2}{\longrightarrow} \iota(x_3 \mathbb{I}_v + M) + \text{sym} \nabla_\gamma \varphi \qquad \text{strongly two-scale in } L^2. \quad (33)$$

Furthermore,

$$\limsup_{h \to 0} h \| E_h(v_h) \|_{L^\infty} = 0 \quad \text{and} \quad \lim_{h \to 0} \| \det(\nabla_h v_h) - 1 \|_{L^\infty} = 0.$$

Finally, if v *satisfies boundary conditions in the sense that* $v \in \mathcal{A}_{BC}$ *(see* Definition 2.11*), and if*

$$M(x') + \delta I_{2\times2} \geq 0 \quad \text{in the sense of quadratic forms,}$$

for some $\delta > 0$ *and a.e.* $x' \in S$, *then there exists a sequence* (v_h) *satisfying* (33) *and the boundary condition* (13).

(See Sect. 7.5 for the proof.)

Proposition 3.2 is the key ingredient for determining the Γ-limit of $\mathcal{I}^{\varepsilon(h),h}$, cf. (3): In the proof of Theorem 2.8, with help of Proposition 3.2 we shall first establish Γ-convergence of $\mathcal{I}^{\varepsilon(h),h}$ to the functional $\widetilde{\mathcal{I}}^\gamma$, whose definition (see (28)) is closely related to (32). Indeed, the argument of the quadratic form under the integral in (28) is precisely the difference of the right-hand side of (32) and the prestrain B. Furthermore, $\widetilde{\mathcal{I}}^\gamma(v)$ is then obtained by minimizing out M and φ, i.e., the only terms of the right-hand side of (32) that are not uniquely determined by the deformation v.

Proposition 3.2 extends a previous result in Hornung et al. (2014) in various directions: First, the construction of Part (b) takes boundary conditions of the form of

Definition 2.11 into account. Secondly, "grained" composites, i.e., composites with a periodic microstructure whose reference lattice changes from grain to grain, are considered. Thirdly and most importantly, Proposition 3.2 closes a gap in the characterization of the limiting strain on regions where the second fundamental form vanishes. More precisely, Hornung et al. (2014) proves Part (a) in the single grain case $J = 1$, $\Lambda_1 = I_{2 \times 2}$, and establishes Part (b) only under the additional assumption that the matrix M in (32) vanishes on all flat parts of the bending deformation u, i.e.,

$$M = 0 \text{ a.e. in } \{x' \in S \ : \ \mathbb{II}_v(x') = 0\}. \tag{34}$$

This assumption is critical for the construction in Hornung et al. (2014). Nevertheless, in the case without prestrain, the construction of Hornung et al. (2014) is sufficient for deriving the Γ-limit. In contrast, when a prestrain is present, it is necessary to treat the case where (34) is not satisfied to retrieve the Γ-limit. In the case without homogenization, this has recently been achieved by the third author in Padilla-Garza (2022) using a flexibility result for isometric immersions that was inspired by Lewicka and Pakzad (2017). In our proof of Proposition 3.2(b), we combine this method with the two-scale ansatz of Hornung et al. (2014) and thus give a complete characterization of the two-scale limits of the nonlinear strain.

3.2 Strong Two-Scale Convergence of the Nonlinear-Strain for Almost-Minimizing Sequences

Theorem 2.8 implies that a sequence of almost-minimizers (v_h) converges (after possibly extracting a subsequence) to a minimizer of the limiting energy. The next result shows that the nonlinear strain $E_h(v_h)$ defined in (29) strongly two-scale converges along such a sequence to a two-scale strain that is uniquely determined by the second fundamental form of the limiting deformation. More precisely, if the limiting deformation is given by $v_* \in H^2_{\mathrm{iso}}(S; \mathbb{R}^3)$, then the limiting strain takes the form

$$E_*(x, y) = \iota\big(x_3 \mathbb{II}_{v_*}(x') + M_*(x')\big) + \operatorname{sym} \nabla_\gamma \varphi_*(x, y), \tag{35}$$

where

$$M_* \in L^2(S; \mathbb{R}^{2 \times 2}_{\mathrm{sym}}) \text{ and } \varphi_* \in L^2\big(S; H^1_{\gamma, \mathrm{uloc}}\big)$$

satisfy, for all $j \in J$ and a.e. $x' \in S_j$, the weak corrector problem

$$\int_{\square_{\Lambda_j}} \mathbb{L}(x', \cdot)\big(\iota(x_3 \mathbb{II}_{v_*}(x') + M_*(x'))$$
$$+ \operatorname{sym}(\nabla_\gamma \varphi_*(x', \cdot))\big) : \big(\iota(M') + \operatorname{sym}(\nabla_\gamma \varphi')\big) \mathrm{d}(x_3, y) = 0,$$
$$\text{for all } M' \in \mathbb{R}^{2 \times 2}_{\mathrm{sym}} \text{ and } \varphi' \in H^1_\gamma(\square_{\Lambda_j}; \mathbb{R}^3) \tag{36}$$

subject to the mixed boundary and zero-mean conditions

$$\varphi_*(x', \cdot) \in H_\gamma^1(\square_{\Lambda_j}; \mathbb{R}^3) \quad \text{and} \quad \fint_{\square_{\Lambda_j}} \varphi_*(x', x_3, y) \mathrm{d}(x_3, y) = 0.$$

Remark 3.3 (*Corrector representation of E_**) By linearity of equation (36), for each $x' \in S$ we have the corrector representation

$$\left(M_*(x'), \varphi_*(x', \cdot)\right) = \sum_{i=1}^3 \widehat{\mathbb{I}_{v_*}(x')}_i \, (M_i, \varphi_i),$$

where the (M_i, φ_i), $i = 1, 2, 3$ are the correctors of Proposition 2.25 (applied with $Q = Q(x', \cdot)$ and $B = B(x', \cdot)$), and where $\widehat{\mathbb{I}_{v_*}(x')} \in \mathbb{R}^3$ denotes the coefficient vector of $\mathbb{I}_{v_*}(x') \in \mathbb{R}^{2\times2}_{\mathrm{sym}}$ with respect to the basis G_1, G_2, G_3 of Proposition 2.25.

Next, we establish strong two-scale convergence of the nonlinear strain for sequences of deformations whose energy is converging. In particular, it applies to sequences of (almost) minimizers.

Proposition 3.4 *Let Assumptions 2.1 and 2.5 be satisfied. Consider a sequence (v_h) in $H^1(\Omega; \mathbb{R}^3)$ that strongly converges in $L^2(\Omega)$ to some $v_* \in H_{\mathrm{iso}}^2(S; \mathbb{R}^3)$. Assume that the energy converges in the sense that*

$$\lim_{h\to0} \mathcal{I}^{\varepsilon(h),h}(v_h) = \mathcal{I}_{\mathrm{hom}}^\gamma(v_*) + \mathcal{I}_{\mathrm{res}}^\gamma(B). \tag{37}$$

Then

$$E_h(v_h) \xrightarrow{\ 2\ } E_* \quad \text{strongly two-scale in } L^2,$$

where E_* is defined in (35).

Proposition 3.4, proved in Sect. 7.6, extends (Friesecke et al. 2002, Theorem 7.1), where strong "single-scale" convergence of $E_h(v_h)$ was established in the case without homogenization. Also related is Theorem 7.5.1 of Neukamm (2010), which shows the result for two-scale homogenization and rods.

Remark 3.5 (*Application to almost-minimizers*) Proposition 3.4 applies in particular to almost-minimizers: When (v_h) is a sequence of almost-minimizers, that is, a sequence such that

$$\lim_{h\to0} \left(\mathcal{I}^{\varepsilon(h),h}(v_h) - \inf_{v\in H^1(\Omega;\mathbb{R}^3)} \mathcal{I}^{\varepsilon(h),h}(v) \right) = 0,$$

then Theorem 2.8 implies that a subsequence of (v_h) converges strongly in H^1 to a minimizer of $\mathcal{I}^\gamma(\cdot) + \mathcal{I}_{\mathrm{res}}^\gamma(B)$. Hence, Proposition 3.4 implies that (along the same subsequence) $E_h(v_h) \xrightarrow{\ 2\ } E_*$ strongly two-scale in L^2.

4 The Microstructure–Properties Relations

In this and the following section we investigate the relation between the microstructure of the composite material and the effective shape of the plate in equilibrium, i.e., we want to predict the geometry of a minimizer $v_* \in H^2_{\text{iso}}(S; \mathbb{R}^3)$ of $\mathcal{I}^\gamma_{\text{hom}}$ based on knowledge of the microstructure of the composite and of the prestrain. We focus here on "free" minimizers, i.e., we do not take boundary conditions or external loads into account. The relationship can then be split into two parts:

(Q1) How do the effective stiffness Q^γ_{hom} and prestrain B^γ_{eff} depend on the microstructure of the composite and its prestrain?

(Q2) How do the minimizers of $\mathcal{I}^\gamma_{\text{hom}}$ depend on Q^γ_{hom} and B^γ_{eff}?

Note that in the general case, both problems can only be studied by numerical simulations: Question (Q1) requires solving a system of linear PDEs that admits closed-form solutions only in special cases. Question (Q2) is even more delicate since it generally requires solving a nonlinear, singular PDE. Solving PDEs, however, can be mostly avoided when studying the homogeneous case, i.e., when Q^γ_{hom} and B^γ_{eff} are independent of $x' \in S$. In this case it is known that free minimizers have a constant second fundamental form; see (Schmidt 2007a) and Lemma 5.1 below. The problem then reduces to an algebraic minimization problem. This is the case that the present paper focuses on. The numerical investigation of Question (Q2) in the case of spatial heterogeneity will be the subject of a further paper.

In this section we investigate Question (Q1), and thus study the connection between the microstructure (the linearized elastic energy Q, and the prestrain B) and the effective properties of the thin plate (Q^γ_{hom} and B^γ_{eff}). In Sect. 4.1, we first introduce a class of examples in which some symmetries of Q^γ_{hom} and B^γ_{eff} can be deduced from the symmetries of Q and B. Later, we further specialize that class to one for which explicit formulas for Q^γ_{hom} and B^γ_{eff} are available. Section 4.2 then numerically explores these formulas. The discussion of Question (Q2) shall follow in Sect. 5.

4.1 The Case of Orthotropic Effective Stiffness

In this section we introduce a special class of composites that feature simplified formulas for the effective quantities. We shall discuss a series of examples that become progressively more specific. Our final example consists of a parametrized laminate that is composed of two isotropic materials with zero-Poisson ratio. The upshot of the example is that it features a closed-form expression for Q^γ_{hom} and B^γ_{eff} that can be evaluate at low computational cost — an advantage that we shall exploit in our numerical studies.

In the following, we use the representation of a matrix $G \in \mathbb{R}^{2\times 2}_{\text{sym}}$ as

$$G = \sum_{i=1}^{3} \widehat{G}_i G_i, \quad \text{where } G_1 := e_1 \otimes e_1, \ G_2 := e_2 \otimes e_2, \ G_3 := \frac{1}{\sqrt{2}}(e_1 \otimes e_2 + e_2 \otimes e_1),$$

(38)

denotes the canonical orthonormal basis of $\mathbb{R}^{2\times2}_{\text{sym}}$. We call $\widehat{G}_1, \widehat{G}_2, \widehat{G}_3 \in \mathbb{R}$ the coefficients of G. We start by introducing the following notion of orthotropocity for Q^γ_{hom}, and note that all examples in this section shall feature this material symmetry.

Definition 4.1 (*Orthotropicity*) We call a quadratic form $Q^\gamma_{\text{hom}} : \mathbb{R}^{2\times2}_{\text{sym}} \to \mathbb{R}$ *orthotropic*, if there exist $q_1, q_2, q_{12}, q_3 \in \mathbb{R}$ such that

$$Q^\gamma_{\text{hom}}(G) = \left(\widehat{G}_1^2 q_1 + \widehat{G}_1\widehat{G}_2 q_{12} + \widehat{G}_2^2 q_2\right) + \widehat{G}_3^2 q_3.$$

We call q_1, q_2, q_{12}, q_3 the coefficients of Q^γ_{hom}.

In the rest of this section we consider composites that are Λ-periodic with $\Lambda = I_{2\times2}$. For convenience we introduce for the representative volume element the shorthand $\square := \square_\Lambda = \left(-\frac{1}{2}, \frac{1}{2}\right) \times \left[-\frac{1}{2}, \frac{1}{2}\right)^2$. The following lemma yields a sufficient condition on the quadratic form Q for orthotropicity.

Lemma 4.2 (A sufficient condition for orthotropicity) *Let the quadratic form Q be admissible in the sense of* Definition 2.15, *and assume that $\Lambda = I_{2\times2}$. Suppose that Q is independent of y_2 and takes the form*

$$Q(x_3, y, G) = \lambda(x_3, y_1)\text{tr}(G)^2 + 2\mu(x_3, y_1)|\text{sym } G|^2 \tag{39}$$

with Lamé coefficients λ, μ satisfying the symmetry conditions

$$\lambda(x_3, y_1) = \lambda(-x_3, y_1) = \lambda(x_3, -y_1) \quad\text{and}\quad \mu(x_3, y_1) = \mu(-x_3, y_1) = \mu(x_3, -y_1)$$

for all $x_3 \in \left(-\frac{1}{2}, \frac{1}{2}\right)$ and a.e. $y_1 \in \left(-\frac{1}{2}, \frac{1}{2}\right)$. Then Q^γ_{hom} associated with Q via Definition 2.17 *is orthotropic. Moreover, the corrector pair (M_i, φ_i) associated with G_i via* (20) *satisfies the following properties:*

$$M_1 = M_2 = M_3 = 0, \tag{40}$$

and a.e. in $\square_\Lambda$ we have,

$$\partial_{y_2}\varphi_1 = \partial_{y_2}\varphi_2 = \partial_{y_2}\varphi_3 = \varphi_1 \cdot e_2 = \varphi_2 \cdot e_2 = \varphi_3 \cdot e_1 = \varphi_3 \cdot e_3 = 0, \tag{41}$$

$$\mathbb{L}\big(\iota(x_3 G_3) + \text{sym } \nabla_\gamma \varphi_3\big) : (e_j \otimes e_j) = 0 \quad\text{for } j = 1, 2, 3. \tag{42}$$

Above, we denote by e_1, e_2, e_3 the canonical basis of $\mathbb{R}^3$.

(See Sect. 7.7 for the proof.)

Next, we specialize the situation further to a class of examples for which we have explicit solutions to the corrector problem (20): In addition to the assumptions of Lemma 4.2, in the following result we consider a composite in which the elastic law described by Q is additionally independent of x_3 and thus describes a laminate. Furthermore, we assume that the components of the composite have a Poisson ratio that vanishes (i.e., $\lambda = 0$). We shall also derive simplified formulas for B^γ_{eff} in the case of a prestrain B that is rotationally invariant, i.e., of the form $B = \rho I_{2\times2}$ for a scalar function ρ.

Lemma 4.3 (Laminate of isotropic materials with vanishing Poisson ratio) *Let* (Q, B) *be admissible in the sense of* Definition 2.15, *and assume that* $\Lambda = I_{2 \times 2}$. *Suppose that Q takes the form*

$$Q(x_3, y, G) = 2\mu(y_1)|\operatorname{sym} G|^2,$$

and assume that $\mu(-y_1) = \mu(y_1)$ *for a.e.* $y_1 \in (-\frac{1}{2}, \frac{1}{2})$. *We denote the harmonic and arithmetic means of μ by*

$$\langle \mu \rangle_{\mathrm{h}} := \left(\int_{-\frac{1}{2}}^{\frac{1}{2}} \frac{1}{\mu} \, dy_1 \right)^{-1} \quad and \quad \overline{\mu} := \int_{-\frac{1}{2}}^{\frac{1}{2}} \mu \, dy_1, \qquad (43a)$$

respectively, and introduce for $\gamma \in (0, \infty)$ *the following weighted average*

$$\mu_\gamma := \min_{w \in \mathcal{H}} \fint_{\square} \mu \left(\left(\sqrt{12} x_3 + \partial_{y_1} w \right)^2 + \left(\tfrac{1}{\gamma} \partial_3 w \right)^2 \right) d(x_3, y), \qquad (43b)$$

where

$$\mathcal{H} := \left\{ w \in H^1_\gamma(\square; \mathbb{R}) \, : \, \fint_{\square} w = 0, \ \partial_{y_2} w = 0 \text{ a.e. in } \square \right\}.$$

Let Q^γ_{hom} *and* B^γ_{eff} *denote the effective quantities associated with* (Q, B) *defined via Definitions 2.17 and 2.22. Then the following properties hold:*

(a) *We have*

$$\langle \mu \rangle_{\mathrm{h}} \le \mu_\gamma \le \overline{\mu} \quad \text{for all } \gamma \in (0, \infty). \qquad (44)$$

　　Furthermore, the map $(0, \infty) \ni \gamma \mapsto \mu_\gamma$ *is continuous and monotonically decreasing, and satisfies*

$$\lim_{\gamma \to 0} \mu_\gamma = \overline{\mu} \quad and \quad \lim_{\gamma \to \infty} \mu_\gamma = \langle \mu \rangle_{\mathrm{h}}. \qquad (45)$$

　　Furthermore, if μ is non-constant, then $\gamma \mapsto \mu_\gamma$ *is strictly monotone.*

(b) Q^γ_{hom} *is orthotropic with coefficients*

$$q_1 = \frac{1}{6} \langle \mu \rangle_{\mathrm{h}}, \quad q_2 = \frac{1}{6} \overline{\mu}, \quad q_3 = \frac{1}{6} \mu_\gamma, \quad q_{12} = 0. \qquad (46)$$

(c) *Assume that* $B(x_3, y) = \rho(x_3, y_1) I_{3 \times 3}$ *for a scalar function ρ. Then the coefficients of B^γ_{eff} are given by*

$$\widehat{B}^\gamma_{\mathrm{eff},1} = 12 \fint_{\square} \rho \, x_3 \, d(x_3, y), \quad \widehat{B}^\gamma_{\mathrm{eff},2} = \frac{12}{\overline{\mu}} \fint_{\square} \mu \rho x_3 \, d(x_3, y), \quad \widehat{B}^\gamma_{\mathrm{eff},3} = 0. \qquad (47)$$

(See Sect. 7.7 for the proof.)

Remark 4.4 (*Physical interpretation*) The harmonic mean $\langle \mu \rangle_{\mathrm{h}}$ and the arithmetic mean $\overline{\mu}$ are typical averages in homogenization of laminates: By assumption, the

(a) Prestrain strength $\rho(x_3, y_1)$ **(b)** Lamé parameter $\mu(x_3, y_1)$
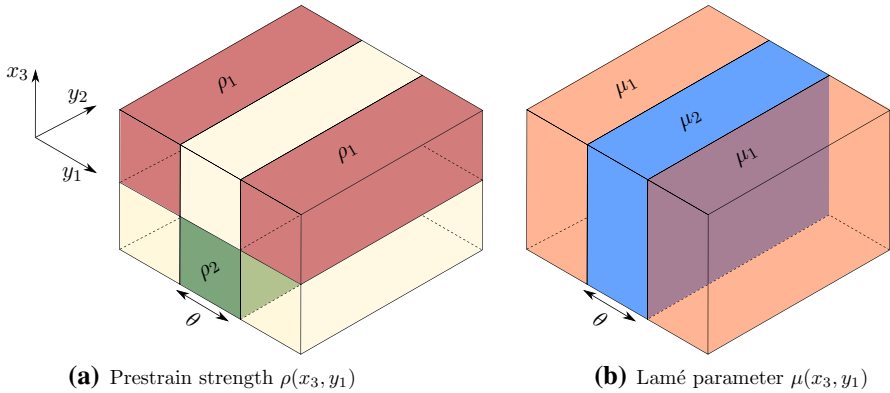
Fig. 4 Schematic view of the microstructure of Lemma 4.5

laminate under consideration oscillates in the y_1-coordinate, while it is constant with respect to y_2. As a consequence, the corrector associated with G_2 vanishes and leads to the arithmetic mean for the effective coefficient q_2. On the other hand, the corrector associated with G_1 oscillates and leads to the harmonic mean for q_1. Furthermore, since $\fint_\square |\sqrt{12}x_3|^2 \, d(x_3, y) = 1$, the quantity μ_γ is a weighted average that interpolates between the arithmetic and harmonic mean.

We will now specialize the particular case of Lemma 4.3 even further: We divide the representative volume element of the composite $\square = (-\frac{1}{2}, \frac{1}{2}) \times [-\frac{1}{2}, \frac{1}{2}]^2$ into two regions in the x_3-axis (top and bottom) and two regions in the y_1-axis (middle and its complement). The middle region has width θ. The remaining Lamé parameter μ takes one value in the middle and another value in the complement region. The prestrain strength ρ takes one value in the top, complement region, another value in the bottom, middle region, and is 0 elsewhere. The setting is illustrated in Fig. 4, and formalized in the following lemma.

Lemma 4.5 (A parametrized laminate) *For parameters $\mu_1 > 0$, $\rho_1 \in \mathbb{R}$, $\theta \in [0, 1]$, $\theta_\rho \in \mathbb{R}$, and $\theta_\mu > 0$, we consider the situation of* Lemma 4.3 *where ρ and μ are defined by*

$$\rho(x_3, y_1) := \begin{cases} \rho_1 & \text{if } |y_1| > \frac{\theta}{2} \text{ and } x_3 > 0, \\ \rho_2 & \text{if } |y_1| < \frac{\theta}{2} \text{ and } x_3 < 0, \\ 0 & \text{else,} \end{cases} \quad \text{and} \quad \mu(x_3, y_1) := \begin{cases} \mu_1 & \text{if } |y_1| > \frac{\theta}{2}, \\ \mu_2 & \text{else,} \end{cases}$$

where $\rho_2 := \theta_\rho \rho_1$ and $\mu_2 := \theta_\mu \mu_1$. Then we have

$$q_1 = \mu_1 \frac{\theta_\mu}{6(\theta + (1 - \theta)\theta_\mu)}, \qquad q_2 = \frac{\mu_1}{6}\big((1 - \theta) + \theta\theta_\mu\big), \qquad (48)$$

Table 1 Parameters for the parametrized laminate introduced in Lemma 4.5

θ	: Volume fraction of the components
θ_μ	: Stiffness ratio
θ_ρ	: Prestrain contrast
μ_1	: Material stiffness
ρ_1	: Strength of the isotropic prestrain

Parameters	θ_μ	θ_ρ	θ
	2	2	$\frac{1}{2}$
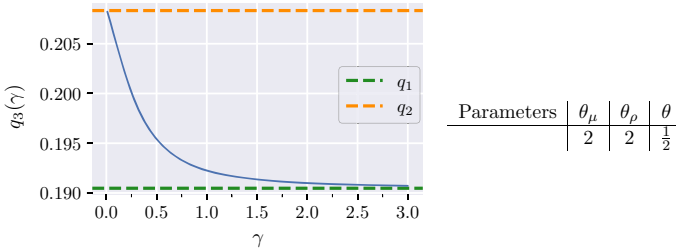
Fig. 5 Numerical approximation of $q_3(\gamma) = \frac{1}{6}\mu_\gamma$

and

$$\widehat{B}^\gamma_{\mathrm{eff},1} = \frac{3\rho_1}{2}\big(1 - \theta(1 + \theta_\rho)\big), \quad \widehat{B}^\gamma_{\mathrm{eff},2} = \frac{3\rho_1}{2}\left(\frac{1 - \theta(1 + \theta_\mu\theta_\rho)}{1 - \theta + \theta\theta_\mu}\right), \quad \widehat{B}^\gamma_{\mathrm{eff},3} = 0. \tag{49}$$

(See Sect. 7.7 for the proof.)

4.2 Numerical Computation of the Effective Quantities

In this section we answer Question (Q1) for the parametrized laminate introduced in Lemma 4.5 by numerically exploring the parameter dependence of the effective quantities Q^γ_{hom} and B^γ_{eff}. Recall that by Lemma 4.5, Q^γ_{hom} is orthotropic with coefficients q_1, q_2 given by (48), $q_{12} = 0$, and $q_3(\gamma) = \frac{1}{6}\mu_\gamma$ with μ_γ given by (43b). The coefficients of B^γ_{eff} are given by (49). These coefficients (and thus Q^γ_{hom} and B^γ_{eff}) depend on the parameters of the model shown in Table 1. As can be seen by a close look at the formulas for the coefficients, the following scaling properties hold:

$$Q^\gamma_{\mathrm{hom}}(G; \theta, \theta_\mu, \theta_\rho, \mu_1, \rho_1) = \mu_1 Q^\gamma_{\mathrm{hom}}(G; \theta, \theta_\mu, 1, 1, 1),$$
$$B^\gamma_{\mathrm{eff}}(\theta, \theta_\mu, \theta_\rho, \mu_1, \rho_1) = \rho_1 B^{\gamma=1}_{\mathrm{eff}}(\theta, \theta_\mu, \theta_\rho, 1, 1). \tag{50}$$

In particular, Q^γ_{hom} does not depend on θ_ρ and ρ_1, and B^γ_{eff} does not depend on μ_1 and the scaling parameter γ. In view of this, we set $\mu_1 = \rho_1 = 1$ in the following. With the idea in mind that the volume fraction θ can be controlled during the fabrication of the composite, we shall mainly focus on the functional dependence of Q^γ_{hom} and B^γ_{eff} on θ for various values of θ_μ and θ_ρ.
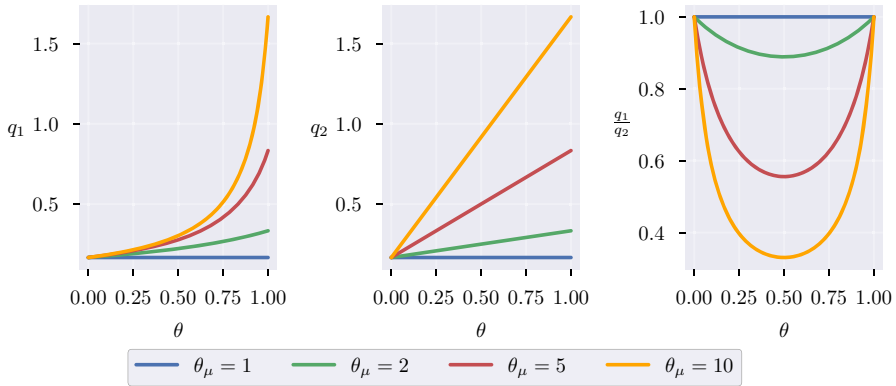
Fig. 6 Coefficients q_1, q_2 and the ratio q_1/q_2 as functions of the volume fraction θ of the constituents, for different values of θ_μ

In view of the definition of the coefficients (cf. (48), (46), and (49)) all except the coefficient $q_3(\gamma)$ are given by explicit formulas, which can be evaluated without computational effort. In contrast, for $q_3(\gamma)$ we need to solve the Euler–Lagrange equation for the minimization problem (43b). It is a two-dimensional, elliptic system that we solve using a finite element method implemented in C++ using the DUNE libraries (Blatt et al. 2016; Sander 2020). We also note that $q_3(\gamma)$ is the only coefficient that depends on the scaling parameter γ. Figure 5 shows the value of $q_3(\gamma)$ obtained numerically for different values of the relative scaling parameter γ. We clearly observe property (44), i.e., $q_1 < q_3(\gamma) < q_2$ for $\gamma \in (0, \infty)$, continuity and monotonicity of $\gamma \mapsto q_3(\gamma)$, and the asymptotic behavior

$$\lim_{\gamma \to 0} q_3(\gamma) = q_2 \quad \text{and} \quad \lim_{\gamma \to \infty} q_3(\gamma) = q_1, \tag{51}$$

as predicted by Lemma 4.3. Furthermore, $q_3(\gamma)$ appears to be a convex function with a rapid decay for values of γ close to zero. Let us anticipate that in the next section we shall appeal to the asymptotic behavior (51) to avoid the computational effort required to solve (43b) numerically: in view of (51), in the extreme cases $0 < \gamma \ll 1$ and $\gamma \gg 1$, we may use q_2 and q_1 as approximations for $q_3(\gamma)$, respectively.

Figure 6 shows the elastic moduli q_1, q_2, and their ratio $\frac{q_1}{q_2}$ as functions of the volume fraction θ for different values of the stiffness ratio θ_μ. The ratio $\frac{q_1}{q_2}$ serves as a measure for the in-plane anisotropy of the effective material. As expected from (48) we observe a nonlinear dependence of q_1 on the volume fraction θ, and a linear dependence of q_2 on θ. Note that for $\theta_\mu = 1$ the laminate reduces to a homogeneous material. By increasing the stiffness ratio θ_μ, the slopes of q_1 and q_2 as functions of θ increase while the ratio $\frac{q_1}{q_2}$ decreases. We note that as θ_μ increases, so does the possible anisotropy. Additionally, for all $\theta_\mu > 1$ the ratio $\frac{q_1}{q_2}$ assumes its minimum at $\theta = \frac{1}{2}$. Next, we study the effective prestrain B_{eff}^γ and its dependence on the laminate
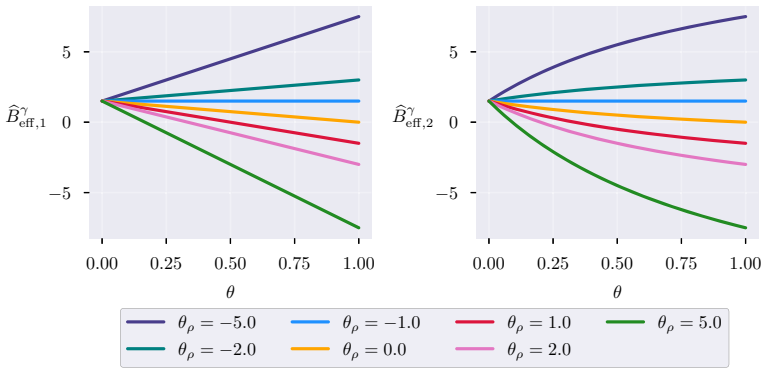
Fig. 7 Effective prestrain components $\widehat{B}^{\gamma}_{\text{eff},1}$ (left) and $\widehat{B}^{\gamma}_{\text{eff},2}$ (right) for a fixed value of $\theta_{\mu} = 2$ with different values of θ_{ρ}
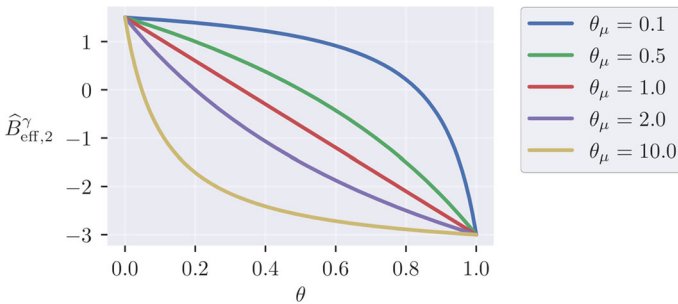
Fig. 8 Effective prestrain $\widehat{B}^{\gamma}_{\text{eff},2}$ for a fixed value of $\theta_{\rho} = 2$ with different values of θ_{μ}

parameters. Recall that $\widehat{B}^{\gamma}_{\text{eff},3} = 0$ by Lemma 4.3. (Here and below, we use the notation introduced in (38) for the coefficients of B^{γ}_{eff}.)

Figure 7 displays the effective prestrain coefficients $\widehat{B}^{\gamma}_{\text{eff},1}$ and $\widehat{B}^{\gamma}_{\text{eff},2}$ as functions of the volume fraction θ for different values of the prestrain ratio θ_{ρ}. Note that the dependence of $\widehat{B}^{\gamma}_{\text{eff},1}$ on θ is linear, while the dependence of $\widehat{B}^{\gamma}_{\text{eff},2}$ on θ is nonlinear. This is somewhat surprising, since the corrector associated to G_1 is non-zero, while the corrector associated to G_2 is zero, cf. the proof of Lemma 4.3. Furthermore, note that the effective prestrain is not zero if $\theta = 0$, and the sign, as well as the slope of the effective prestrain depends on the prestrain ratio θ_{ρ}.

In a similar way, Fig. 8 shows the dependence of $\widehat{B}^{\gamma}_{\text{eff},2}$ on the volume fraction θ but for different stiffness ratios θ_{μ}. Note that $\widehat{B}^{\gamma}_{\text{eff},1}$ is independent of θ_{μ}, see Lemma 4.5. Again, the dependence of $\widehat{B}^{\gamma}_{\text{eff},2}$ on θ is nonlinear except for the homogeneous case $\theta_{\mu} = 1.0$, where the dependence becomes affine.

5 The Microstructure–Shape Relation

In this section, we investigate Question (Q2) and combine it with the results of Sect. 4 in order to explore the parameter-dependence of the shapes of free minimizers of the homogenized energy functional $\mathcal{I}_{\text{hom}}^{\gamma}$ for the parametrized laminate material of Lemma 4.5. Note that unless stated otherwise, with "minimizer" we always refer to a *global* minimizer. As mentioned before, in the present paper, we restrict our analysis to the spatially homogeneous case and thus assume that

$$Q_{\text{hom}}^{\gamma} \text{ and } B_{\text{eff}}^{\gamma} \text{ are independent of } x' \in S. \tag{52}$$

A sufficient condition for (52) is the global periodicity of the composite's microstructure. Condition (52) allows to simplify the minimization of $\mathcal{I}_{\text{hom}}^{\gamma}$ drastically: Every bending deformation that minimizes $\mathcal{I}_{\text{hom}}^{\gamma}$ has a constant fundamental form and thus parametrizes a cylindrical surface with constant curvature. Note that for $v \in H_{\text{iso}}^2(S; \mathbb{R}^3)$, thanks to the isometry constraint $(\nabla' v)^\top \nabla' v = I_{2 \times 2}$, we have

$$\mathbb{I}_v(x') \in \mathcal{G} := \left\{ G \in \mathbb{R}_{\text{sym}}^{2 \times 2} : \det G = 0 \right\} \qquad \text{for a.e. } x' \in S.$$

Thus, under condition (52), minimization of the non-convex integral functional $\mathcal{I}_{\text{hom}}^{\gamma}$ reduces to the following *algebraic minimization problem*:

$$\mathcal{S} := \arg\min_{G \in \mathcal{G}} Q_{\text{hom}}^{\gamma}(G - B_{\text{eff}}^{\gamma}). \tag{53}$$

More precisely, we recall the following result from Schmidt (2007a):

Lemma 5.1 (Schmidt 2007a, Theorem 3.2) *In the situation of* Theorem 2.8 *suppose that Q_{hom}^{γ} and B_{eff}^{γ} are independent of $x' \in S$. Then $v \in H_{\text{iso}}^2(S; \mathbb{R}^3)$ is a minimizer of $\mathcal{I}_{\text{hom}}^{\gamma}$, if and only if there exists G solving (53) such that $\mathbb{I}_v = G$ almost everywhere in S, where $\mathbb{I}_v$ denotes the second fundamental form of v.*

In view of this, we study the dependence of the solution set $\mathcal{S}$ on the effective coefficients of Q_{hom}^{γ} and B_{eff}^{γ}. Having the parametrized laminate of Lemma 4.5 in mind, we focus on the orthotropic case of Definition 4.1. In Sect. 5.1 we present a classification result that describes $\mathcal{S}$ for a general orthotropic quadratic form and a general effective, diagonal prestrain. In Sect. 5.2 we then explore the microstructure–shape relation by analyzing the dependence of $\mathcal{S}$ on the parameters of the parametrized laminate material of Sect. 4.2.

Remark 5.2 (*Cylindrical surfaces and their parametrization by angle and curvature*) The geometry of a cylindrical surface can be conveniently parametrized by an angle and a scalar curvature. We shall use this parametrization in the characterization and visualization of the set $\mathcal{S}$ in the upcoming section. Let us first fix our terminology: Recall that $v \in H_{\text{iso}}^2(S; \mathbb{R}^3)$ is called *cylindrical* if $\mathbb{I}_v$ is constant, i.e., if there exists $G \in \mathcal{G}$ such that $\mathbb{I}_v = G$ a.e. in S. We note that for any $G \in \mathcal{G}$ there exists a

deformation $v_G \in H^2_{\mathrm{iso}}(S; \mathbb{R}^3)$ with $\mathbb{I}_{v_G} = G$. To see this, first note that any $G \in \mathcal{G}$ can be represented as

$$G = \kappa \xi \otimes \xi \qquad \text{for some unique } \kappa \in \mathbb{R} \text{ and a vector } \xi \in \mathbb{R}^2 \text{ with } |\xi| = 1. \tag{54}$$

In the case $G \neq 0$, the line spanned by ξ is uniquely determined by G.

A direct calculation shows that the map $v_G : S \to \mathbb{R}^3$,

$$v_G(x') := \left(\int_0^{x' \cdot \xi} \cos(-\kappa s) \, \mathrm{d}s, \ x' \cdot \xi^\perp, \ \int_0^{x' \cdot \xi} \sin(-\kappa s) \, \mathrm{d}s \right)^\top, \qquad \xi^\perp := \begin{pmatrix} 0 & -1 \\ 1 & 0 \end{pmatrix} \xi,$$

defines a bending deformation with its second fundamental form satisfying $\mathbb{I}_{v_G} = G$.

In fact, by the rigidity theorem for surfaces (see, e.g., (Ciarlet and Larsonneur 2002, Theorem 3)), any parametrized surface $v \in H^2_{\mathrm{iso}}(S; \mathbb{R}^3)$ with $\mathbb{I}_v = G$ a.e. in S equals v_G modulo a superposition with a Euclidean transformation of $\mathbb{R}^3$.

Geometrically, v_G parametrizes a cylindrical surface, whose (nonzero) principal curvature is given by κ and with associated principal direction (expressed in local coordinates) $\pm \xi$, see Fig. 9.

For $\kappa < 0$ the surface is bent in the direction of the surface normal $\partial_1 v \wedge \partial_2 v$.

For visualizations it is convenient to parametrize the set $\mathcal{G} \setminus \{0\}$ by associating to each $G = \kappa \xi \otimes \xi \in \mathcal{G}$ the curvature κ and the angle

$$\alpha(G) := \begin{cases} \arctan \dfrac{\xi \cdot e_2}{\xi \cdot e_1} & \text{if } \xi \cdot e_1 \neq 0, \\ \dfrac{\pi}{2} & \text{else.} \end{cases} \tag{55}$$
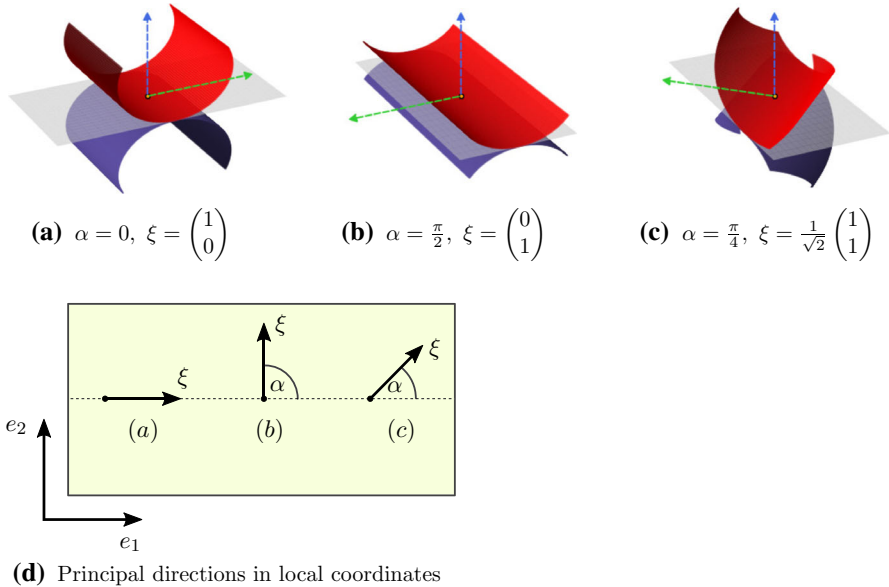
Note that the expression on the right-hand side is the same for ξ and $-\xi$ and thus $\alpha(G)$ is well-defined. Geometrically, $\alpha(G)$ is the angle required to rotate the line spanned by e_1 to the line spanned by ξ (in counterclockwise direction). The map $\mathcal{G} \setminus \{0\} \mapsto (\alpha, \kappa) \in (-\frac{\pi}{2}, \frac{\pi}{2}] \times \mathbb{R} \setminus \{0\}$ is a bijection. It is even a homeomorphism if we identify the end points of $(-\frac{\pi}{2}, \frac{\pi}{2}]$.

5.1 Classification of $\mathcal{S}$ in the Orthotropic Case

We analyze the algebraic minimization problem (53) in the case of an orthotropic quadratic form Q^γ_{hom} and a diagonal prestrain B^γ_{eff}. For the upcoming discussion it is not important that Q^γ_{hom} and B^γ_{eff} are defined via the homogenization formulas of Sect. 2.3. We rather consider a generic quadratic form and prestrain, which we denote by Q and B to simplify the notation.

More precisely, with G_1, G_2, G_3 the orthonormal basis of $\mathbb{R}^{2 \times 2}_{\mathrm{sym}}$ introduced in (38), let $Q : \mathbb{R}^{2 \times 2}_{\mathrm{sym}} \to \mathbb{R}$ be a positive definite quadratic form, $B \in \mathbb{R}^{2 \times 2}_{\mathrm{sym}}$, and assume that

$$Q \text{ is orthotropic in the sense of Definition 4.1 with coefficients } q_1, q_2, q_3, q_{12}, \tag{56a}$$

(a) $\alpha = 0$, $\xi = \begin{pmatrix} 1 \\ 0 \end{pmatrix}$ **(b)** $\alpha = \frac{\pi}{2}$, $\xi = \begin{pmatrix} 0 \\ 1 \end{pmatrix}$ **(c)** $\alpha = \frac{\pi}{4}$, $\xi = \frac{1}{\sqrt{2}} \begin{pmatrix} 1 \\ 1 \end{pmatrix}$

(d) Principal directions in local coordinates

Fig. 9 Deformations with constant second fundamental form $\mathrm{II} = \kappa \xi \otimes \xi$ and $|\kappa| = 2$. Blue color corresponds to positive values of the curvature κ and red to negative values of κ. The green vector shows $(\nabla u)\xi$ while the blue vector represents the surface normal $\partial_1 v \wedge \partial_2 v$

and

$$B \text{ is diagonal and invertible, i.e., } \det B \neq 0. \tag{56b}$$

We remark that in view of (56) the positive definiteness of Q is equivalent to

$$q_1, q_2, q_3 > 0 \quad \text{and} \quad -2\sqrt{q_1 q_2} < q_{12} < 2\sqrt{q_1 q_2}. \tag{57}$$

Our goal is to determine the set of minimizers

$$\mathcal{S}_{Q,B} := \arg\min_{G \in \mathcal{G}} Q(G - B).$$

This is a quadratic minimization problem on the non-convex set $\mathcal{G}$, and thus a rich behavior can be expected. We first note that by the positive definiteness of Q and in view of the assumption $\det B \neq 0$ we have $\mathcal{S}_{Q,B} \neq \emptyset$ and $0 \notin \mathcal{S}_{Q,B}$. Thus, minimizers $G \in \mathcal{S}_{Q,B}$ exist and correspond to non-flat, cylindrical surfaces.

Axial minimizers. An important role for the upcoming discussion is played by $G \in \mathcal{G}$ with angle $\alpha(G) \in \{0, \frac{\pi}{2}\}$. Such G correspond to a cylindrical surface with a principal direction that in local coordinates is parallel to one of the coordinate axes of $\mathbb{R}^2$ (Fig. 9). We call such matrices *axial*, and note that

$$G \in \mathcal{G} \setminus \{0\} \text{ is axial} \quad \Longleftrightarrow \quad G \in \text{span}\{G_1\} \cup \text{span}\{G_2\}.$$

Since Q is positive definite, the restrictions of $G \mapsto Q(G - B)$ to $\text{span}\{G_1\}$ or $\text{span}\{G_2\}$ are strictly convex. They thus admit unique minimizers, which can be com-

puted by elementary calculations. We obtain

$$\left\{ G \in \mathcal{S}_{Q,B} : G \text{ is axial} \right\} \subseteq \left\{ \frac{2q_1 \widehat{B}_1 + q_{12}\widehat{B}_2}{2q_1} G_1, \ \frac{2q_{12}\widehat{B}_1 + q_2 \widehat{B}_2}{2q_2} G_2 \right\}, \quad (58)$$

where $\widehat{B}_1$, $\widehat{B}_2$ denote the coefficients of B in the sense of (38).

As we shall see, for most choices of Q and B, every $G \in \mathcal{S}_{Q,B}$ is axial. In this case, $\mathcal{S}_{Q,B}$ consists of at most two (global) minimizers, and to determine $\mathcal{S}_{Q,B}$ we only need to compare the energy values associated with the elements in the set on the right-hand side in (58). However, we shall see that for certain choices of Q and B, the set $\mathcal{S}_{Q,B}$ contains two or even a one-parameter family of infinitely many non-axial minimizers. In the following, we develop an algorithm to compute the set $\mathcal{S}_{Q,B}$ in this case.

Mirror symmetry of the solution set. Consider the bijective transformation

$$T : \mathcal{G} \to \mathcal{G}, \quad \begin{pmatrix} a_1 & a_3 \\ a_3 & a_2 \end{pmatrix} \mapsto \begin{pmatrix} a_1 & -a_3 \\ -a_3 & a_2 \end{pmatrix}.$$

Then by orthotropicity of Q and diagonality of B we have $Q(G - B) = Q(TG - B)$, and thus

$$G \in \mathcal{S}_{Q,B} \quad \Longleftrightarrow \quad TG \in \mathcal{S}_{Q,B}. \quad (59)$$

Geometrically, the transformation T is a reflection in the following sense: If G describes a cylindrical surface with curvature κ and angle $\alpha \in (-\frac{\pi}{2}, \frac{\pi}{2})$, then TG corresponds to a cylindrical surface with the same curvature κ but angle $-\alpha$. From (59) we conclude that

$$\mathcal{S}_{Q,B} = \left\{ G, TG : G \in \mathcal{S}_{Q,B}^+ \right\},$$
$$\text{where } \mathcal{S}_{Q,B}^+ := \arg\min_{G \in \mathcal{G}^+} Q(G - B), \quad \mathcal{G}^+ := \left\{ G \in \mathcal{G} \text{ with } G : G_3 \geq 0 \right\}. \quad (60)$$

Moreover, we note that for all $G \in \mathcal{G} \setminus \{0\}$ we have $G = TG$, if and only if G is axial.

Classification of minimizers. The set $\mathcal{G}^+$ can be conveniently parametrized by the nonlinear, bijective transformation

$$\Phi : \mathcal{G}_{\mathbb{R}^2}^+ \to \mathcal{G}^+, \quad \Phi(a_1, a_2) := a_1 G_1 + a_2 G_2 + \sqrt{2a_1 a_2} G_3,$$
$$\mathcal{G}_{\mathbb{R}^2}^+ := \left\{ a = (a_1, a_2) \in \mathbb{R}^2 : a_1 a_2 \geq 0 \right\}.$$

We remark that the boundary $\partial \mathcal{G}_{\mathbb{R}^2}^+$ corresponds to axial $G \in \mathcal{G}^+$, i.e., $\Phi(\partial \mathcal{G}_{\mathbb{R}^2}^+) = \{G \in \mathcal{G}^+ : G \text{ is axial}\}$. In order to express $\mathcal{G}^+ \ni G \mapsto Q(G-B)$ in these coordinates, we introduce the quadratic function

$$\mathcal{E}_{Q,B} : \mathbb{R}^2 \to \mathbb{R}, \quad \mathcal{E}_{Q,B}(a) := \frac{1}{2} a \cdot Ha - 2a \cdot Ab,$$

where

$$H := \begin{pmatrix} 2q_1 & q_{12} + 2q_3 \\ q_{12} + 2q_3 & 2q_2 \end{pmatrix}, \qquad A := \begin{pmatrix} q_1 & \frac{q_{12}}{2} \\ \frac{q_{12}}{2} & q_2 \end{pmatrix}, \qquad b := (\widehat{B}_1, \widehat{B}_2)^\top. \quad (61)$$

One can easily check that for all $a \in \mathcal{G}_{\mathbb{R}^2}^+$ we have $\mathcal{E}_{Q,B}(a) = Q(\Phi(a) - B) + c$ for a constant c that is independent of a. We thus conclude that

$$\mathcal{S}_{Q,B}^+ = \Phi\left(\arg\min_{a \in \mathcal{G}_{\mathbb{R}^2}^+} \mathcal{E}_{Q,B}(a) \right). \quad (62)$$

The problem on the right-hand side is a quadratic minimization problem subject to the nonlinear constraint $a_1 a_2 \geq 0$. Since $q_1, q_2 > 0$, the quadratic part of $\mathcal{E}_{Q,B}$ is elliptic, parabolic, or hyperbolic, if and only if $\det H > 0$, $\det H = 0$, or $\det H < 0$, respectively. In the case $\det H > 0$ the minimizer of $\mathcal{E}_{Q,B}$ is unique and given by

$$g_* := 2H^{-1}Ab. \quad (63)$$

We can always compute g_* in closed form using Cramer's rule.

We obtain the following classification of the set of minimizers:

Lemma 5.3 (Trichotomy of minimizers) *Let $Q : \mathbb{R}_{\text{sym}}^{2\times 2} \to \mathbb{R}$ be a positive definite quadratic form that is orthotropic in the sense of* Definition 4.1. *Let further $B \in \mathbb{R}^{2\times 2}$ be diagonal with $\det B \neq 0$. Then exactly one of the following three cases has to hold:*

(a) (Axial minimizers). All minimizers $G \in \mathcal{S}_{Q,B}$ are axial. Furthermore, $\mathcal{S}_{Q,B}$ is characterized as follows:

$$\emptyset \neq \mathcal{S}_{Q,B} \subseteq \left\{ \frac{2q_1 \widehat{B}_1 + q_{12} \widehat{B}_2}{2q_1} G_1, \ \frac{2q_{12} \widehat{B}_1 + q_2 \widehat{B}_2}{2q_2} G_2 \right\}, \quad (64)$$

and equality holds if and only if $\frac{(\widehat{B}_2)^2}{q_1} = \frac{(\widehat{B}_1)^2}{q_2}$.

(b) (Two non-axial minimizers). We have $\det H > 0$ and g_* defined in (63) is an interior point of $\mathcal{G}_{\mathbb{R}^2}^+$. Furthermore, $\mathcal{S}_{Q,B}$ is characterized as follows:
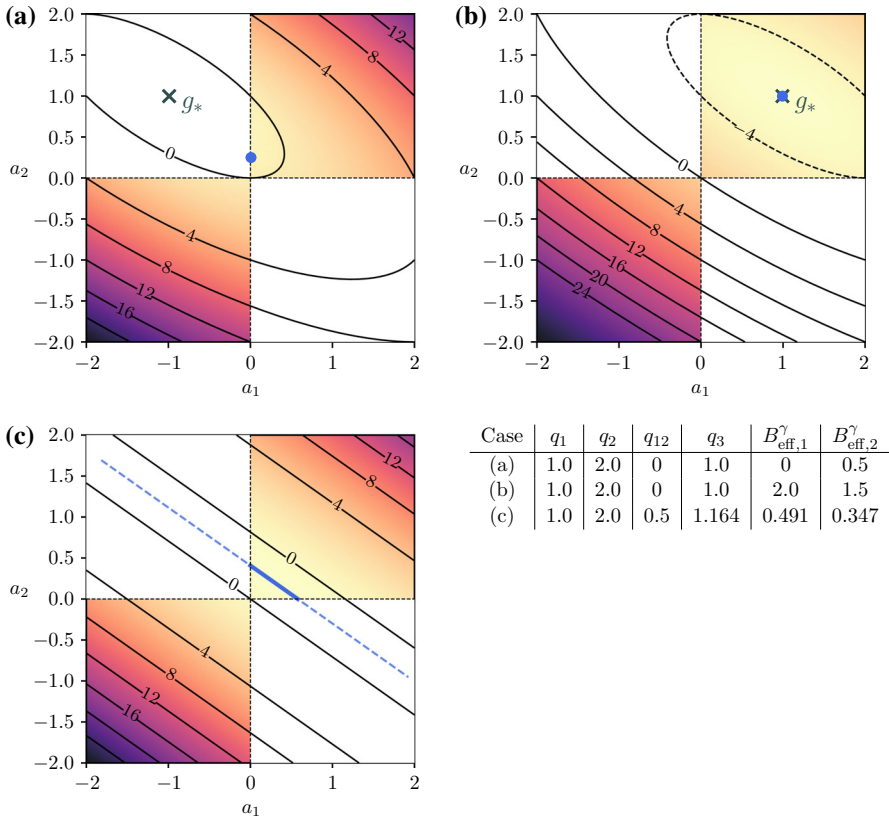
$$\mathcal{S}_{Q,B} = \{G, TG\}, \qquad G := \Phi(g_*).$$

(c) (One-parameter family of minimizers). We have $\det H = 0$ and $Ab \in$ range H. Furthermore, $\mathcal{S}_{Q,B}$ is characterized as follows:

$$\mathcal{S}_{Q,B} = \left\{ G, TG \ : \ G = \Phi(a) \text{ for all } a \in \mathcal{G}_{\mathbb{R}^2}^+ \text{ s.t. } a \cdot q_* = s_* \right\},$$

where

$$q_* := \frac{1}{\sqrt{(q_{12} + 2q_3)^2 + 4q_2^2}} \begin{pmatrix} q_{12} + 2q_3 \\ 2q_2 \end{pmatrix} \quad \text{and} \quad s_* := \frac{q_* \cdot Ab}{q_1 + q_2}. \quad (65)$$

Case	q_1	q_2	q_{12}	q_3	$B_{\mathrm{eff},1}^{\gamma}$	$B_{\mathrm{eff},2}^{\gamma}$
(a)	1.0	2.0	0	1.0	0	0.5
(b)	1.0	2.0	0	1.0	2.0	1.5
(c)	1.0	2.0	0.5	1.164	0.491	0.347

Fig. 10 Visualization of $\mathcal{G}_{\mathbb{R}^2}^{+}$ and the level lines of $\mathcal{E}_{Q,B}$ with each subfigure (**a**–**c**) corresponding to one Case of Lemma 5.3. The set of minimizers of $\mathcal{E}_{Q,B}|_{\mathcal{G}_{\mathbb{R}^2}^{+}}$ is highlighted in blue. The table contains the effective quantities rounded to 3 decimal places

(See Sect. 7.7 for the proof.)

In Fig. 10 we illustrate the three Case of Lemma 5.3 by visualizing the level lines of $\mathcal{E}_{Q,B}$ and its minimizers in $\mathcal{G}_{\mathbb{R}^2}^{+}$ for different choices of the coefficients.

Remark 5.4 (*Qualitative properties of $\mathcal{S}_{Q,B}$*)

(a) (*Sufficient and necessary conditions*). A sufficient condition for the axiality of minimizers is $\det H = 4q_1 q_2 - (q_{12} + 2q_3)^2 < 0$, which is a condition only depending on Q. Likewise, a necessary condition for two non-axial minimizers is $\det H = 4q_1 q_2 - (q_{12} + 2q_3)^2 > 0$.

(b) (*Stability with respect to perturbations of Q and B*). In contrast to the case of a single axial minimizer and the case of Lemma 5.3 (b), the condition in Lemma 5.3 (c) is very sensitive with respect to perturbations of Q and B. In applications, we shall evaluate Q and B numerically and thus case (c) can typically be neglected. The same holds for the case of two global axial minimizers.

(c) *(One-parameter family).* Figure 11 visualizes the one-parameter family $\mathcal{S}_{Q,B}$ in the case of Lemma 5.3 (c). In Fig. 12 that very same one-parameter family is visualized as a subset of $\mathcal{G}^+$ and of $\mathcal{G}^+_{\mathbb{R}^2}$. One can show that angles $\alpha(G)$ associated with $G \in \mathcal{S}_{Q,B}$ span the whole interval $(-\pi/2, \pi/2]$. Furthermore, one can show that $\mathcal{S}_{Q,B}$ is a one-dimensional compact manifold.

(d) *(Continuous dependence).* Lemma 5.3 reveals that minimizers may not depend continuously on the prestrain B. For instance, even in the stable case (a), the global minimizer may jump from an axial minimizer with angle $\alpha = 0$ to one with angle $\alpha = \frac{\pi}{2}$. On the other hand, in case (b), the two global minimizers continuously depend on $b \in \frac{1}{2} A^{-1} H(\mathcal{G}^+_{\mathbb{R}^2} \setminus \partial \mathcal{G}^+_{\mathbb{R}^2})$.

(e) *(Local minimizers).* The same techniques can be used to handle local minimizers. In the case of Lemma 5.3 (a) both axial matrices on the right-hand side of (64) turn out to be local minimizers in the case $\det H > 0$. In the case of Lemma 5.3 (b) the two global minimizers are also the only local minimizers, and in the case of Lemma 5.3 (c), the one-parameter families

Remark 5.5 (*The case $q_{12} = 0$ and the isotropic case*) In the case $q_{12} = 0$ we may simplify the statement of Lemma 5.3 further. In particular, A is diagonal and the following holds:

(a) In the case of Lemma 5.3 (a) we have

$$\mathcal{S}_{Q,B} \subseteq \{\widehat{B}_1 G_1, \widehat{B}_2 G_2\}$$

(b) Formula (63) for g_* simplifies to

$$g_* = \left(\frac{q_1 q_2 \widehat{B}_1 - q_3 q_2 \widehat{B}_2}{q_1 q_2 - q_3^2}, \frac{q_1 q_2 \widehat{B}_2 - q_3 q_1 \widehat{B}_1}{q_1 q_2 - q_3^2} \right).$$

Furthermore, we note that if Q is isotropic, i.e., $q_1 = q_2 = q_3$ and $q_{12} = 0$, and B is a multiple of the identity, we are always in the case of Lemma 5.3 (c) and $\mathcal{S}$ consists of all matrices of the form $G = \sqrt{\det B}(\xi \otimes \xi)$ with $\xi \in \mathbb{R}^2$, $|\xi| = 1$.
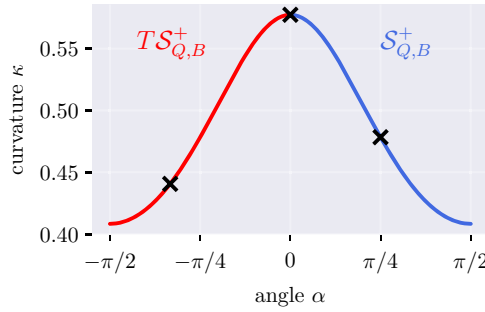
5.2 Microstructure–Shape Relation for the Parametrized Laminate

We continue our study of the parametrized laminate considered in Sect. 4.2 (shown in Fig. 4), and now focus on the microstructure–shape relation. We thus consider the algebraic minimization problem (53) with Q^γ_{hom} and B^γ_{eff} defined as in Lemma 4.5, and study the dependence of the set of minimizers $\mathcal{S}$ on the parameters listed in Table 1. Throughout this section we set $\mu_1 = \rho_1 = 1$; the set $\mathcal{S}$ for other values can then be easily obtained with the help of (50).

Visualization of $\mathcal{S}$. Before we start our exploration, we briefly comment on how we visualize the set $\mathcal{S}$. As we shall see, except for the special case of a homogeneous composite or for parameters $(\theta, \theta_\mu, \theta_\rho)$ in a small exceptional set, $\mathcal{S}$ consists of

$$\text{one unique axial minimizer} \quad \text{or} \quad \text{two non-axial minimizers.} \tag{66}$$

(a) Plot of $\mathcal{S}_{Q,B}$ in (α, κ)-coordinates.

(b) $\alpha = -\frac{\pi}{3}, \kappa \approx 0.44$ **(c)** $\alpha = 0, \kappa \approx 0.58$ **(d)** $\alpha = \frac{\pi}{4}, \kappa \approx 0.48$
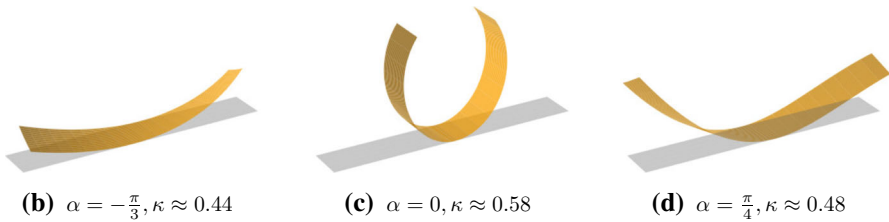
Fig. 11 Visualization of the one-parameter family of minimizers $\mathcal{S}_{Q,B}$ in the case of Lemma 5.3 (c) with parameters $q_1 = 1, q_2 = 2, q_{12} = 1/2$ and $q_3 = \frac{1}{2}(\sqrt{4q_1q_2} - q_{12})$. Furthermore, we chose $b = A^{-1}q_*$ in order to enforce the condition of Lemma 5.3 (c). Subfigures **b**–**d** show the deformations corresponding to the points on $\mathcal{S}_{Q,B}$ marked in Subfigure **a**
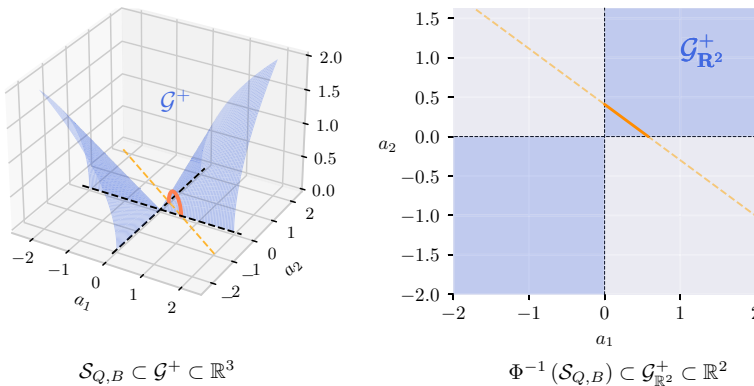

$\mathcal{S}_{Q,B} \subset \mathcal{G}^+ \subset \mathbb{R}^3$ $\Phi^{-1}(\mathcal{S}_{Q,B}) \subset \mathcal{G}^+_{\mathbb{R}^2} \subset \mathbb{R}^2$

Fig. 12 The one-parameter family $\mathcal{S}_{Q,B}$ (orange) of Fig. 11 as a subset of $\mathcal{G}^+$ and of $\mathcal{G}^+_{\mathbb{R}^2}$

Hence, in view of (59) there exists a unique $G_* \in \mathcal{G}^+$ such that $\mathcal{S} = \{G_*, TG_*\}$; note that $G_* = TG_*$ if and only if G_* is axial. This allows to visualize $\mathcal{S}$ by visualizing G_*. We use the angle–curvature parametrization introduced in Remark 5.2, i.e., we shall plot the angle $\alpha(G_*)$ and the curvature $\kappa(G_*)$ as functions of the parameters under consideration. In fact, the exceptional set of parameters $(\theta_\rho, \theta_\mu, \theta)$ that violate condition (66) are precisely those that lead to minimizers of Case (c) of Lemma 5.3.

In view of Remark 5.4, these exceptional parameters belong to a set of zero Lebesgue measure and thus can be neglected in the following presentation.

Remark 5.6 (*The homogeneous case*: $\theta \in \{0, 1\}$ or $\theta_\mu = 1$) When $\theta \in \{0, 1\}$ or $\theta_\mu = 1$, Condition (66) is not satisfied, and thus $\mathcal{S}$ cannot be visualized in terms of the angle–curvature parametrization.

In the case $\theta \in \{0, 1\}$, both the composite and the prestrain are homogeneous. In the case $\theta_\mu = 1$ only the composite is homogeneous. In both cases we conclude that

$$q_1 = q_2 = q_3, \quad \text{and} \quad \widehat{B}^\gamma_{\text{eff},1} = \widehat{B}^\gamma_{\text{eff},2},$$

and we are thus in the isotropic case of Remark 5.5. In particular, we deduce that $\mathcal{S} = \{\kappa \xi \otimes \xi : \xi \in \mathbb{R}^2, \ |\xi| = 1\}$ with

$$\kappa := \begin{cases} \frac{3}{2}\rho_1 & \text{if } \theta = 0, \\ \frac{3}{2}\theta_\rho \rho_1 & \text{if } \theta = 1, \\ \frac{3}{2}\rho_1 \left(1 - \theta(1 + \theta_\rho)\right) & \text{if } \theta_\mu = 1. \end{cases}$$

In the following discussion, we exclude the homogeneous case and focus on the dependence of $\mathcal{S}$ on parameters $(\theta_\rho, \theta_\mu, \theta)$ in the set

$$\mathcal{P} := \left\{ \begin{pmatrix} \theta \\ \theta_\mu \\ \theta_\rho \end{pmatrix} : \theta_\mu > 1, \ \theta_\mu \neq 1 \text{ and } \theta \in (0, 1) \right\} \subset \mathbb{R}^3. \tag{67}$$

We note that parameters $(\theta, \theta_\mu, \theta_\rho)$ with $\theta_\mu \in (0, 1)$ are also covered by the following discussion: In view of the symmetry of the composite, the associated set $\mathcal{S}$ is obtained by considering the parameters $(1 - \theta, \frac{1}{\theta_\mu}, \frac{1}{\theta_\rho}) \in \mathcal{P}$.

Computation of $\mathcal{S}$. The computation of the set of minimizers $\mathcal{S}$ associated with Q^γ_{hom} and B^γ_{eff} for prescribed parameters $(\theta, \theta_\mu, \theta_\rho) \in \mathcal{P}$ uses Lemma 5.3 and the simplifications in Remark 5.5. The resulting algorithm is summarized as a flow-chart in Fig. 13. Recall that we denote by q_1, q_2, q_{12}, q_3 the coefficients of Q^γ_{hom} as in Definition 4.1, and by $\widehat{B}^\gamma_{\text{eff},1}, \widehat{B}^\gamma_{\text{eff},2}, \widehat{B}^\gamma_{\text{eff},3}$ the coefficients of B^γ_{eff} with respect to the basis in (38).

Dependence of $\mathcal{S}$ on γ and the critical value γ_*. According to Lemma 4.3, B^γ_{eff} is independent of γ, and the only coefficient of Q^γ_{hom} that depends on γ is $q_3 = q_3(\gamma)$. By (44) we have $q_1 < q_3(\gamma) < q_2$, and for $(\theta, \theta_\mu, \theta_\rho) \in \mathcal{P}$ the map, $\gamma \mapsto q_3(\gamma)$ is continuous and strictly monotonically decreasing. Thus, in view of (45), we can find a unique value $\gamma_* \in (0, \infty)$ such that

$$q_3(\gamma_*) = q_3^* := \sqrt{q_1 q_2}.$$

We call γ_* the *critical value* for the following reason: For $\gamma < \gamma_*$ we have $\det H < 0$ and we are thus in Case (a) of Lemma 5.3, which, in particular, means that all minimizers are axial. On the other hand, for $\gamma > \gamma_*$ we have $\det H > 0$, which is
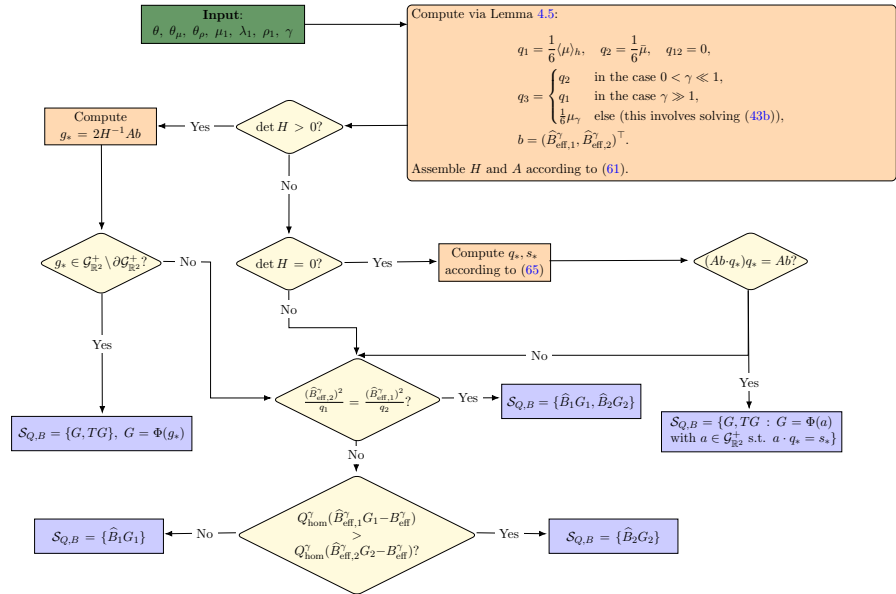
Fig. 13 The algorithm for evaluating the set of minimizers $\mathcal{S}$ of the algebraic minimization problem (53) in the case of the parametrized laminate of Lemma 4.5. Note that in the cases $0 < \gamma \ll 1$ and $\gamma \gg 1$ we use the approximation $q_3 = q_2$ and $q_3 = q_1$, respectively, see (45) for the justification

a necessary condition for the case (b). We conclude that non-axial minimizers may only emerge for $\gamma > \gamma_*$. The critical condition $\gamma = \gamma_*$ is equivalent to $\det H = 0$, and therefore necessary for the case Lemma 5.3 (c), which is the only case where a one-parameter family of minimizers may emerge.

In order to demonstrate the dependence of $\mathcal{S}$ on the relative scaling parameter γ we show in Fig. 14 the angle $\alpha(G_*)$ and the curvature $\kappa(G_*)$ as a function of γ. The three columns of Fig. 14 feature different values of the prestrain ratio θ_ρ, each resulting in qualitatively different behavior: The angle $\alpha(G_*)$ and the curvature $\kappa(G_*)$ may increase, decrease or remain constant in γ. Furthermore, Fig. 14 also includes a vertical dotted line to indicated the value of γ^*. Recall that $\gamma > \gamma^*$ is a necessary (but not sufficient) condition for the existence of non-axial minimizers, while $\gamma < \gamma^*$ is a sufficient condition for axiality of minimizers. The curvature $\kappa(G_*)$ remains constant if $\gamma < \gamma^*$. Finally, note that both the angle $\alpha(G_*)$ and the curvature $\kappa(G_*)$ appear to depend continuously on γ.

Dependence of $\mathcal{S}$ on θ, θ_μ and θ_ρ. We investigate the dependence of $\mathcal{S}$ on the parameters $(\theta, \theta_\mu, \theta_\rho) \in \mathcal{P}$ (see (67)). Since we shall consider a high number of sample points in the parameter set $\mathcal{P}$, we mostly focus on the extreme regimes $0 < \gamma \ll 1$ and $\gamma \gg 1$. In these regimes, we can use the approximations $q_3 = q_2$ for $0 < \gamma \ll 1$ and $q_3 = q_1$ for $\gamma \gg 1$ in order to avoid the high computational cost of solving (43b) numerically, which would be required to evaluate $q_3(\gamma)$ for $\gamma \in (0, \infty)$. Note that the regimes $0 < \gamma \ll 1$ and $1 \ll \gamma$ illustrate the possible range of behaviors, since the behavior for $0 < \gamma < \infty$ is a middle ground between these extreme cases. We
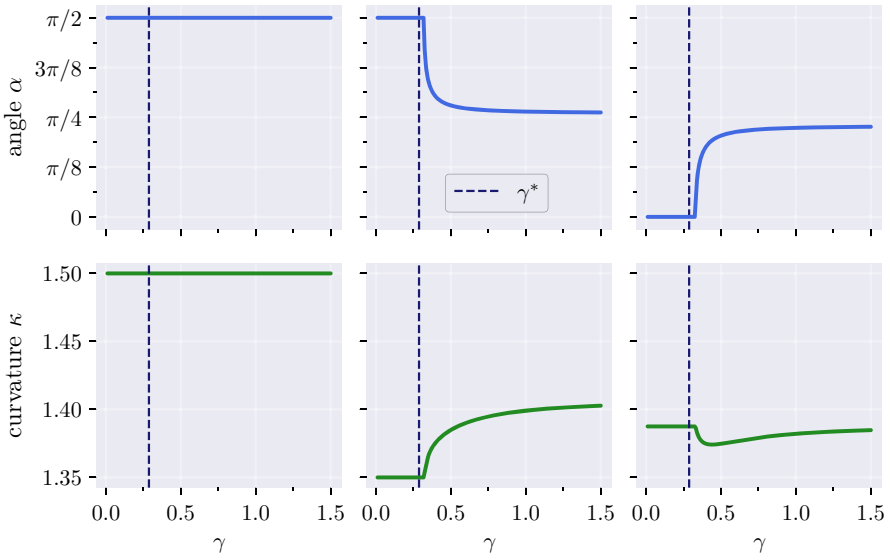
Fig. 14 Angle $\alpha(G_*)$ (top) and curvature $\kappa(G_*)$ (bottom) for different values of γ with $\theta_\mu = 2$, $\theta = \frac{1}{4}$. The three columns correspond to $\theta_\rho = -1.0$ (left), $\theta_\rho = -0.75$ (middle), and $\theta_\rho = -0.7$ (right). The dotted line shows the critical value γ_*

illustrate this at the end of this section. Figure 15 visualizes G_* in the extreme regimes $0 < \gamma \ll 1$ and $\gamma \gg 1$ for 300^3 uniformly spaced sample points in the parameter set $\mathcal{P}$. The transparent and blue regions in these plots corresponds to axial minimizers with $\alpha(G_*) = \frac{\pi}{2}$ and $\alpha(G_*) = 0$, respectively. The region with $\alpha(G_*) = \frac{\pi}{2}$ seems to consist of two connected components that are divided by a region where $\alpha(G_*)$ takes other values. We refer to that later region as the *transition region*.

We first discuss the regime $0 < \gamma \ll 1$. In that case only angles 0 and $\frac{\pi}{2}$ appear, which is in agreement with the trichotomy of minimizers, since $0 < \gamma \ll 1$ is a sufficient condition for Lemma 5.3 (a). We see that the angle has a discontinuity at the boundary of the transition region. This means that minimizers may flip from one axial state to the other when parameters close to the boundary of the transition region are perturbed. Figure 16 (top, left) shows a cut through the diagram of Fig. 15 (top, left) along the plane with $\theta_\mu = 2$. We see that the boundary of the transition is tilted (left boundary) or curved (right boundary) with respect to the θ-axis. This means that for certain values of $\theta_\rho \in (-1, -0.5) \cup (0, \infty)$ the angle $\alpha(G_*)$ can be influenced by changing the volume fraction θ. Figure 17 (top, left) visualizes the discontinuous dependence of the angle on the prestrain ratio θ_ρ for fixed parameters θ_μ and θ. The marked points correspond to the boundary of the transition region. The bottom left plots of Figs. 15, 16 and 17 visualize the curvature $\kappa(G_*)$. Figure 16 (bottom, left) suggests that the curvature is continuous as a function of θ in regions where the angle $\alpha(G_*)$ is constant, while we observe a jump in the curvature whenever the angle jumps. It would further be natural to expect that the curvature is monotone in θ_ρ, but Fig. 17 (bottom, left) shows that this is not the case: The curvature jumps upwards at the first point of discontinuity. This observation can be seen more easily in Fig. 18 (left), where
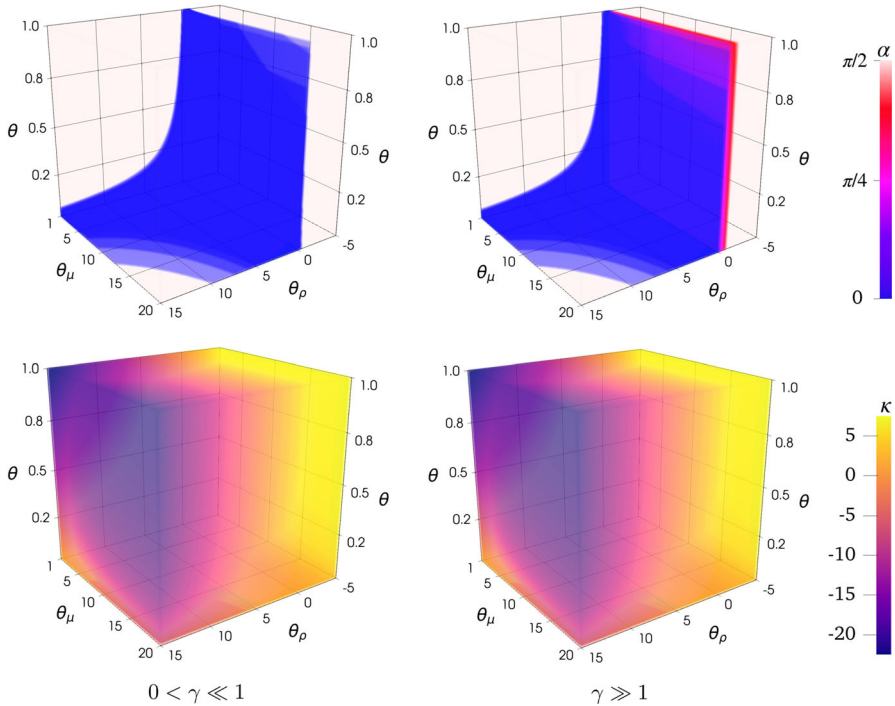
Fig. 15 The angle $\alpha(G_*)$ (top) and curvature $\kappa(G_*)$ (bottom) as a functions of θ_ρ, θ_μ and θ in the extreme regimes $0 < \gamma \ll 1$ (left) and $\gamma \gg 1$ (right). In the plots for the angle, transparent regions correspond to the angle $\frac{\pi}{2}$

we consider the larger value $\theta_\mu = 10$. Next, we discuss the regime $\gamma \gg 1$. The phase diagram in Fig. 15 (top, right) shows that in that regime the transition region features non-axial minimizers. Again, this is in agreement with the trichotomy of minimizers, since $\gamma \gg 1$ is a necessary condition for Case (b) of Lemma 5.3. The cut shown in Fig. 16 (top, right) indicates that the transition on the left boundary of the transition region is continuous, while the transition on the right boundary is not. In particular, the plot suggests that for a fixed volume fraction $\theta \in (0, 1)$ we can obtain any angle in $[0, \frac{\pi}{2}]$ by choosing a suitable $\theta_\rho \in [-1, -0.5]$. This is even more visible in Fig. 17 (top, right), which shows the θ_ρ-dependence of the angle. The marked points ① and ③ correspond to the boundary of the transition region. Furthermore, we observe a monotone behavior for $\theta_\rho \in [-1, -0.5]$. Finally, a close look at the isolines of Fig. 16 (top, right) shows that for $\theta_\rho \in [-1, -0.5]$ the angle is monotone in the volume fraction θ.

Figure 15 (bottom, right) visualizes the curvature in the regime $\gamma \gg 1$. The phase diagram looks similar to the one in the regime $0 < \gamma \ll 1$. However, the two are not identical, as becomes apparent by comparing the plots in Fig. 17 (bottom). The bottom right plots of Figs. 15, 16 and 17 suggest that also in the regime $\gamma \gg 1$, the curvature is continuous at points where the angle is continuous, and jumps if and only if the angle jumps. In particular, Fig. 17 (bottom, right) shows that the curvature as a function of
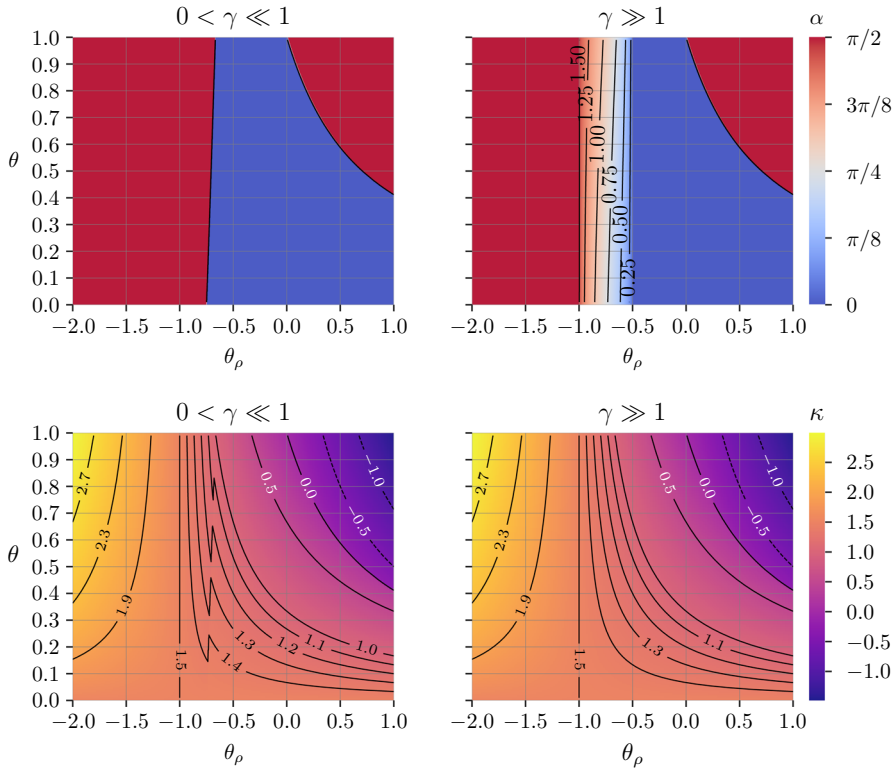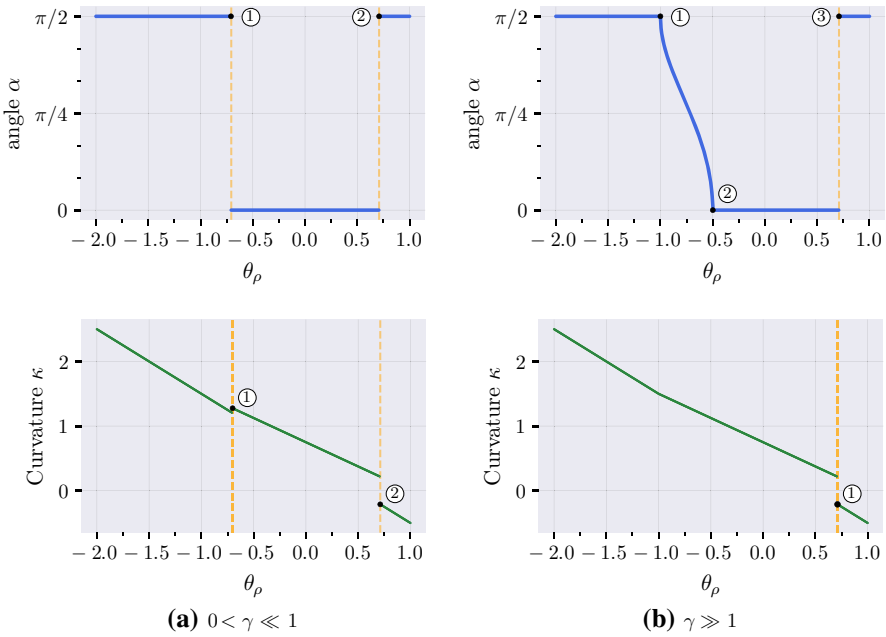
Fig. 16 The angle $\alpha(G_*)$ (top) and curvature $\kappa(G_*)$ (bottom) in the case $0 < \gamma \ll 1$ (left) and $\gamma \gg 1$ (right) for points in the parameter set $\mathcal{P}$, with $\theta_\mu = 2$

θ_ρ has only a single discontinuity at the marked point ①, which corresponds to the right boundary of the transition region. In contrast to the regime $0 < \gamma \ll 1$, we observe in Fig. 17 (bottom, right) a monotone dependence on θ_ρ.

So far we have only analyzed the extreme regimes $0 < \gamma \ll 1$ and $1 \ll \gamma$. We now briefly consider the intermediate regime $0 < \gamma < \infty$. We show these plots in Fig. 19. We note that the region of θ_ρ for which non-axial minimizers are observed is largest at $\gamma = \infty$. This region gets progressively smaller as γ tends to 0, and finally for values $\gamma < \gamma^*$ it disappears and we observe a discontinuous transition between two axial minimizers. If $\theta_\mu = 10$, this region appears to lie always between -1 and 0.

Discussion of the θ_ρ-dependence. In the case $\theta_\rho = 0$ the prestrain is only active in the top layer of the two-layer microstructure of Fig. 4. More precisely, the "fibres" in the top layer want to expand isotropically by a factor $\rho_1 = 1$ to gain equilibrium. In view of this we expect that the plate bends downwards either in parallel or orthogonal to the fibres. This corresponds to $\kappa(G_*) > 0$ and $\alpha(G_*) \in \{0, \frac{\pi}{2}\}$. Indeed, Figs. 16 and 19 show that this is indeed the case: Independently of γ, for $\theta_\mu \in \{2, 10\}$ and all $\theta \in (0, 1)$, we have $\alpha(G_*) = 0$ and $\kappa(G_*) > 0$. This means that the plate bends in a direction orthogonal to the fibres. For $\theta_\rho \neq 0$ the prestrain is active in both layers. For $\theta_\rho < 0$ the prestrain in the top and bottom layer have the opposite sign,

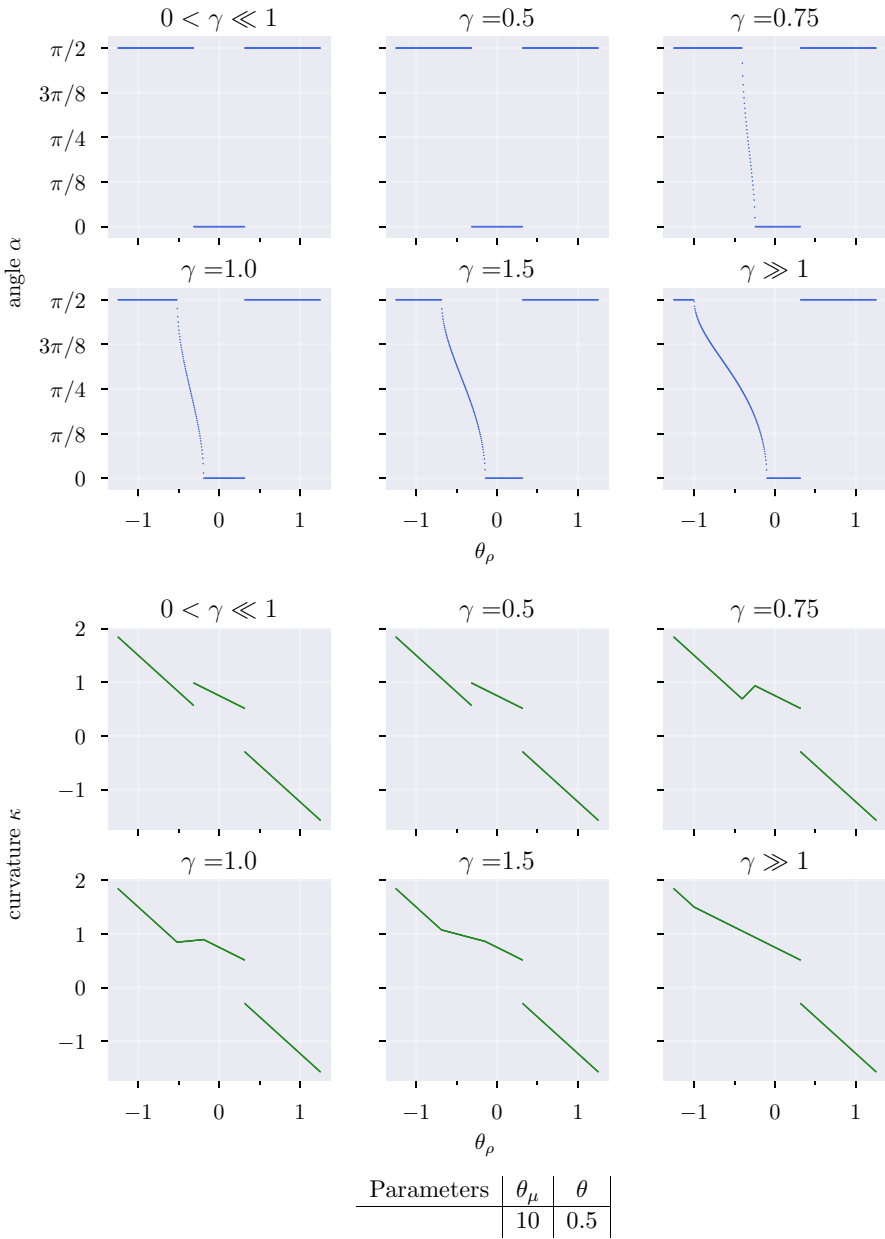| Parameters	θ_μ	θ
	2	0.5

Fig. 17 Angle $\alpha(G_*)$ (top) and curvature $\kappa(G_*)$ (bottom) as a function of the prestrain ratio θ_ρ with $0 < \gamma \ll 1$ (left) and $\gamma \gg 1$ (right)
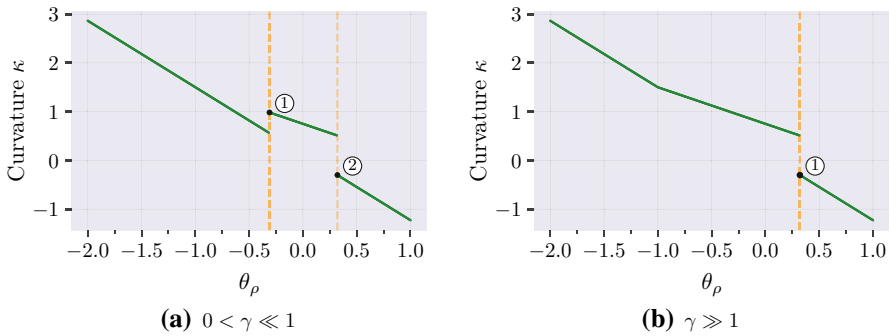
Parameters	θ_μ	θ
	10	$\frac{1}{2}$

Fig. 18 Curvature $\kappa(G_*)$ as a function of the prestrain ratio θ_ρ

Fig. 19 Angle $\alpha(G_*)$ (blue) and curvature $\kappa(G_*)$ (green) as a function of the prestrain ratio θ_ρ for different values of γ

and thus "push" into the same direction. Hence, one could expect that the curvature monotonically increases when θ_ρ decreases. But in the regime $0 < \gamma \ll 1$ we observe a downwards jump of the curvature, see Fig. 17 (bottom, left). In the case $\theta_\rho > 0$ the sign of the prestrain in the two layers is the same, and thus they are competing with regard to energy minimization. We expect that for θ_ρ sufficiently large the bending induced by the fibres in the bottom layer dominate the behavior, which would mean that the plate bends "upwards". Indeed, as shown by Fig. 16, for θ_ρ above the threshold (which decreases with the volume fraction θ), the curvature changes its sign from negative to positive. Surprisingly, at that point the angle jumps from $\alpha(G_*) = 0$ to $\alpha(G_*) = \frac{\pi}{2}$.

Conclusion. Our analysis shows that the parametrized, prestrained laminate features a complex behavior. In particular, we make the following observations:

(a) We observe a discontinuous dependence of the set of minimizers on the parameters.
(b) We observe non-uniqueness of the global minimizers: In the regime $\gamma \gg 1$ we find parameters leading to non-axial minimizers. Those always come in pairs of the form $\{G_*, TG_*\}$. Likewise, for the special cases of Remark 5.6 we have a one-parameter family of minimizers.
(c) The mechanical system features a break of symmetry: For $\theta_\mu = 1$, which corresponds to a homogeneous material, the set of minimizers is of the form $\{\kappa(\xi \otimes \xi) : \xi \in \mathbb{R}^2, |\xi| = 1\}$ and *rotationally symmetric*, while for $\theta_\mu \neq 1$ the set of minimizers degenerates to a set with one axial or two (possibly non-axial) minimizers.
(d) The mechanical properties for $0 < \gamma \ll 1$ and $\gamma \gg 1$ are qualitatively and quantitatively different: In the former regime minimizers are always axial and G_* as a function of θ_ρ is non-monotone and has two discontinuities, while the latter regime features minimizers of arbitrary angle and G_* as a function of θ_ρ is monotone and only has one discontinuity.

6 Shape Programming

This section is devoted to the problem of shape programming: given *a target shape* that can be parametrized by a bending deformation with second fundamental form $\mathbb{I}_*$, can we construct a *simple* prestrained composite such that minimizers of the corresponding three-dimensional elastic energy approximate the target shape for $(\varepsilon, h) \to 0$? If the target shape is *cylindrical* the problem can be solved relatively easily with the help of the parametrized laminate composite studied in Sect. 5. In the general case, the problem is more complex and requires a composite whose microstructure changes with the in-plane position. We first discuss the simpler case of a cylindrical target shape in Sect. 6.1 and then turn to general target shapes in Sect. 6.2. That section culminates in Theorem 6.6 which provides our analytical answer to the problem of shape programming.

6.1 The Case of a Cylindrical Shape and the Notion of a Composite Template

In the following we consider the problem of shape programming in the special case of a cylindrical target shape, that is, we are looking for a deformation with second fundamental form $\mathrm{II}_* = \kappa_*(\xi_* \otimes \xi_*)$ a.e. in S for some $\kappa_* \in \mathbb{R}$ and a unit vector $\xi_* \in \mathbb{R}^2$. Our task is to identify a composite such that minimizers of the corresponding 3d-energy "effectively" describe a surface that coincides with the target shape. Here, "effectively" means that we consider accumulation points of sequences of minimizers of the 3d energy along the limit $(\varepsilon, h) \to 0$. As we explain next, for the cylindrical shapes the problem of shape programming can solved explicitly with the help of the parametrized laminate considered in Lemma 4.5. Specifically, let W_1, W_2 be two isotropic stored energy functions satisfying (W1) – (W4) with Lamé-parameters $\mu_1 = 1$, $\mu_2 = 2$, and $\lambda_1 = \lambda_2 = 0$. We consider a $\Lambda := I_{2\times 2}$-periodic laminate that is constant in e_2-direction and composed of the materials described by W_1 and W_2. We denote by $\theta \in [0, 1]$ the volume fraction of the material described by W_2, and we model the parametrized composite by a stored energy function $W(\theta; \cdot) : \mathbb{R} \times \mathbb{R}^{3\times 3} \to [0, +\infty]$, $(y_1, F) \mapsto W(\theta; y_1, F)$. We assume that $W(\theta; y_1, F)$ is 1-periodic in y_1, and

$$W(\theta; y_1, F) := \begin{cases} W_1(F) & \text{if } |y_1| > \frac{\theta}{2}, \\ W_2(F) & \text{else}, \end{cases} \quad \text{for } y_1 \in (-\tfrac{1}{2}, \tfrac{1}{2}], \ F \in \mathbb{R}^{3\times 3}.$$

(By periodicity, $W(\theta; \cdot)$ is uniquely defined by this identity.) Let $Q(\theta; \cdot)$ be the quadratic form associated with $W(\theta; \cdot)$. Furthermore, for $\rho_1 > 0$ fixed, consider a prestrain B that is $\Lambda = I_{2\times 2}$-periodic and admissible in the sense of Definition 2.15, and that satisfies

$$B(\theta; x_3, y) := \begin{cases} \rho_1 I_{3\times 3} & \text{if } |y_1| > \frac{\theta}{2} \text{ and } x_3 > 0, \\ 0 & \text{else}. \end{cases}$$

Then $Q(\theta; \cdot)$ and $B(\theta; \cdot)$ coincide with the parametrized laminate considered in Lemma 4.5 with parameters $\mu_1 = 1$, $\theta_\mu = 2$, and $\theta_\rho = 0$. By Lemma 4.5, the coefficients of the associated homogenized quadratic form $Q_{\text{hom}}^\gamma(\theta; \cdot)$ and effective prestrain $B_{\text{eff}}^\gamma(\theta)$ are given by

$$\widehat{B}_{\text{eff},1}^\gamma = \frac{3\rho_1}{2}(1 - \theta), \qquad \widehat{B}_{\text{eff},2}^\gamma = \frac{3\rho_1}{2}\frac{1 - \theta}{1 + \theta}, \qquad \widehat{B}_{\text{eff},3}^\gamma = 0,$$

$$q_1 = \frac{1}{3(2 - \theta)}, \qquad q_2 = \frac{1 + \theta}{6}, \qquad q_{12} = 0.$$

There is no explicit expression for $q_3(\gamma)$, but we know that $q_1 \le q_3(\gamma) \le q_2$ by (44). In the following we fix an arbitrary value for $\gamma \in (0, \infty)$. For any $\theta \in (0, 1]$ one can check (with help of a computer algebra system and only using $q_1 \le q_3(\gamma) \le q_2$) that for this specific composite Case of (a) of Lemma 5.3 always applies. In view of this, Lemma 5.3 implies that the algebraic minimization problem

$$\min_{\substack{G \in \mathbb{R}^{2\times 2} \\ \det G = 0}} Q_{\text{hom}}^\gamma\big(\theta; G - B_{\text{hom}}^\gamma(\theta)\big)$$

admits a unique axial minimizer, which is given by

$$\kappa(\theta)e_1 \otimes e_1, \qquad \text{where } \kappa(\theta) = \frac{3\rho_1}{2}(1-\theta).$$

In the following let $\mathcal{I}^{\varepsilon,h}(\theta; \cdot)$ denote the 3d-energy defined by (3) with $W_\varepsilon(x, F) := W(\theta; \frac{x_1}{\varepsilon}, F)$ and $B_{\varepsilon,h}(x) = B(\theta; \frac{x_1}{\varepsilon})$. Also, let $\mathcal{I}^\gamma_{\text{hom}}(\theta; \cdot)$ denote the bending energy defined by (7) with Q^γ_{hom} and B^γ_{eff} replaced by $Q^\gamma_{\text{hom}}(\theta; \cdot)$ and $B^\gamma_{\text{eff}}(\theta)$, respectively. Finally, let (v_h) in $H^1(\Omega; \mathbb{R}^3)$ be an arbitrary sequence of almost minimizers for $\mathcal{I}^{\varepsilon(h),h}(\theta; \cdot)$. From Theorem 2.8 we conclude that any accumulation point v of $\left(v_h - \fint_\Omega v_h\right)$ for $h \to 0$ is a bending deformation that minimizes the energy $\mathcal{I}^\gamma_{\text{hom}}(\theta; \cdot)$. Furthermore, with the help of Lemma 5.1 we conclude that $\mathrm{II}_v = \kappa(\theta)e_1 \otimes e_1$. We may summarize this observation by saying that the composite described by $W(\theta; \cdot)$ and $B(\theta; \cdot)$ *effectively programs* the target shape $\mathrm{II}_* = \kappa(\theta)(e_1 \otimes e_1)$.

Since the map $(0, 1] \ni \theta \mapsto \kappa(\theta) \in [0, \frac{3\rho_1}{2})$ is a homeomorphism, we can *program* any target shape $\mathrm{II}_* = \kappa_*(e_1 \otimes e_1)$ with κ_* in the range $[0, \frac{3\rho_1}{2})$—we just need to make an appropriate choice of $\theta_* \in (0, 1]$. Moreover, a non-positive target curvature κ_* in the range $(-\frac{3\rho_1}{2}, 0]$ can be obtained by considering the reflected prestrain $(x_3, y) \mapsto B(\theta; -x_3, y)$. For a general unit vector $\xi_* \in \mathbb{R}^2$ we can recover target shapes of the form $\mathrm{II}_* = \kappa_*(\xi_* \otimes \xi_*)$ by introducing a rotation of the laminate microstructure such that the direction of the rotated laminate is given by ξ_*; this is made precise by the transformation rule of Corollary 6.3 below. In conclusion, with help of the parametrized, two-phase laminate introduced above, we can program any cylindrical shape with curvature $\kappa_* \in \mathcal{K} := (-\frac{3\rho_1}{2}, \frac{3\rho_1}{2})$ by an appropriate choice of the volume fraction θ and the laminate direction. Since the map $\theta \mapsto \kappa(\theta)$ is bijective, we may consider directly $\kappa \in \mathcal{K}$ (instead of θ) as the design parameter of the composite.

Figure 20 illustrates some examples of cylindrical deformations of a strip obtained with a two-phase laminate. Similarly, Fig. 1 shows cylindrical shapes which were experimentally observed for 3d–printed, two–layer composite plates with a laminar microstructure consisting of prestrained fibres. As in our analysis, the orientation and the volume fraction of the fibres are design parameters. Qualitatively, our analysis reproduces the relation between these parameters and the geometry of the strip.

The two-phase laminate discussed above is an example of what we call a *composite template*:

Definition 6.1 (*Composite template*) Let $\gamma \in (0, \infty)$, $\Lambda \in \mathbb{R}^{2\times 2}$ be invertible, and let $\mathcal{K} \subset \mathbb{R}$ be an open interval. The one-parameter family $(\bar{W}(\kappa, \cdot), \bar{B}(\kappa, \cdot))_{\kappa \in \mathcal{K}}$ is called a *composite template*, if the following properties hold:

(i) For all $\kappa \in \mathcal{K}$ the energy density $\bar{W}(\kappa; \cdot) : (-\frac{1}{2}, \frac{1}{2}) \times \mathbb{R}^2 \times \mathbb{R}^{3\times 3} \to [0, +\infty]$ is a Borel function, and $\bar{W}(\kappa; x_3, y, \cdot) \in \mathcal{W}(\alpha, \beta, \rho, r)$ for a.e. $(x_3, y) \in (-\frac{1}{2}, \frac{1}{2}) \times \mathbb{R}^2$. Furthermore, $\bar{Q}(\kappa; \cdot)$ and $\bar{B}(\kappa; \cdot)$ are Λ-periodic and admissible in the sense of Definition 2.15, and

$$\fint_{\square_\Lambda} |\bar{B}(\kappa; x_3, y)|^2 \mathrm{d}(x_3, y) \leq C_B,$$

for a constant C_B that is independent of κ.
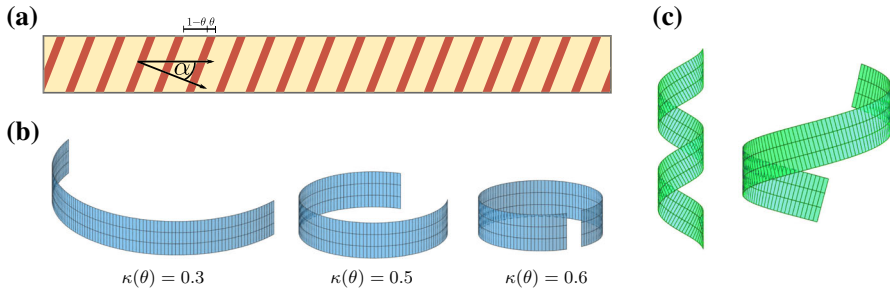
Fig. 20 Cylindrical shapes programmed via a two-phase laminate composite. **a** shows the reference configuration $S = (0, 10) \times (0, 1)$ of a composite plate. The plate is filled with the parametrized composite of Lemma 4.5 with fixed parameters $\mu_1 = 1$, $\theta_\mu = 2$, $\lambda_1 = \lambda_2 = 0$, $\theta_\rho = 0$, and $\rho_1 > 0$. The volume fraction θ and the rotation angle α are considered as design parameters. We use the same color coding as in Fig. 4a: yellow refers to the material with energy W_1 and no prestrain, while red refers to the prestrained material with energy W_2. **b** shows global minimizers of the effective energy for the case when $\alpha = 0$; from left to the right the value of θ decreases. Specifically, θ is chosen such that $\kappa(\theta) \in \{0.3, 0.5, 0.6\}$. **c** shows (from left to right) the global minimizers of the effective energy for $\alpha \in \{15°, 30°\}$ and a choice of θ with $\kappa(\theta) = 1.5$

(ii) For any sequence $\kappa_j \to \kappa$ in $\mathcal{K}$, we have

$$\bar{Q}(\kappa_j; x_3, y, G) \to \bar{Q}(\kappa; x_3, y, G) \qquad \text{for all } G \in \mathbb{R}^{3\times3} \text{ and a.e. } (x_3, y),$$
$$\bar{B}(\kappa_j; \cdot) \to \bar{B}(\kappa; \cdot) \qquad \text{strongly in } L^2(\square_\Lambda; \mathbb{R}^{3\times3}).$$

(iii) For all $\kappa \in \mathcal{K}$ the matrix $\kappa(e_1 \otimes e_1)$ is a unique global minimizer of the algebraic minimization problem

$$\min_{\substack{G \in \mathbb{R}^{2\times2} \\ \det G = 0}} \bar{Q}^\gamma_{\text{hom}}(\kappa; G - \bar{B}^\gamma_{\text{eff}}(\kappa)),$$

where $\bar{Q}^\gamma_{\text{hom}}(\kappa; \cdot)$ and $\bar{B}^\gamma_{\text{eff}}(\kappa)$ are the effective quantities associated with $\bar{Q}(\kappa; \cdot)$ and $\bar{B}(\kappa; \cdot)$ by Definitions 2.17 and 2.22, respectively.

With a composite template we can directly program shapes of the form $\mathbb{I}_* = \kappa(e_1 \otimes e_1)$ for any $\kappa \in \mathcal{K}$. As already indicated, by combining the composite template with an in-plane rotation we can also program shapes with arbitrary bending direction. This can be seen from the following two transformation results:

Lemma 6.2 (Transformation of microstructures) *Let* Λ, $T \in \mathbb{R}^{2\times2}$ *be invertible, and let* (Q, B) *be* Λ-*periodic and admissible in the sense of* Definition 2.15. *Consider the transformation*

$$\widetilde{Q}(x_3, y, \tilde{G}) := Q(x_3, T^{-1}y, \widehat{T}^\top \tilde{G} \widehat{T}),$$
$$\tilde{B}(x_3, y) := \widehat{T}^{-\top} B(x_3, T^{-1}y) \widehat{T}^{-1}, \qquad \widehat{T} := \begin{pmatrix} T & \\ & 1 \end{pmatrix}.$$

Then $(\tilde{Q}, \tilde{B})$ is $\tilde{\Lambda} := T\Lambda$-periodic and admissible. Furthermore, for all $\tilde{G} \in \mathbb{R}^{2\times2}_{\text{sym}}$ we have

$$\tilde{Q}^\gamma_{\text{hom}}(\tilde{G}) = Q^\gamma_{\text{hom}}(T^\top \tilde{G} T) \text{ and } \tilde{B}^\gamma_{\text{eff}} = T^{-\top} B^\gamma_{\text{eff}} T^{-1}.$$

Above, Q^γ_{hom}, $\tilde{Q}^\gamma_{\text{hom}}$, B^γ_{eff}, and $\tilde{B}^\gamma_{\text{eff}}$ are associated with $Q, \tilde{Q}, B,$ and $\tilde{B}$ via Definitions 2.17 and 2.22, respectively.

(See Sect. 7.8 for the proof.)

As a corollary of Lemma 6.2 we obtain the following transformation rule for minimizers of the algebraic minimization problem (53). Roughly speaking, it states that the transformation by an in-plane rotation and the passage to the effective quantities commute.

Corollary 6.3 (Rotation of microstructure of a composite template) *Let $\big(\bar{W}(\kappa; \cdot),$ $\bar{B}(\kappa; \cdot)\big)_{\kappa\in\mathcal{K}}$ be a composite template as in Definition 6.1. For $R \in SO(2)$ and $\widehat{R} := \text{diag}(R, 1)$ consider the transformation*

$$W(R, \kappa; x_3, y, F) := \bar{W}(\kappa; x_3, R^\top y, F\widehat{R}), \qquad B(R; \kappa; x_3, y) := \widehat{R}\bar{B}(\kappa; x_3, R^\top y)\widehat{R}^\top.$$

Then:

(a) For all $R \in SO(2)$ the transformed composite $\big(W(R, \kappa; \cdot), B(R, \kappa; \cdot)\big)_{\kappa\in\mathcal{K}}$ satisfies Properties (i) and (ii) of Definition 6.1.

(b) For all $R \in SO(2)$ and $\kappa \in \mathcal{K}$ we have

$$Q^\gamma_{\text{hom}}(R, \kappa; G) = \bar{Q}^\gamma_{\text{hom}}(\kappa; R^\top GR) \text{ for all } G \in \mathbb{R}^{2\times2}_{\text{sym}} \text{ and } B^\gamma_{\text{eff}}(R, \kappa) = R\bar{B}^\gamma_{\text{eff}}(\kappa)R^\top.$$

Here, $Q^\gamma_{\text{hom}}(R, \kappa; \cdot)$ and $B^\gamma_{\text{eff}}(R, \kappa)$ denote the effective quantities associated with $\big(W(R, \kappa; \cdot), B(R, \kappa; \cdot)\big)$. Likewise, $\bar{Q}^\gamma_{\text{hom}}(\kappa; \cdot)$ and $\bar{B}^\gamma_{\text{eff}}(\kappa)$ denote the effective quantities associated with $\big(\bar{W}(\kappa; \cdot), \bar{B}(\kappa; \cdot)\big)$.

(c) For all $G \in R^{2\times2}_{\text{sym}}$ the map

$$SO(2) \times \mathcal{K} \ni (R, \kappa) \mapsto \Big(Q^\gamma_{\text{hom}}(R, \kappa; G), B^\gamma_{\text{eff}}(R; \kappa)\Big)$$

is continuous.

(d) For all $R \in SO(2)$ and $\kappa \in \mathcal{K}$ the matrix $\kappa(Re_1 \otimes Re_1)$ is the unique minimizer of the algebraic minimization problem

$$\min_{\substack{G\in\mathbb{R}^{2\times2} \\ \det G=0}} Q^\gamma_{\text{hom}}\big(R, \kappa; G - B^\gamma_{\text{eff}}(R; \kappa)\big).$$

(See Sect. 7.8 for the proof.)

6.2 The General Case

We turn to the shape programming problem for surfaces parametrized by general bending deformations. More precisely, given a second fundamental form $\mathbb{II}_*$ associated

with a bending deformation $v_* \in H^2_{\text{iso}}(S; \mathbb{R}^3)$, the task is to identify a *simple* composite such that any accumulation point $v \in H^2_{\text{iso}}(S; \mathbb{R}^3)$ of a sequence of almost minimizers for the associated 3d-energy, parametrizes a surface that coincides with the target shape in the sense that $\mathrm{II}_v = \mathrm{II}_*$. The problem is trivial if we allow arbitrarily complex composites. Instead, we shall only consider a restricted class of composites that are *simple* in the following sense:

- We assume that the 3d-plate is *finitely structured* in the sense that Ω is partitioned into finitely many "grains" of the form $S_j \times (-\frac{1}{2}, \frac{1}{2})$, $j \in J$ (cf. Assumption 2.4).
- A *composite template* $\left(W(\kappa; \cdot), B(\kappa; \cdot) \right)_{\kappa \in \mathcal{K}}$ shall be given and each grain is filled with the composite template, possibly rotated in–plane.

We formalize this concept in the following definition:

Definition 6.4 (*Structured composite*) Let $(\bar{W}(\kappa, \cdot), \bar{B}(\kappa, \cdot))_{\kappa \in \mathcal{K}}$ be a composite template. Let $\{S_j\}_{j \in J}$ denote a partition of S as in Assumption 2.4. A *structured composite* (based on the composite template and subordinate to the partition) is a pair (W, B) consisting of Borel functions $W : \Omega \times \mathbb{R}^2 \times \mathbb{R}^{3 \times 3} \to [0, +\infty]$ and $B : \Omega \times \mathbb{R}^2 \to \mathbb{R}^{3 \times 3}$ such that for all $j \in J$ there exists a rotation $R_j \in SO(2)$ and a parameter $\kappa_j \in \mathcal{K}$ such that for all $x' \in S_j$,

$$W(x', x_3, y, F) = \bar{W}(\kappa_j, x_3, R_j^\top y, F \widehat{R}_j),$$

$$B(x', x_3, y) = \widehat{R}_j \bar{B}(\kappa_j; x_3, R_j^\top y) \widehat{R}_j^\top, \qquad \text{where } \widehat{R}_j := \begin{pmatrix} R_j \\ & 1 \end{pmatrix}.$$

If J is finite, then (W, B) is called a *finitely structured composite*.

Remark 6.5 Note that a structured composite is a special case of a prestrained composite satisfying Assumption 2.5. Specifically, if (W, B) is a structured composite, then $W_\varepsilon(x, F) := W(x, \frac{x'}{\varepsilon}, F)$ and $B_{\varepsilon(h), h}(x) := B(x, \frac{x'}{\varepsilon(h)})$ satisfy Assumption 2.5. Also note that once the composite template $(\bar{W}, \bar{B})$ is fixed, the structured composite is fully characterized by the partition $\{S_j\}_{j \in J}$, the parameters $\{\kappa_j\}_{j \in J} \subseteq \mathcal{K}$, and the rotations $\{R_j\}_{j \in J} \subseteq SO(2)$.

For an example of a composite template and a schematic picture of an associated finitely structured composite, see Fig. 21 below. The following main result states that any target shape (satisfying a certain restriction on its curvature, see (68) below) can effectively be approximated by almost–minimizers of a 3d-energy associated with a finitely structured composite.

Theorem 6.6 (Shape programming) *Let* Assumption 2.1 *be satisfied. Let* $(\bar{W}(\kappa; \cdot), \bar{B}(\kappa; \cdot))_{\kappa \in \mathcal{K}}$ *be a composite template, and let* II_* *be the second fundamental form of a bending deformation in* $H^2_{\text{iso}}(S; \mathbb{R}^3)$ *such that*

$$\mathrm{II}_*(x') \in \left\{ \kappa(\xi \otimes \xi) : \kappa \in \mathcal{K}, \xi \in \mathbb{R}^2, |\xi| = 1 \right\} \quad \textit{for a.e. } x' \in S. \tag{68}$$

Then for all $\delta > 0$, there exists a finitely structured composite (W, B) (based on the composite template and subordinate to a finite partition of S that depends on δ) such that the following holds: Consider the functional

$$\mathcal{I}^h(v) := \frac{1}{h^2} \int_\Omega W\left(x, \tfrac{x'}{\varepsilon(h)}, \nabla_h v(x)\left(I_{3\times 3} - h B\left(x, \tfrac{x'}{\varepsilon(h)}\right)\right)\right) \mathrm{d}x,$$

and let (v_h) denote a sequence with $\fint_\Omega v_h \, \mathrm{d}x = 0$ that satisfies $\mathcal{I}^h(v_h) \leq \inf \mathcal{I}^h + h$. Then any accumulation point v of (v_h) (viewed as a sequence in $L^2(\Omega; \mathbb{R}^3)$) is a bending deformation, i.e., $v \in H^2_{\mathrm{iso}}(S; \mathbb{R}^3)$, and satisfies

$$\|\mathbb{I}_v - \mathbb{I}_*\|_{L^2(S)} \leq \delta. \tag{69}$$

(See Sect. 7.8 for the proof.)

Condition (68) is a restriction on the curvature of the target shape. In view of Definition 6.1 (iii), the set $\mathcal{K}$ is the curvature range that can be recovered by the composite template under consideration. For example, if we consider the model composite of Sect. 6.1 as a composite template, then (68) takes the form of the restriction $|\mathbb{I}_*(x')| < \frac{3\rho_1}{2}$. We see that the range of admissible shapes increases for larger values of the parameter ρ_1, which in the model composite is the magnitude of the prestrain.

In a nutshell our result is: For any composite template and any target shape satisfying the constraint on the curvature (68), we can find a partition and a subordinate, finitely structured composite that programs the target shape up to a tolerance that is quantified by the parameter δ. As shall become clear from the proof of Theorem 6.6, in order to decrease δ one needs to refine the partition. We note that the proof of Theorem 6.6 yields a partition of S into dyadic squares and a boundary layer.

An illustration of a finitely structured composite designed to approximate a conically deformed strip is shown in Fig. 21. Figure 21a shows an isometrically deformed paper strip glued to the surface of a symmetric cone. The associated reference domain $S = (0, 4) \times (0, 1)$ is shown in Fig. 21a. The asymptotic lines of the deformed strip are indicated in blue. The deformation is affine along these lines. Since the deformed strip lies on a cone, these lines intersect in a single point. The principal curvature curves of the strip are shown in red. In the conical setting, the curves lie on circles whose center is given by the intersection point of the blue lines. The mean curvature is constant along these red curves. Moreover, we note that the curvature increases when moving along the blue lines (from lower–left to upper–right).

As indicated in Fig. 21b, the reference domain S is equipartitioned into small squares $\{S_j\}_{j \in J}$. An example of a finitely structured composite can be defined by filling each 3d-cube $S_j \times (-\frac{1}{2}, \frac{1}{2})$, $j \in J$, with a rotated instance of the composite template introduced in Sect. 6.1. It is based on the parametrized laminate shown in Fig. 4 and features the volume fraction θ as a parameter. In order to obtain a finitely structured composite that leads to an approximation of the deformed strip, in each box $S_j \times (-\frac{1}{2}, \frac{1}{2})$ the rotation of the composite template needs to be chosen according to the direction of the asymptotic (blue) line in S_j, and the parameter θ needs to be chosen in dependence of the curvature in S_j. The two schematic drawings in Fig. 21c illustrate this: The left drawing is the parametrized composite in the lower–left square of S and
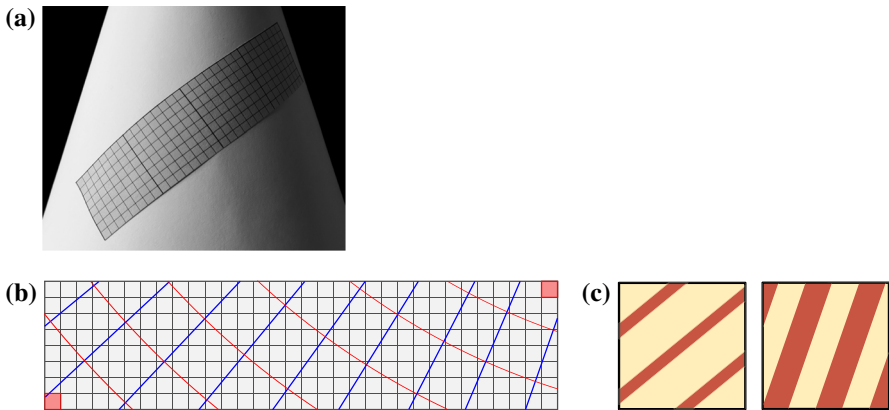
Fig. 21 A finitely structured composite designed for a conically deformed strip. **a** shows a conically deformed strip. **b** shows the reference domain S= $(0, 4) \times (0, 1)$ of the strip. The blue lines are asymptotic lines of the deformed strip and the red curves are integral curves of the principal direction along which the strip curved. **c** illustrates the specific composite template that is assigned to the lower-left and upper-right subsquares of S

the right drawing is the parametrization in the upper–right square. In Fig. 21c the yellow color refers to the domain occupied by the material with energy W_1 (where no prestrain is present), while the red color refers to the prestrained material with energy W_2. We see that the laminate direction is aligned with the asymptotic line. Furthermore, we see that in the composite assigned to the lower-left square, the volume fraction of the prestrained material is smaller than in the composite assigned with the upper–right square. This corresponds to the fact that the curvature in the lower-left square is smaller than the curvature in the upper–right one.

The idea of the proof of Theorem 6.6 is as follows: Similarly to Sect. 6.1, by the properties of the composite template and with the help of the transformation rule for in-plane rotations of Corollary 6.3, we find parameter fields $\kappa : S \to \mathcal{K}$ and $R : S \to \mathrm{SO}(2)$ such that for each $x' \in S$ the composite template with parameter $\kappa(x')$ and in-plane rotation $R(x')$ leads to an algebraic minimization problem

$$\min_{\substack{G \in \mathbb{R}^{2 \times 2} \\ \det G = 0}} Q_{\mathrm{hom}}^{\gamma}\Big(R(x'), \kappa(x'); G - B_{\mathrm{eff}}^{\gamma}\big(R(x'), \kappa(x')\big)\Big)$$

which is uniquely minimized by $G = \mathbb{I}_*(x')$; see Corollary 6.3 for the definition of $Q_{\mathrm{hom}}^{\gamma}(R, \kappa; \cdot)$ and $B_{\mathrm{eff}}^{\gamma}(R, \kappa)$. In particular, we shall see that the associated bending energy is minimized by bending deformations $v \in H_{\mathrm{iso}}^2(S; \mathbb{R}^3)$ satisfying $\mathbb{I}_v = \mathbb{I}_*$. In order to obtain a *finitely* structured composite, we approximate the parameter fields (R, κ) by fields (κ_n, R_n) that are piecewise constant subordinate to a finite partition of S, and we shall prove that minimizers of the bending energy associated with (κ_n, R_n) converge to a minimizer of the bending energy associated with (κ, R). For this we use the following approximation result for bending energies. It shows that pointwise

convergence of the quadratic form and of the prestrain implies Γ-convergence of the bending energy.

Lemma 6.7 (Γ-convergence of parametrized bending energies) *For $n \in \mathbb{N} \cup \{\infty\}$ consider a Borel function $Q_n : S \times \mathbb{R}^{2\times2}_{\mathrm{sym}} \to \mathbb{R}$ such that*

$$\alpha|G|^2 \leq Q_n(x', G) \leq \beta|G|^2 \quad \text{for a.e. } x' \in S \text{ and all } G \in \mathbb{R}^{2\times2}_{\mathrm{sym}}, \quad (70)$$

where $0 < \alpha \leq \beta$ are independent of n. Moreover, let $B_n \in L^2(S; \mathbb{R}^{2\times2}_{\mathrm{sym}})$. Consider the functional

$$\mathcal{I}_n : H^2_{\mathrm{iso}}(S; \mathbb{R}^3) \to \mathbb{R}, \quad \mathcal{I}_n(v) := \int_S Q_n(x', \mathrm{II}(x') - B_n(x')) \, dx'.$$

Suppose that for $n \to \infty$,

$$Q_n(\cdot, G) \to Q_\infty(\cdot, G) \qquad \text{a.e. in S and for all } G \in \mathbb{R}^{2\times2}_{\mathrm{sym}},$$
$$B_n \to B_\infty \qquad \text{strongly in } L^2(S).$$

Then:

(a) *(Equicoercivity). Let (v_n) have equibounded energy, i.e., $\limsup_{n\to 0} \mathcal{I}_n(v_n) < \infty$. Then there exists $v \in H^2_{\mathrm{iso}}(S; \mathbb{R}^3)$ with $\fint_S v \, dx' = 0$ such that*

$$v_n - \fint_S v_n \, dx' \rightharpoonup v \quad \text{weakly in } H^2(S; \mathbb{R}^3),$$

for a subsequence.

(b) *(Γ-convergence). For $n \to \infty$, the functional $\mathcal{I}_n$ Γ-converges to $\mathcal{I}_\infty$ with respect to weak convergence in $H^2(S; \mathbb{R}^3)$.*

(c) *(Strong convergence of minimizers). Let $(v_n) \subset H^2_{\mathrm{iso}}(S; \mathbb{R}^3)$ be a sequence such that for all $n \in \mathbb{N}$, v_n is a minimizer of $\mathcal{I}_n$ subject to $\fint_S v_n = 0$. Then, up to extraction of a subsequence, we have $v_n \to v_\infty$ strongly in $H^2(S; \mathbb{R}^3)$ where v_∞ is a minimizer of $\mathcal{I}_\infty$.*

(See Sect. 7.8 for the proof.)

Remark 6.8 Convergence of minimizers in the weak topology of $H^2(S; \mathbb{R}^3)$ follows directly from the general theory of Γ-convergence. The upgrade to strong convergence requires an additional argument that exploits the fact that $\mathcal{I}_n(v)$ is quadratic when seen as a function II_v, see Step 3 in the proof of Lemma 6.7.

7 Proofs

In the following we present the proofs of our results. We start in Sect. 7.1 to prove results concerning the definition of the effective quantities (Q^γ_{hom}, B^γ_{eff}) and their representation via correctors. In Sects. 7.2–7.4 are devoted to the proofs of Theorems 2.8

and 2.13. Our results on the two-scale structure of the nonlinear strain are proven in Sect. 7.5. In Sect. 7.6 we present the argument for the results on the microstructure–properties–shape relation and in Sect. 7.8 we prove the results on shape programming.

7.1 Homogenization Formula: Proofs of Lemmas 2.20, 2.29, 2.23, Proposition 2.25, and Lemma 2.26

Proof of Lemma 2.20 We first note that since $Q \in \mathcal{Q}(\alpha, \beta)$ (see Definition 2.2), it suffices to prove

$$\alpha \fint_{\square_\Lambda} |\iota(x_3 G)|^2 \leq \|P_{\text{rel},\Lambda}^{\gamma,\perp}(\iota(x_3 G))\|_\Lambda^2 \leq \beta \fint_{\square_\Lambda} |\iota(x_3 G)|^2.$$

Since $P_{\text{rel},\Lambda}^{\gamma,\perp}$ is a projection, we have

$$\|P_{\text{rel},\Lambda}^{\gamma,\perp}(\iota(x_3 G))\|_\Lambda^2 \leq \|\iota(x_3 G)\|_\Lambda^2,$$

and thus the upper bound follows. For the lower bound note that by definition of $\mathbf{H}_{\text{rel},\Lambda}^{\gamma}$ we have

$$\|P_{\text{rel},\Lambda}^{\gamma,\perp}(\iota(x_3 G))\|_\Lambda^2 = \inf_{M,\varphi} \|\iota(x_3 G) + \iota(M) + \text{sym}\,\nabla_\gamma \varphi\|_\Lambda^2, \tag{71}$$

where the infimum is taken over all $M \in \mathbb{R}_{\text{sym}}^{2\times2}$ and $\varphi \in H_\gamma^1(\square_\Lambda; \mathbb{R}^3)$. Since $Q \in \mathcal{Q}(\alpha, \beta)$, we have for all $M \in \mathbb{R}_{\text{sym}}^{2\times2}$ and $\varphi \in H_\gamma^1(\square_\Lambda; \mathbb{R}^3)$,

$$\|\iota(x_3 G) + \iota(M) + \text{sym}\,\nabla_\gamma \varphi\|_\Lambda^2 \geq \alpha \fint_{\square_\Lambda} |\iota(x_3 G) + \iota(M) + \text{sym}\,\nabla_\gamma \varphi|^2 \geq \alpha \fint_{\square_\Lambda} |\iota(x_3 G)|^2, \tag{72}$$

where the last inequality holds thanks to the orthogonality

$$\fint_{\square_\Lambda} \iota(x_3 G) : (\iota(M) + \text{sym}\,\nabla_\gamma \varphi) = 0,$$

which can be checked by a direct computation. In combination with (71), the lower bound follows. □

Proof of Lemma 2.29 For the argument, fix $j \in J$, $x' \in S_j$, and note that for all $\chi \in \mathbf{H}_{\text{rel},\Lambda_j}^{\gamma}$ we have

$$\fint_{\square_{\Lambda_j}} Q\Big(x', x_3, y, \iota(x_3 \mathbb{I}_v(x'))) + \chi - B(x', x_3, y)\Big) d(x_3, y)$$
$$= \|\iota(x_3 \mathbb{I}_v(x')) + \chi - P_{\Lambda_j}^{\gamma}(\text{sym}\,B(x', \cdot))\|_{\Lambda_j}^2 + \|(I - P_{\Lambda_j}^{\gamma})(\text{sym}\,B((x', \cdot))\|_{\Lambda_j}^2,$$

where I denotes the identity operator on $\mathbf{H}_{\Lambda_j}$. Moreover, by Lemma 2.20, Definition 2.22, and Definition 2.17,

$$\inf_{\chi \in \mathbf{H}_{\text{rel},\Lambda_j}^{\gamma}} \|\iota(x_3 \mathbb{I}_v(x')) + \chi - P_{\Lambda_j}^{\gamma}(\text{sym}\,B(x', \cdot)))\|_{\Lambda_j}^2 = \|P_{\text{rel},\Lambda_j}^{\gamma,\perp}\Big(\iota(x_3 (\mathbb{I}_v(x') - B_{\text{eff}}^{\gamma}(x')))\Big)\|_{\Lambda_j}^2$$
$$= Q_{\text{hom}}^{\gamma}(x', \mathbb{I}_v(x') - B_{\text{eff}}^{\gamma}(x')).$$

Now, the claim follows by combining the previous two identities, integration over S_j and summation in $j \in J$. $\qquad\square$

Proof of Lemma 2.23 and Proposition 2.25

Step 1 (Representation of $\mathbf{H}^{\gamma}_{\mathrm{rel},\Lambda}$) We claim that for all $\chi \in \mathbf{H}^{\gamma}_{\mathrm{rel},\Lambda}$ there exists a unique pair (M, φ) with $M \in \mathbb{R}^{2\times 2}_{\mathrm{sym}}$ and $\varphi \in H^1_{\gamma}(\square_{\Lambda}; \mathbb{R}^3)$ such that

$$\chi = \iota(M) + \mathrm{sym}\,\nabla_{\gamma}\varphi \quad \text{and} \quad \fint_{\square_{\Lambda}} \varphi = 0, \tag{73}$$

and

$$|M|^2 + \fint_{\square_{\Lambda}} |\varphi|^2 + |\nabla_{\gamma}\varphi|^2 \le C \|\chi\|^2_{\Lambda}, \tag{74}$$

for a constant C only depending on α, γ and C_{Λ}.

Here comes the argument: The existence of (M, φ) is clear by definition. Moreover we have $\fint_{\square_{\Lambda}} \iota(M) : \mathrm{sym}\,\nabla_{\gamma}\varphi = 0$, since φ is in-plane periodic. Combined with the Korn inequality in Lemma 8.5 and the Poincaré–Wirtinger inequality, the bound (74) follows. Uniqueness of the representation is a consequence of (74).

Step 2 (Proof of Lemma 2.23)
Let $G \in \mathbb{R}^{2\times 2}_{\mathrm{sym}}$. Let $\chi_G \in \mathbf{H}^{\gamma}_{\mathrm{rel},\Lambda}$ denote the unique minimizer to

$$\|\iota(x_3 G) + \chi_G\|^2_{\Lambda} = \min_{\chi \in \mathbf{H}^{\gamma}_{\mathrm{rel},\Lambda}} \|\iota(x_3 G) + \chi\|^2_{\Lambda},$$

and note that χ_G is characterized by the variational problem

$$\big(\iota(x_3 G) + \chi_G, \chi\big)_{\Lambda} = 0 \quad \text{for all } \chi \in \mathbf{H}^{\gamma}_{\mathrm{rel},\Lambda}, \tag{75}$$

with $(\cdot, \cdot)_{\Lambda}$ denoting the inner product of $\mathbf{H}_{\Lambda}$. Since projections are contractions and $Q \in \mathcal{Q}(\alpha, \beta)$, we have

$$\|\chi_G\|_{\Lambda} \le \|\iota(x_3 G)\|_{\Lambda} \le \sqrt{\tfrac{\beta}{12}} |G|. \tag{76}$$

For future reference, we also note that we have the identity

$$\iota(x_3 G) + \chi_G = P^{\gamma,\perp}_{\mathrm{rel},\Lambda}(\iota(x_3 G)) = \mathbf{E}^{\gamma}_{\Lambda}(G). \tag{77}$$

Now, let (M_G, φ_G) denote the unique pair associated with χ_G via (73). Then, we deduce from (75) that (M_G, φ_G) is characterized by (20), and we obtain (21) from (76) and (74).

Step 3 (Proof of Proposition 2.25 (a))
First, we recall that the definition of $Q^{\gamma}_{\mathrm{hom}}$ can be rephrased as $Q^{\gamma}_{\mathrm{hom}}(G) = \|P^{\gamma,\perp}_{\mathrm{rel},\Lambda}(\iota(x_3 G))\|_{\Lambda}$ for all $G \in \mathbb{R}^{2\times 2}_{\mathrm{sym}}$. Using the orthonormal basis G_1, G_2, G_3, we

write $G = \widehat{G}_i G_i$, where here and below we appeal to Einstein's summation convention. By (77) and linearity we have $P_{\text{rel},\Lambda}^{\gamma,\perp}(\iota(x_3 G)) = \widehat{G}_i(\iota(x_3 G_i) + \chi_{G_i})$, and thus

$$Q_{\text{hom}}^{\gamma}(G) = \widehat{G}_i \widehat{G}_k \Big(\iota(x_3 G_i) + \chi_{G_i},\, \iota(x_3 G_k) + \chi_{G_k}\Big)_{\Lambda}$$
$$= \widehat{G}_i \widehat{G}_k \Big(\iota(x_3 G_i) + \chi_{G_i},\, \iota(x_3 G_k) + \chi_{G_k}\Big)_{\Lambda} = \widehat{G}_i \widehat{G}_k \widehat{Q}_{ik},$$

where the last two identities hold thanks to (75) and the definition of $\widehat{Q}$, respectively. The identity shows that $\widehat{Q}$ is symmetric. The bound (22) is a direct consequence of (18).

Step 4 (Proof of Proposition 2.25 (b))
Set $\tilde{B} := \sum_{i=1}^{3} \big(\widehat{Q}^{-1}\widehat{B}\big)_i G_i$. In view of the definition of B_{eff}^{γ}, cf. (19), and since $\mathbf{E}_{\Lambda}^{\gamma}$ is injective, it suffices to show that

$$\mathbf{E}_{\Lambda}^{\gamma}(\tilde{B}) = P_{\text{rel},\Lambda}^{\gamma,\perp}(\text{sym}\, B). \tag{78}$$

Since $P_{\text{rel},\Lambda}^{\gamma,\perp}$ is a projection onto $\mathbf{H}_{\text{rel},\Lambda}^{\gamma,\perp}$, and since the latter is spanned by the fields $\iota(x_3 G_i) + \chi_{G_i}$, the above identity is equivalent to

$$\big(\mathbf{E}_{\Lambda}^{\gamma}(\tilde{B}),\, \iota(x_3 G_i) + \chi_{G_i}\big)_{\Lambda} = \big(\text{sym}\, B,\, \iota(x_3 G_{G_i}) + \chi_{G_i}\big)_{\Lambda} \tag{79}$$

for all $i = 1, 2, 3$. By definition, the right-hand side is equal to $\widehat{B}_i$. On the other hand, by (77) and linearity, we have $\mathbf{E}_{\Lambda}^{\gamma}(\tilde{B}) = \sum_{k=1}^{3} \big(\widehat{Q}^{-1}\widehat{B}\big)_k (\iota(x_3 G_k) + \chi_{G_k})$. Thus, (79) is equivalent to $\big(\widehat{Q}^{-1}\widehat{B}\big)_i = \widehat{B}_i$, and we conclude (78). □

Proof of Lemma 2.26 It suffices to prove (25) and (26). The other statements then follow with help of Proposition 2.25.

We first note that there exists $\tilde{M}$ and $\tilde{\varphi}$ such that for a subsequence (not relabeled) we have

$$M_{n,i} \to \tilde{M} \quad \text{and} \quad \varphi_{n,i} \rightharpoonup \tilde{\varphi} \text{ weakly in } H_{\gamma}^1(\square_{\Lambda}; \mathbb{R}^3). \tag{80}$$

Indeed, this follow from (21), the variant of Korn's inequality of Lemma 8.5 and weak compactness of bounded sequences in Hilbert spaces. Thanks to the assumed convergence of (Q_n), we may pass to the limit in the corrector equation (20) for $(M_{n,i}, \varphi_{n,i})$ and deduce that

$$\int_{\square_{\Lambda}} \mathbb{L}_{\infty}\big(\iota(x_3 G_i + \tilde{M}) + \text{sym}(\nabla_{\gamma}\tilde{\varphi})\big) : \big(\iota(M') + \text{sym}(\nabla_{\gamma}\varphi')\big) = 0$$

for all test functions M' and φ'. Above, $\mathbb{L}_{\infty}$ denotes the fourth-order tensor associated with Q_{∞} via the polarization identity (4). By uniqueness of the corrector (see Lemma 2.23), we conclude that $\tilde{M} = M_{\infty,i}$ and $\tilde{\varphi} = \varphi_{\infty,i}$, and thus the convergence (80) holds for the entire sequence. It remains to show that $\varphi_{n,i} \to \varphi_{\infty,i}$ strongly in H^1. In view of Korn's inequality, cf. Lemma 8.5, it suffices to show that

$\| \operatorname{sym} \nabla_\gamma \varphi_{n,i} - \operatorname{sym} \nabla_\gamma \varphi_{\infty,i} \|_{L^2(\square_\Lambda)} \to 0$. Since $Q_n \in \mathcal{Q}(\alpha, \beta)$ and by appealing to the corrector equations (20) for $\varphi_{n,i}$ and $\varphi_{\infty,i}$, we have

$$
\alpha \fint_{\square_\Lambda} | \operatorname{sym} \nabla_\gamma \varphi_{n,i} - \operatorname{sym} \nabla_\gamma \varphi_{\infty,i} |^2
$$

$$
\leq \fint_{\square_\Lambda} \mathbb{L}_n \Big(\iota(M_n - M_\infty) + \operatorname{sym} \nabla_\gamma (\varphi_{n,i} - \varphi_{\infty,i}) \Big) :
$$

$$
\Big(\iota(M_n - M_\infty) + \operatorname{sym} \nabla_\gamma (\varphi_{n,i} - \varphi_{\infty,i}) \Big)
$$

$$
= \fint_{\square_\Lambda} (\mathbb{L}_\infty - \mathbb{L}_n) \Big(\iota(x_3 G_i + M_\infty) + \operatorname{sym} \nabla_\gamma \varphi_{\infty,i} \Big) :
$$

$$
\Big(\iota(M_\infty - M_n) + \operatorname{sym} \nabla_\gamma (\varphi_{n,i} - \varphi_{\infty,i}) \Big).
$$

Note that the last integral converges to 0, since we have $(\mathbb{L}_\infty - \mathbb{L}_n)\Big(\iota(x_3 G_i + M_\infty) + \operatorname{sym} \nabla_\gamma \varphi_{\infty,i} \Big) \to 0$ strongly in L^2, and $\iota(M_\infty - M_n) + \operatorname{sym} \nabla_\gamma (\varphi_{n,i} - \varphi_{\infty,i}) \rightharpoonup 0$ weakly in L^2.   □

7.2 Compactness: Proof of Theorem 2.8 (a)

Proof of Theorem 2.8(a) By the triangle inequality and Young's inequality, for all $F \in \mathbb{R}^{3 \times 3}$ and $h > 0$, we have

$$
\frac{1}{2} \operatorname{dist}(F, \mathrm{SO}(3)) \leq \operatorname{dist}\Big(F(I_{3 \times 3} - h B_{\varepsilon(h),h}), \mathrm{SO}(3) \Big) + \frac{1}{2} h^2 |B_{\varepsilon(h),h}|^2 + h |B_{\varepsilon(h),h}| \tag{81}
$$

almost everywhere in Ω. Together with Assumption 2.5 (iv) this yields the implication

$$
\limsup_{h \to 0} \mathcal{I}^{\varepsilon(h),h}(v_h) < \infty \quad \Rightarrow \quad \limsup_{h \to 0} \frac{1}{h^2} \int_\Omega \operatorname{dist}^2(\nabla_h v_h(x), \mathrm{SO}(3)) \mathrm{d}x < \infty.
$$

Hence, the statement of Theorem 2.8 (a) follows from (Friesecke et al. 2002, Theorem 4.1).   □

7.3 Lower Bound: Proof of Theorem 2.8 (b)

We only need to consider the case when (8) is satisfied since otherwise, the claim is trivial. We note that by Theorem 2.8 (a) we have $v \in H^2_{\mathrm{iso}}(S; \mathbb{R}^3)$. In view of Lemma 2.29 it suffices to prove that

$$
\liminf_{h \to 0} \mathcal{I}^{\varepsilon(h),h}(v_h) \geq \widetilde{\mathcal{I}}^\gamma(v),
$$

where $\widetilde{\mathcal{I}}^\gamma$ is defined in (28). For the proof we modify the argument in (Neukamm 2012, Proof of Theorem 3.3 (Lower bound)) as follows: Without loss of generality,

we may assume that

$$\liminf_{h \to 0} \mathcal{I}^{\varepsilon(h),h}(v_h) = \lim_{h \to 0} \mathcal{I}^{\varepsilon(h),h}(v_h) < \infty.$$

Hence, by Theorem 2.8 (a), (v_h) is a sequence of finite bending energy in the sense of (9). By appealing to Proposition 3.2 (a) we can pass to a subsequence (that we do not relabel) such that

$$E_h(v_h) \overset{2}{\rightharpoonup} E := \iota(x_3 \mathbb{I}_v + M) + \text{sym} \, \nabla_\gamma \varphi, \tag{82}$$

for some $M \in L^2(S; \mathbb{R}^{2\times2}_{\text{sym}})$ and $\varphi \in L^2(S; H^1_{\gamma, \text{uloc}})$ that is locally periodic in the sense of (6). Set

$$\theta_h(x) := \begin{cases} 1 & \text{if } \text{dist}(\nabla_h v_h(x), \text{SO}(3)) \leq h^{1/2}, \\ 0 & \text{else,} \end{cases} \tag{83}$$

and note that (9) yields

$$\limsup_{h \to 0} \frac{1}{h} \int_\Omega |1 - \theta_h| \leq \limsup_{h \to \infty} \frac{1}{h^2} \int_\Omega \text{dist}^2(\nabla_h v_h(x), \text{SO}(3)) \mathrm{d}x < \infty. \tag{84}$$

By polar factorization (of $\nabla_h v_h(x)$ for $x \in \{\theta_h = 1\}$) and by Assumption 2.5 (iv), there exists a rotation field $R_h : \Omega \to \text{SO}(3)$ such that $\theta_h \nabla_h v_h = \theta_h R_h (I_{3\times3} + h E_h(v_h))$. Thus, $\theta_h \nabla_h v_h (I_{3\times3} - h B_{\varepsilon(h),h}) = \theta_h R_h (I_{3\times3} + h G_h)$ where

$$G_h := \frac{1}{h} \Big((I_{3\times3} + h\theta_h E_h(v_h))(I_{3\times3} - h\theta_h B_{\varepsilon(h),h}) - I_{3\times3} \Big) \to 0 \text{ uniformly in } \Omega. \tag{85}$$

Frame-indifference (W1) and the natural state condition (W3) thus yield

$$\frac{\theta_h}{h^2} W_{\varepsilon(h)}(x, \nabla_h v_h (I_{3\times3} - h B_{\varepsilon(h),h})) = \frac{1}{h^2} W_{\varepsilon(h)}(x, I_{3\times3} + h G_h(x)).$$

Combined with (W4) and (85), we get

$$\limsup_{h \to 0} \Big| \frac{1}{h^2} \int_\Omega \theta_h W_{\varepsilon(h)}(x, \nabla_h v_h (I_{3\times3} - h B_{\varepsilon(h),h})) \mathrm{d}x$$
$$- \int_\Omega Q_{\varepsilon(h)} \Big(x, \theta_h \big(E_h(v_h) - B_{\varepsilon(h),h} \big) \Big) \mathrm{d}x \Big| = 0, \tag{86}$$

and thus (by non-negativity of $W_{\varepsilon(h),h}$),

$$\liminf_{h \to 0} \mathcal{I}^{\varepsilon(h),h}(v_h) \geq \liminf_{h \to 0} \int_\Omega Q_{\varepsilon(h)} \Big(x, \theta_h \big(E_h(v_h) - B_{\varepsilon(h),h} \big) \Big) \mathrm{d}x. \tag{87}$$

By appealing to Assumption 2.5 (i) and Assumption 2.5 (iv) , the right-hand side is equal to

$$\liminf_{h \to 0} \int_\Omega Q\left(x, \tfrac{x'}{\varepsilon(h)}, \theta_h\big(E_h(v_h) - B(x, \tfrac{x'}{\varepsilon(h)})\big)\right) dx. \tag{88}$$

We claim that

$$\theta_h\big(E_h(v_h) - B(x, \tfrac{x'}{\varepsilon(h)})\big) \overset{2}{\rightharpoonup} E - B \qquad \text{weakly two-scale in } L^2, \tag{89}$$

where E is defined in (82). For the argument, we first note that $E_h(v_h) - B\left(x, \tfrac{x'}{\varepsilon(h)}\right)$ weakly two-scale converges to the right-hand side thanks to (82) and Assumption 2.5 (iv). The left-hand side of (89) converges to the same limit, since (θ_h) is bounded in L^∞ and $\theta_h \to 1$ in L^1 by (84).

In view of (87), (88), (89), and (82), the two-scale lower semicontinuity result Lemma 8.4 yields the lower bound

$$\liminf_{h \to 0} \mathcal{I}^{\varepsilon(h),h}(v_h) \geq \sum_{j \in J} \int_{S_j} \fint_{\square_{\Lambda_j}} Q(x, y, \iota(x_3 \mathbb{II}_v + M) + \operatorname{sym} \nabla_\gamma \varphi - B) d(x_3, y) dx'.$$

In view of the definition of $\widetilde{I}^\gamma$ (see (2.29)) the claim follows by taking the infimum on the right-hand side over M and φ. $\qquad \square$

7.4 Recovery Sequence: Proofs of Theorem 2.8 (c) and Theorem 2.13

We only discuss the proof of Theorem 2.13, since, in comparison to Theorem 2.8 (c), it features the additional difficulty to take care of the clamped boundary conditions (13).

Proof of Theorem 2.13 *Step 1* (A priori estimate on M and choice of δ)
Let $\tilde{v} \in H^2_{\text{iso}}(S; \mathbb{R}^3)$. Set $\widetilde{\mathbb{II}} := \mathbb{II}_{\tilde{v}}$, and denote by $(\tilde{M}, \tilde{\varphi})$ the associated pair of correctors satisfying

$$\mathcal{I}^\gamma_{\text{hom}}(\tilde{v}) = \sum_{j=1}^\infty \int_{S_j} \fint_{\square_{\Lambda_j}} Q(x', x_3, y, \iota(x_3 \widetilde{\mathbb{II}} + \tilde{M}) + \operatorname{sym} \nabla_\gamma \tilde{\varphi} - \widetilde{B}) d(x_3, y) dx',$$

where

$$\widetilde{B}(x', \cdot) := P^\gamma_{\Lambda_j}(\operatorname{sym} B(x', \cdot)) \qquad \text{for } x' \in S_j \text{ and } j \in J. \tag{90}$$

We claim that there exists a constant $C = C(\alpha, \beta, \gamma, C_J, C_B)$ such that

$$|\tilde{M}(x')|^2 \leq C(|\widetilde{\mathbb{II}}(x')|^2 + 1). \tag{91}$$

Before we prove this estimate, we note that this implies that

$$\tilde{M}(x') + \delta I_{2 \times 2} \geq 0 \text{ a.e. in } \{\widetilde{\mathbb{II}} = 0\}, \tag{92}$$

for a constant $\delta = \delta(\alpha, \beta, \gamma, C_J, C_B) \geq 0$ that is independent of the specific isometry $\tilde{v}$. We now prove (91) and first argue that for all $j \in J$,

$$\fint_{\square_{\Lambda_j}} |\widetilde{B}(x', x_3, y)|^2 \mathrm{d}(x_3, y) \lesssim 1 \quad \text{for a.e. } x' \in S_j; \tag{93}$$

where here and below, $\lesssim$ means $\leq$ up to a multiplicative constant that only depends $\alpha, \beta, \gamma, C_J, C_B$. Indeed, since $Q(x, y, \cdot) \in \mathcal{Q}(\alpha, \beta)$, and since $P_{\Lambda_j}^\gamma$ is a projection (adapted to $Q(x', \cdot)$), we have

$$\fint_{\square_{\Lambda_j}} |\widetilde{B}(x', x_3, y)|^2 \mathrm{d}(x_3, y) \lesssim \fint_{\square_{\Lambda_j}} Q(x', \widetilde{B}(x', x_3, y)) \mathrm{d}(x_3, y)$$

$$\lesssim \fint_{\square_{\Lambda_j}} Q(x', \mathrm{sym}\, B(x', x_3, y)) \mathrm{d}(x_3, y)$$

$$\lesssim \fint_{\square_{\Lambda_j}} |\mathrm{sym}\, B(x', x_3, y)|^2 \mathrm{d}(x_3, y),$$

and thus the claim follows from (14). Next, we note that by orthogonality,

$$|\tilde{M}(x')|^2 \leq \fint_{\square_{\Lambda_j}} |\iota(x_3 \tilde{\mathbb{I}} + \tilde{M}) + \mathrm{sym}\, \nabla_\gamma \tilde{\varphi}|^2$$

$$\leq 2 \fint_{\square_{\Lambda_j}} |\iota(x_3 \tilde{\mathbb{I}} + \tilde{M}) + \mathrm{sym}\, \nabla_\gamma \tilde{\varphi} - \widetilde{B}|^2 + 2 \fint_{\square_{\Lambda_j}} |\widetilde{B}|^2.$$

With (93) and since $Q \in \mathcal{Q}(\alpha, \beta)$, we conclude

$$|\tilde{M}(x')|^2 \lesssim \fint_{\square_{\Lambda_j}} Q(x', x_3, y, \iota(x_3 \tilde{\mathbb{I}} + \tilde{M}) + \mathrm{sym}\, \nabla_\gamma \tilde{\varphi} - \widetilde{B}) \mathrm{d}(x_3, y) + 1.$$

Since $(\tilde{M}(x'), \tilde{\varphi}(x', \cdot))$ is the corrector pair, we conclude that

$$|\tilde{M}(x')|^2 \lesssim Q_{\text{hom}}^\gamma(x', \tilde{\mathbb{I}}(x')) + 1 \lesssim |\tilde{\mathbb{I}}(x')|^2 + 1,$$

as claimed.

Step 2 (Construction in the smooth case)
Let $\delta \geq 0$ be as in (92) and denote by

$$\mathcal{A}_{BC}^h := \{v_h \in H^1(\Omega; \mathbb{R}^3) \,:\, v_h \text{ satisfies } (13)\},$$

the space of deformations that satisfy the 3d-boundary conditions. We claim that for all $\rho > 0$ there exists $v_\rho \in \mathcal{A}_{BC} \cap C^\infty(\bar{S}; \mathbb{R}^3)$ with

$$\|v_\rho - v\|_{L^2(S)} + |\mathcal{I}_{\text{hom}}^\gamma(v_\rho) - \mathcal{I}_{\text{hom}}^\gamma(v)| \leq \rho, \tag{94}$$

and a recovery sequence $(v_{h,\rho})$ with $v_{h,\rho} \in \mathcal{A}^h_{BC}$ satisfying the claim of Theorem 2.13 with v replaced by v_ρ. Here comes the argument: First, since $\mathcal{I}^\gamma_{\text{hom}}$ is continuous w.r.t. strong convergence in $H^2(S; \mathbb{R}^3)$ and in view of the approximation result (15), we can find v_ρ such that (94) holds. Let (M_ρ, φ_ρ) denote the pair of correctors associated with v_ρ, that is,

$$\mathcal{I}^\gamma_{\text{hom}}(v_\rho) = \sum_{j=1}^\infty \int_{S_j} \fint_{\square_{\Lambda_j}} Q(x', x_3, y, \iota(x_3 \mathbb{I}_{v_\rho} + M_\rho) + \text{sym}\, \nabla_\gamma \varphi_\rho - \widetilde{B}) \mathrm{d}(x_3, y) \mathrm{d}x',$$

where $\widetilde{B}$ is defined in (90). By (92) we have $M_\rho + \delta I_{2\times 2} \geq 0$ on $\{\mathbb{I}_{v_\rho} = 0\}$. Therefore, we can apply Proposition 3.2 to obtain a recovery sequence $v_{h,\rho} \in \mathcal{A}^h_{BC}$ such that $v_{h,\rho} \to v_\rho$ in $L^2(\Omega)$,

$$E_h(v_{h,\rho}) \xrightarrow{\;2\;} \iota(x_3 \mathbb{I}_{v_\rho} + M_\rho) + \text{sym}\, \nabla_\gamma \varphi_\rho \quad \text{strongly two-scale,}$$

and in addition

$$\limsup_{h \to 0} h \|E_h(v_{h,\rho})\|_{L^\infty} = 0 \quad \text{and} \quad \lim_{h \to 0} \|\det(\nabla_h v_{h,\rho}) - 1\|_{L^\infty} = 0.$$

Note that the latter implies that (for h sufficiently small) there exists a rotation field $R_{h,\rho} \in L^\infty(\Omega; SO(3))$ such that

$$\nabla_h v_{h,\rho}(I_{3\times 3} - h B_{\varepsilon(h),h}) = R_{h,\rho}(I_{3\times 3} + h E_h(v_{h,\rho}))(I_{3\times 3} - h B_{\varepsilon(h),h}).$$

Moreover, with Assumption 2.5 (iv),

$$\nabla_h v_{h,\rho}(I_{3\times 3} - h B_{\varepsilon(h),h}) = R_{h,\rho}(I_{3\times 3} + h G_h + h o_h), \qquad G_h = E_h(v_{\rho,h}) - B_{\varepsilon(h),h},$$

for some remainder $o_h : \Omega \to \mathbb{R}^{3\times 3}$ and $h(\|G_h\|_{L^\infty(\Omega)} + \|o_h\|_{L^\infty(\Omega)}) \to 0$. We thus conclude by frame-indifference and a Taylor expansion at $I_{3\times 3}$ of $W_{\varepsilon(h)}$ that

$$\limsup_{h \to \infty} \mathcal{I}^{\varepsilon(h),h}(v_{\rho,h}) = \limsup_{h \to \infty} \int_\Omega Q_{\varepsilon(h)}(x, G_h(x)) \mathrm{d}x.$$

In view of Assumption 2.5 (ii), we have

$$\limsup_{h \to \infty} \int_\Omega Q_{\varepsilon(h)}(x, G_h(x)) \mathrm{d}x = \limsup_{h \to \infty} \int_\Omega Q(x', x_3, \tfrac{x'}{\varepsilon(h)}, G_h(x)) \mathrm{d}x, \qquad (95)$$

and in view of Assumption 2.5 (iv), we have

$$G_h \xrightarrow{\;2\;} \iota(x_3 \mathbb{I}_{v_\rho} + M_\rho) + \text{sym}\, \nabla_\gamma \varphi_\rho - B \qquad \text{strongly two-scale in } L^2.$$

By the continuity of the convex functional on the right-hand side of (95) w.r.t. strong two-scale convergence, cf. Lemma 8.4, we conclude that

$$
\begin{aligned}
\limsup_{h \to \infty} &\, \mathcal{I}^{\varepsilon(h),h}(v_{\rho,h}) \\
&= \sum_{j=1}^{\infty} \int_{S_j} \fint_{\square_{\Lambda_j}} Q(x', x_3, y, \iota(x_3 \mathbb{II}_{v_\rho} + M_\rho) + \operatorname{sym} \nabla_\gamma \varphi_\rho - \operatorname{sym} B) \mathrm{d}(x_3, y) \mathrm{d}x' \\
&= \mathcal{I}^{\gamma}_{\mathrm{hom}}(v_\rho) + \mathcal{I}^{\gamma}_{\mathrm{res}}(B),
\end{aligned}
$$

see Lemma 2.29. This concludes the argument.

Step 3 (Extraction of a diagonal sequence)
Consider

$$
c_{h,\rho} := |\mathcal{I}^{\varepsilon(h),h}(v_{h,\rho}) - (\mathcal{I}^{\gamma}_{\mathrm{hom}}(v) + \mathcal{I}^{\gamma}_{\mathrm{res}}(B))| + \int_{\Omega} |v_{h,\rho} - v|^2.
$$

Step 2 yields $\limsup_{h \to 0} \limsup_{\rho \to 0} c_{h,\rho} = 0$, and thus there exists a diagonal sequence $h \mapsto \rho(h)$ such that $c_{h,\rho(h)} \to 0$. Hence, $v_h := v_{h,\rho(h)}$ defines the recovery sequence (v_h) we were looking for. $\qquad\square$

7.5 Characterization of the Limiting Strain: Proof of Proposition 3.2 and Lemma 2.29

We start with the proof of Proposition 3.2 (a), which is almost a direct consequence of (Hornung et al. 2014, Proposition 3.2), where the "single-grain" case with $\Lambda_j = I_{2 \times 2}$ is considered.

Proof of Proposition 3.2(a) By Lemma 8.2 (a) we may pass to a subsequence (not relabeled) such that

$$
E_h(v_h) \overset{2}{\rightharpoonup} E \qquad \text{weakly two-scale in } L^2,
$$

where $E \in L^2(\Omega; L^2_{\mathrm{uloc}}(\mathbb{R}^2; \mathbb{R}^{3 \times 3}_{\mathrm{sym}}))$. In view of Lemma 8.1, it suffices to show that for all $j \in J$, we have (after possibly passing to a further subsequence)

$$
E_h(v_h) \overset{2}{\rightharpoonup} \iota(x_3 \mathbb{II} + M_j) + \operatorname{sym} \nabla_\gamma \varphi_j,
$$

weakly two-scale in the sense of (128) for some $M_j \in L^2(S_j; \mathbb{R}^{2 \times 2}_{\mathrm{sym}})$ and $\varphi_j \in L^2(S_j; H^1_\gamma(\square_{\Lambda_j}; \mathbb{R}^3))$. In the case $\Lambda_j = I_{2 \times 2}$, (128) directly follows from (Hornung et al. 2014, Proposition 3.2). With help of Proposition 8.3 and the variant of Korn's inequality Lemma 8.5, the argument of (Hornung et al. 2014, Proposition 3.2) extends verbatim to the case of general invertible $\Lambda_j \in \mathbb{R}^{2 \times 2}$. $\qquad\square$

We turn to the proof of Proposition 3.2 (b). We only discuss the construction in the case with prescribed boundary data, since this adds an additional layer of difficulties.

The construction is based on the density of $\mathcal{A}_{BC} \cap C^\infty(\bar{S}; \mathbb{R}^3)$ in $\mathcal{A}_{BC}$, see (15), and a "single-scale" approximation result that we recently obtained together with M. Griehl et al. in Bartels et al. (2022). We recall it in the following (slightly weaker) form:

Proposition 7.1 (cf. Bartels et al. 2022, Proposition 4.4) *Let* $v \in H^2_{\mathrm{iso}}(S; \mathbb{R}^3) \cap C^\infty(\bar{S}; \mathbb{R}^3)$, $M \in L^2(S; \mathbb{R}^{2\times2}_{\mathrm{sym}})$, $d \in L^2(\Omega; \mathbb{R}^3)$ *and assume that there exists* $\delta \geq 0$ *such that*

$$M + \delta I_{2\times2} \geq 0 \text{ a.e. in } \{\mathbb{I}_v = 0\}.$$

Then there exists a sequence $(v_h) \subseteq C^\infty(\bar{\Omega}; \mathbb{R}^3)$ *such that*

$$v_h \to v \quad \text{uniformly in } \Omega,$$
$$E_h(v_h) \to \iota(x_3\mathbb{I} + M) + \mathrm{sym}(d \otimes e_3) \quad \text{strongly in } L^2(\Omega),$$
$$\limsup_{h\to0} h\|E_h(v_h)\|_{L^\infty(\Omega)} = 0 \quad \text{and} \quad \lim_{h\to0} \|\det(\nabla_h v_h) - 1\|_{L^\infty(\Omega)} = 0. \quad (96)$$

Furthermore, if Assumption 2.11 *is satisfied and* $v \in \mathcal{A}_{BC} \cap C^\infty(\bar{S}; \mathbb{R}^3)$, *then we may additionally enforce the clamped, affine boundary condition* (13).

Proof of Proposition 3.2 (b) By (15), for any ρ there exists $v_\rho \in \mathcal{A}_{BC} \cap C^\infty(\bar{S}; \mathbb{R}^3)$ such that

$$\int_S |v - v_\rho|^2 + |\mathbb{I}_v - \mathbb{I}_{v_\rho}|^2 + |(\nabla'v, b_v) - R_\rho|^2 \leq \rho, \qquad \text{where } R_\rho := (\nabla'v_\rho, b_{v_\rho}).$$

We claim that there exists a sequence $(\tilde{v}_{h,\rho}) \subset C^1(\bar{\Omega}; \mathbb{R}^3)$ that satisfies the clamped boundary conditions (13) and

$$\tilde{v}_{h,\rho} \to v_\rho \quad \text{uniformly in } \Omega, \quad (97a)$$
$$E_h(\tilde{v}_{h,\rho}) \xrightarrow{2} \iota(x_3\mathbb{I}_{v_\rho} + M) + \mathrm{sym} \nabla_\gamma \varphi \quad \text{strongly two-scale in } L^2(\Omega), \quad (97b)$$
$$\limsup_{h\to0} h\|E_h(\tilde{v}_{h,\rho})\|_{L^\infty(\Omega)} = 0 \quad \text{and} \quad \lim_{h\to0} \|\det(\nabla_h \tilde{v}_{h,\rho}) - 1\|_{L^\infty(\Omega)} = 0. \quad (97c)$$

Before we prove this claim we note that with the sequence $(\tilde{v}_{h,\rho})$ at hand, the searched for sequence is obtained (similar to Step 3 in the proof of Theorem 2.13) as a diagonal sequence , i.e., $v_h = \tilde{v}_{h,\rho(h)}$ for a suitable function $h \mapsto \rho(h)$ (note that the notion of strong two-scale convergence is metrizable). We leave the details to the reader and turn to the construction of $(\tilde{v}_{h,\rho})$: By Proposition 7.1 we can associate with v_ρ a sequence $(v_{h,\rho}) \subseteq C^1(\bar{\Omega}; \mathbb{R}^3)$ that satisfies (96) with $d = 0$ and the clamped boundary conditions (13). Furthermore, by Proposition 8.3 there exists a sequence $(\varphi_h) \subseteq C^\infty_c(\Omega)$ such that $\nabla_h\varphi_h \xrightarrow{2} \nabla_\gamma(R_\rho\varphi)$, and

$$h\|\varphi_h\|_{L^\infty(\Omega)} + h\|\nabla_h\varphi_h\|_{L^\infty(\Omega)} \to 0.$$

We now define

$$\tilde{v}_{h,\rho} := v_{h,\rho} + h\varphi_h.$$

Obviously, $\tilde{v}_{h,\rho}$ satisfies the clamped boundary conditions (13) (since φ_h is compactly supported in Ω). Statements (97a) and (97c) are also obvious by construction. It remains to prove (97b). To that end, we first note that by (96), for $h > 0$ sufficiently small, we have $\det(\nabla_h v_{h,\rho}(x)) > 0$ for all $x \in \Omega$. Thus, by the polar factorization, there exists a unique rotation field $R_{h,\rho} : \Omega \to SO(3)$ such that

$$\nabla_h v_{h,\rho} = R_{h,\rho}(I_{3\times 3} + h E_h(v_{h,\rho})), \tag{98}$$

and thus

$$\nabla_h \tilde{v}_{h,\rho} = R_{h,\rho}\Big(I_{3\times 3} + h G_h\Big), \qquad G_h := E_h(v_{h,\rho}) + R_{h,\rho}^\top \nabla_h \varphi_h.$$

By construction, we have $h \|G_h\|_{L^\infty(\Omega)} \to 0$, and thus a Taylor expansion yields

$$\sqrt{(\nabla_h \tilde{v}_{h,\rho})^\top \nabla_h \tilde{v}_{h,\rho}} = \sqrt{I_{3\times 3} + 2h \operatorname{sym} G_h + h^2 G_h^\top G_h} = I_{3\times 3} + h \operatorname{sym} G_h + h o_h$$

with a remainder $o_h : \Omega \to \mathbb{R}^{3\times 3}$ satisfying $\|o_h\|_{L^\infty(\Omega)} \to 0$. Thus, in order to prove (97b), we only need to show that

$$\operatorname{sym} G_h = E_h(v_{h,\rho}) + \operatorname{sym}\left(R_{h,\rho}^\top \nabla_h \varphi_h\right)$$
$$\xrightarrow{2} \iota(x_3 \mathbb{II}_{v_\rho} + M) + \operatorname{sym} \nabla_\gamma \varphi \quad \text{strongly two-scale in } L^2.$$

In view of (96), it suffices to show that $R_{h,\rho}^T \nabla_h \varphi_h \xrightarrow{2} \nabla_\gamma \varphi$. We first note that $R_{h,\rho} \to R_\rho$ in $L^2(\Omega)$, since the left-hand side of (98) converges in $L^2(\Omega)$ to R_ρ. We therefore conclude with help of Lemma 8.2 (c) that $R_{h,\rho}^\top \nabla_h \varphi_h \xrightarrow{2} R_\rho^\top (R_\rho \nabla_\gamma \varphi) = \nabla_\gamma \varphi$ weakly two-scale. On the other hand, the norm converges:

$$\|R_{h,\rho}^\top \nabla_h \varphi_h\|_{L^2(\Omega)}^2 = \|\nabla_h \varphi_h\|_{L^2(\Omega)}^2 \to \sum_{j \in J} \int_{S_j} \fint_{\square_{\wedge_j}} |\nabla_\gamma \varphi|^2 \mathrm{d}(x_3, y) \mathrm{d}x',$$

since $|R_{h,\rho}^\top(x') \nabla_h \varphi_h(x)| = |\nabla_h \varphi_h(x)|$ (recall $R_{h,\rho}^\top(x) \in SO(3)$), and because $\nabla_h \varphi_{h,\rho} \xrightarrow{2} R_\rho \nabla_\gamma \varphi$. This completes the proof of (97b). $\qquad\square$

7.6 Strong Two-Scale Convergence of the Nonlinear Strain: Proof of Proposition 3.4

For brevity we only present the proof in the single-grain case, i.e. we assume that $Y_j = Y_1$ for all $j \in J$. The argument extends without larger modifications to the general case.

Step 1 (Reduction of the problem) We first note that

$$
\mathcal{I}_{\mathrm{hom}}^{\gamma}(v_*) + \mathcal{I}_{\mathrm{res}}^{\gamma}(B) = \int_S \fint_{\square_{\Lambda_1}} Q(x, y, E_*(x, y)) \mathrm{d}(x_3, y) \mathrm{d}x'
$$
$$
= \min_{(M, \varphi)} \int_S \fint_{\square_{\Lambda_1}} Q(x, y, \iota(x_3 \mathbb{I}_{v_*} + M) + \mathrm{sym}\, \nabla_\gamma \varphi - B) \mathrm{d}(x_3, y) \mathrm{d}x',
$$

where the minimum runs over all $M \in L^2(S; \mathbb{R}_{\mathrm{sym}}^{2 \times 2})$ and $\varphi \in L^2(S; H_\gamma^1(\square_{\Lambda_1}; \mathbb{R}^3))$, see Lemma 2.29. With help of Theorem 2.8 (c) we choose a recovery sequence $(\tilde{v}_h)$ for v_* satisfying

$$
\lim_{h \to \infty} \mathcal{I}^{\varepsilon(h), h}(\tilde{v}_h) = \mathcal{I}_{\mathrm{hom}}^{\gamma}(v_*) + \mathcal{I}_{\mathrm{res}}^{\gamma}(B).
$$

Note that the recovery sequence constructed in Theorem 2.8 (c) additionally satisfies

$$
E_h(\tilde{v}_h) \xrightarrow{2} E_* \qquad \text{strongly two-scale in } L^2. \tag{99}
$$

We claim that the statement of the Proposition 3.4 follows from the following two claims:

$$
\limsup_{h \to 0} \int_\Omega Q\left(x, \frac{x'}{\varepsilon(h)}, \theta_h E_h(v_h) - E_h(\tilde{v}_h)\right) \mathrm{d}x = 0, \tag{100}
$$

$$
\limsup_{h \to 0} \int_\Omega (1 - \theta_h) |E_h(v_h)|^2 \mathrm{d}x = 0, \tag{101}
$$

where θ_h is the indicator function defined in (83). Indeed, since $E_h(v_h)$ and $E_h(\tilde{v}_h)$ are symmetric and since $Q \in \mathcal{Q}(\alpha, \beta)$, the combination of both statements, implies that $F_h := E_h(v_h) - E_h(\tilde{v}_h) \to 0$ strongly in $L^2(\Omega)$, and thus also strongly two-scale in L^2. In view of (99), this implies that $E_h(v_h) = E_h(\tilde{v}_h) + F_h \xrightarrow{2} E_*$ strongly two-scale in L^2, which is the claim of the Proposition 3.4.

We shall prove (100) and (101) in Steps 3 and 4, respectively.

Step 2 (Weak two-scale convergence towards E_*)
For brevity set $B_h(x) := B(x, \frac{x'}{\varepsilon(h)})$. We claim that

$$
E_h(v_h) \xrightarrow{2} E_* \qquad \text{weakly two-scale in } L^2, \tag{102}
$$

$$
\theta_h(E_h(v_h) - B_h) \xrightarrow{2} E_* - \mathrm{sym}\, B \qquad \text{weakly two-scale in } L^2, \tag{103}
$$

$$
\lim_{h \to 0} \frac{1}{h^2} \int_\Omega \theta_h W_{\varepsilon(h)}(x, \nabla_h v_h (I_{3 \times 3} - h B_{\varepsilon(h), h})) \mathrm{d}x
$$

$$
\begin{aligned}
&= \lim_{h\to 0} \int_\Omega Q\Big(x, \tfrac{x'}{\varepsilon(h)}, \theta_h(E_h(v_h) - B_h)\Big)\mathrm{d}x \\
&= \mathcal{I}^\gamma_{\mathrm{hom}}(v_*) + \mathcal{I}^\gamma_{\mathrm{res}}(B).
\end{aligned} \tag{104}
$$

Here comes the argument: By compactness, see Proposition 3.2 (a), we have (for a subsequence)

$$
E_h(v_h) \overset{2}{\rightharpoonup} \iota(x_3 \mathbb{I}_{v_*}) + M + \mathrm{sym}\, \nabla_\gamma \varphi \qquad \text{weakly two-scale in } L^2,
$$

for some corrector pair (M, φ). Moreover, we may additionally assume that $\int_S |\int_{\square_{\Lambda_1}} \varphi| = 0$. Next, we recall from Step 1 in the proof of Theorem 2.8 part (b) (cf. (86), (87) and (88)) that

$$
\begin{aligned}
\liminf_{h\to 0} \mathcal{I}^{\varepsilon(h),h}(v_h) &\geq \liminf_{h\to 0} \frac{1}{h^2} \int_\Omega \theta_h W_{\varepsilon(h)}(x, \nabla_h v_h(I_{3\times 3} - h B_{\varepsilon(h),h}))\mathrm{d}x \\
&\geq \liminf_{h\to 0} \int_\Omega Q\Big(x, \tfrac{x'}{\varepsilon(h)}, \theta_h(E_h(v_h) - B_h)\Big)\mathrm{d}x \\
&\geq \int_S \fint_{\square_{\Lambda_1}} Q(x', x_3, y, \iota(x_3 \mathbb{I}_{v_*} + M) + \mathrm{sym}\, \nabla_\gamma \varphi - B)\mathrm{d}(x_3, y)\mathrm{d}x' \\
&\geq \mathcal{I}^\gamma_{\mathrm{hom}}(v_*) + \mathcal{I}^\gamma_{\mathrm{res}}(B).
\end{aligned}
$$

In view of the convexity of Q and assumption (37), we can upgrade this lower bound to identity (104) as claimed. Furthermore, with Lemma 2.29 we conclude that (M, φ) are minimizers of the functional in the second last line, and we conclude that $M = M_*$ and $\varphi = \varphi_*$ (that is, $E = E_*$). Thus, (102) holds not only for the subsequence, but the entire sequence. Moreover, (103) then follows from (89).

Step 3 (Proof of (101))
For brevity set $w_h(x) := \frac{1}{h^2} W_{\varepsilon(h)}(x, \nabla_h v_h(x)(I_{3\times 3} - h B_{\varepsilon(h),h}(x)))$. By assumption we have $\int_\Omega w_h(x)\mathrm{d}x = \mathcal{I}^{\varepsilon(h),h}(v_h) \to \mathcal{I}^\gamma_{\mathrm{hom}}(v_*) + \mathcal{I}^\gamma_{\mathrm{res}}(B)$, and by (104) we have $\int_\Omega \theta_h w_h \mathrm{d}x \to \mathcal{I}^\gamma_{\mathrm{hom}}(v_*) + \mathcal{I}^\gamma_{\mathrm{res}}(B)$. Hence, since w_h is non-negative, we conclude that

$$
\int_\Omega (1 - \theta_h)|w_h| = \int_\Omega w_h - \int_\Omega \theta_h w_h \to 0.
$$

On the other hand, from the elementary, pointwise bound $|E_h(v_h)| \leq \frac{1}{h^2}\,\mathrm{dist}^2(\nabla_h v_h, \mathrm{SO}(3))$, (81), and ((W1)), we conclude that

$$
\alpha \int_\Omega (1 - \theta_h)|E_h(v_h)|^2 \leq \int_\Omega (1 - \theta_h)\Big(|w_h| + \frac{1}{2}h^2 |B_{\varepsilon(h),h}(x)|^4 + |B_{\varepsilon(h),h}|^2\Big).
$$

Thus, it remains to show that $\int_\Omega (1 - \theta_h)|B_{\varepsilon(h),h}|^2 \to 0$. The latter is a consequence of $\int_\Omega (1 - \theta_h)|B_{\varepsilon(h),h}|^2 \leq \|1 - \theta_h\|_{L^1(\Omega)} \|B_{\varepsilon(h),h}\|^2_{L^\infty(\Omega)}$, (84), and Assumption 2.5 (iv).

Step 4 (Proof of (100))

By adding and subtracting $B_h := B(x, \frac{x'}{\varepsilon(h)})$, and by expanding the square, we have

$$\int_\Omega Q\left(x, \tfrac{x'}{\varepsilon(h)}, \theta_h E_h(v_h) - E_h(\tilde{v}_h)\right) dx$$

$$= \int_\Omega Q\left(x, \tfrac{x'}{\varepsilon(h)}, \theta_h E_h(v_h) - B_h\right) dx - \int_\Omega Q\left(x, \tfrac{x'}{\varepsilon(h)}, E_h(\tilde{v}_h) - B_h\right) dx$$

$$+ 2 \int_\Omega \mathbb{L}(x, \tfrac{x'}{\varepsilon(h)})(E_h(\tilde{v}_h) - B_h) : (E_h(\tilde{v}_h) - \theta_h E_h(v_h)) dx.$$

It suffices to show that the right-hand side converges to 0 for $h \to 0$. The first integral converges by (104), while the second integral converges to the same limit, since $\tilde{v}_h$ is a recovery sequence. Thus, it remains to show that the third integral vanishes. Note that $E_h(\tilde{v}_h) - \theta_h E_h(v_h) \overset{2}{\rightharpoonup} 0$ weakly in L^2, since (103) and since $\tilde{v}_h$ is a recovery sequence. Since $\mathbb{L}(x, \tfrac{x'}{\varepsilon(h)})(E_h(\tilde{v}_h) - B_h)$ is strongly two-scale convergent in L^2, we may pass to the limit by appealing to Lemma 8.2 (c). We thus conclude that

$$\lim_{h \to 0} \int_\Omega \mathbb{L}(x, \tfrac{x'}{\varepsilon(h)})(E_h(\tilde{v}_h) - B_h) : (E_h(\tilde{v}_h) - \theta_h E_h(v_h)) dx = 0.$$

$\square$

7.7 Formulas for the Orthotopic Case: Proofs of Lemmas 4.2, 4.3, 4.5

Throughout this section we use the shorthand notation $\square := (-\tfrac{1}{2}, \tfrac{1}{2}) \times (-\tfrac{1}{2}, \tfrac{1}{2})^2$.

Proof of Lemma 4.2 *Step 1* (Symmetry properties) For $i = 1, 2, 3$ define $P^{(i)} \in \mathbb{R}^{3 \times 3}$ and $\pi^{(i)} : \square \to \square$ by

$$P^{(i)} := \begin{cases} \text{diag}(-1, 1, 1) & i = 1, \\ \text{diag}(1, -1, 1) & i = 2, \\ \text{diag}(1, 1, -1) & i = 3, \end{cases} \quad \pi^{(i)}(x_3, y_1, y_2) := \begin{cases} (x_3, -y_1, y_2) & i = 1, \\ (x_3, y_1, -y_2) & i = 2, \\ (-x_3, y_1, y_2) & i = 3, \end{cases}$$

and remark that thanks to the symmetries and isotropy of Q we have

$$Q(x_3, y, F) = Q\big(\pi^{(i)}(x_3, y), F\big) = Q\big(x_3, y, P^{(i)} F P^{(i)}\big), \tag{105}$$

for all $F \in \mathbb{R}^{3 \times 3}_{\text{sym}}$, a.e. $(x_3, y) \in \square$, and $i = 1, 2, 3$. As a consequence of these symmetries, we obtain for all $G \in \mathbb{R}^{2 \times 2}_{\text{sym}}$, $M \in \mathbb{R}^{2 \times 2}_{\text{sym}}$, and $\varphi \in H^1_\gamma(\square; \mathbb{R}^3)$ the identity

$$\int_\square Q\big(x_3, y, \iota(x_3 G) + \iota(M) + \text{sym} \nabla_\gamma \varphi\big)$$

$$= \begin{cases} \displaystyle\int_\square Q\big(x_3, y, P^{(i)} \iota(x_3 G) P^{(i)} + \iota(\widetilde{M}^{(i)}) + \text{sym} \nabla_\gamma \widetilde{\varphi}^{(i)}\big) & \text{for } i = 1, 2, \\ \displaystyle\int_\square Q\big(x_3, y, \iota(-x_3 G) + \iota(M) + \text{sym} \nabla_\gamma \widetilde{\varphi}^{(3)}\big) & \text{for } i = 3, \end{cases}$$

$$\text{(106)}$$

where

$$\widetilde{\varphi}^{(i)} := P^{(i)} \varphi \circ \pi^{(i)}, \qquad \widetilde{M}^{(i)} := \begin{cases} \text{diag}(-1, 1) M \text{diag}(-1, 1) & \text{for } i = 1, \\ \text{diag}(1, -1) M \text{diag}(1, -1) & \text{for } i = 2. \end{cases} \tag{107}$$

Indeed, this follows by a direct calculation using (105) and the identities

$$\nabla_\gamma \widetilde{\varphi}^{(i)} = P^{(i)} \big(\nabla_\gamma \varphi \circ \pi^{(i)} \big) P^{(i)}, \qquad P^{(3)} \iota(x_3 G + M) P^{(3)} = \iota(x_3 G + M).$$

Step 2 (Symmetries of the corrector)
Let $G \in \mathbb{R}^{2 \times 2}_{\text{sym}}$ and let (M_G, φ_G) denote the associated corrector in the sense of Lemma 2.23. We claim that

$$M_G = 0 \quad \text{and} \quad \varphi_G = \begin{cases} P^{(i)} \varphi_G \circ \pi^{(i)} & \text{if } i = 1, 2 \text{ and } G \text{ is diagonal,} \\ -P^{(i)} \varphi_G \circ \pi^{(i)} & \text{if } i = 1, 2 \text{ and } G \text{ vanishes on the diagonal,} \\ -P^{(3)} \varphi_G \circ \pi^{(3)} & \text{if } i = 3. \end{cases} \tag{108}$$

The proof is as follows: Identity (106) with $i = 3$ in combination with the characterization of the corrector as a minimizer (see Remark 2.24) implies that $(-M_G, -P^{(3)} \varphi_G \circ \pi^{(3)})$ is also a corrector associated with G. By uniqueness of the corrector, we especially conclude that $M_G = -M_G$. Hence, $M_G = 0$ and (40) follow. Likewise, we conclude that $\varphi_G = -P^{(3)} \varphi_G \circ \pi^{(3)}$. By the same argument and by using that for $i = 1, 2$ and all $G \in \mathbb{R}^{2 \times 2}_{\text{sym}}$ we have

$$P^{(i)} \iota(x_3 G) P^{(i)} = \begin{cases} \iota(x_3 G) & \text{if } G \text{ is diagonal,} \\ \iota(-x_3 G) & \text{if } G \text{ vanishes on the diagonal,} \end{cases}$$

the remaining identities follow. Since Q is independent of y_2 we conclude that $\partial_{y_2} \varphi_G = 0$ and $\varphi_G \circ \pi_2 = \varphi_G$. Combined with (108), we deduce that

$$\varphi_G = (\varphi_{G,1}, 0, \varphi_{G,3}) \quad \text{if } G \text{ is diagonal,}$$
$$\varphi_G = (0, \varphi_{G,2}, 0) \quad \text{if } G \text{ vanishes on the diagonal.} \tag{109}$$

In particular, (41) follows.

Step 3 (Conclusion)
To prove that Q^γ_{hom} is orthotopic, by Proposition 2.25 and since $M_{G_3} = 0$, it suffices to show that for $i = 1, 2$ we have

$$\int_\square \mathbb{L}(x_3, y_1)(\iota(x_3 G_3) + \text{sym} \nabla_\gamma \varphi_{G_3}) : \iota(x_3 G_i) = 0. \tag{110}$$

For the argument, note that in view of (39) we have

$$\mathbb{L}(x_3, y_1)G = \lambda(x_3, y_1)(\operatorname{tr}G)I_{3\times 3} + 2\mu(x_3, y_1)\operatorname{sym}G.$$

Furthermore, from (109) and the fact that φ_{G_3} is independent of y_2, we conclude that all diagonal entries of $\iota(x_3 G_3) + \operatorname{sym}\nabla_\gamma\varphi_{G_3}$ vanish a.e. in $\square$. We conclude (110) (and thus orthotropicity) and the identity (42). $\qquad\square$

Proof of Lemma 4.3 Throughout the proof, we will use the shorthand notation $\varphi_{i,3} = \partial_3\varphi \cdot e_i$ and $\varphi_{i,j} = \partial_{y_j}\varphi \cdot e_i$ for $i = 1, 2, 3$ and $j = 1, 2$. Since the setting under consideration is a special case of Lemma 4.2, we conclude that Q_{hom}^γ is orthotropic. Hence, it suffices to prove the formulas for the coefficients q_1, q_2, q_3, q_{12} and the properties of the map $\gamma \mapsto \mu_\gamma$.

Step 1 (Correctors for $i = 1, 2$ and coefficients q_1, q_2, q_{12})
Consider the following subspace of $H_\gamma^1(\square; \mathbb{R}^3)$,

$$\mathcal{H}_{\text{diag}} := \Big\{\varphi \in H_\gamma^1(\square; \mathbb{R}^3) : \varphi_{1,2} = \varphi_{3,2} = \varphi_2 = 0 \text{ a.e. in } \square, \text{ and } \fint_\square \varphi_1 = \fint_\square \varphi_3 = 0\Big\},$$

and note that by (41) we have $\varphi_{G_1}, \varphi_{G_2} \in \mathcal{H}_{\text{diag}}$. Since $M_{G_i} = 0$ by Lemma 4.2, and in view of the characterization of the corrector as a minimizer, we obtain for $i = 1, 2$ the identity

$$
\begin{aligned}
q_1 = Q_{\text{hom}}^\gamma(G_i) &= \fint_\square Q\big(x_3, y_1, \iota(x_3 G_i) + \operatorname{sym}\nabla_\gamma\varphi_{G_i}\big) \\
&= \min_{\varphi \in \mathcal{H}_{\text{diag}}} \fint_\square \mu(\tfrac{1}{\gamma}\varphi_{1,3} + \varphi_{3,1})^2 + 2\mu(\tfrac{1}{\gamma}\varphi_{3,3})^2 \\
&\quad + 2\mu(\delta_{i1}x_3 + \varphi_{1,1})^2 + 2\mu\delta_{i2}x_3^2,
\end{aligned}
$$

where $\delta_{ij} = 1$ for $i = j$ and $\delta_{ij} = 0$ for $i \neq j$. Based on this identity, one can check that for $i = 1$ we have $\varphi_{G_1} = (x_3 w, 0, W)$ with

$$w(y_1) := \int_{-\frac{1}{2}}^{y_1} \big(\frac{\langle\mu\rangle_\text{h}}{\mu} - 1\big)\mathrm{d}s, \qquad W(y_1) := -\frac{1}{\gamma}\Big(\int_{-\frac{1}{2}}^{y_1} w(s)\mathrm{d}s - \int_{-\frac{1}{2}}^{\frac{1}{2}}\int_{-\frac{1}{2}}^{t} w(s)\mathrm{d}s\mathrm{d}t\Big).$$

We compute

$$\nabla_\gamma\varphi_{G_1} = \big(\frac{\langle\mu\rangle_\text{h}}{\mu} - 1\big)\iota(x_3 G_1) \tag{111}$$

and conclude that $q_1 = Q_{\text{hom}}^\gamma(G_1) = \frac{1}{6}\langle\mu\rangle_\text{h}$ as claimed. Similarly, for $i = 2$, we get $\varphi_{G_2} = 0$ and thus $q_2 = Q_{\text{hom}}^\gamma(G_2) = \frac{1}{6}\overline{\mu}$. Combined with (111) and Proposition 2.25, we further conclude that

$$
\begin{aligned}
q_{12} &= \fint_\square \mathbb{L}(\iota(x_3 G_1 + M_{G_1}) + \operatorname{sym}\nabla_\gamma\varphi_{G_1}) : \iota(x_3 G_2) \\
&= \fint_\square 2\mu\big(\iota(x_3 G_1) + (\frac{\langle\mu\rangle_\text{h}}{\mu} - 1)\iota(x_3 G_1)\big) : \iota(x_3 G_2) = 0,
\end{aligned}
$$

since $\iota(x_3 G_1) : \iota(x_3 G_2) = 0$.

Step 2 (Corrector for $i = 3$, coefficient q_3, and properties of μ_γ)
For the argument it is convenient to introduce for $\gamma \in (0, \infty)$ the functional

$$\mathcal{E}_\gamma : \mathcal{H} \to \mathbb{R}, \quad \mathcal{E}_\gamma(w) := \fint_\square \mu\big((\sqrt{12}x_3 + \partial_{y_1} w)^2 + (\frac{1}{\gamma}\partial_3 w)^2\big).$$

We note that by construction, we have $\mu_\gamma = \min \mathcal{E}_\gamma$ where μ_γ is defined by (43b).
Moreover, by (41) in Lemma 4.2 we have $\varphi_{G_3} = (0, w_*, 0)$ for some $w_* \in \mathcal{H}$. As in
the previous step we thus conclude that

$$q_3 = Q_{\text{hom}}^\gamma(G_3) = \min_{w \in \mathcal{H}} \fint_\square \mu\big((\sqrt{2}x_3 + \partial_{y_1} w)^2 + (\frac{1}{\gamma}\partial_3 w)^2\big) = \frac{1}{6} \min_{w \in \mathcal{H}} \mathcal{E}_\gamma(w),$$
(112)

and thus the identity for q_3 in (46) follows.

Substep 2.1 (Proof of (44)). Taking $w = 0$ as a test function in (112), we obtain
$\frac{1}{6}\mu_\gamma \leq \fint_\square 2\mu x_3^2 = \frac{1}{6}\overline{\mu}$. On the other hand,

$$\langle\mu\rangle_{\text{h}} = \min_{w \in \mathcal{H}} \fint_\square \mu\big(\sqrt{12}x_3 + \partial_{y_1} w\big)^2 \leq \min_{w \in \mathcal{H}} \fint_\square \mu\big((\sqrt{12}x_3 + \partial_{y_1} w)^2 + (\frac{1}{\gamma}\partial_3 w)^2\big) = \mu_\gamma,$$

and thus (44) follows.

Substep 2.2 (Continuity of μ_γ). Let (γ_n) be a sequence that converges to $\gamma \in (0, \infty)$.
It is straightforward to check that $\mathcal{E}_{\gamma_n}$ Γ-converges to $\mathcal{E}_\gamma$ w.r.t. weak convergence in $\mathcal{H}$,
where we consider $\mathcal{H}$ as a closed subspace of $H_\gamma^1(\square; \mathbb{R})$. Hence, standard arguments
from the theory of Γ-convergence show that $\min \mathcal{E}_{\gamma_n} \to \min \mathcal{E}_\gamma$ and we conclude that
$\gamma \mapsto \mu_\gamma$ is continuous.

Substep 2.3 (Asymptotic behavior of μ_γ). We show that $\lim_{\gamma \to \infty} \mu_\gamma = \langle\mu\rangle_{\text{h}}$. Since
the map $\gamma \mapsto \mu_\gamma$ is monotone and bounded by (44), the limit $\lim_{\gamma \to \infty} \mu_\gamma$ exists.
To identify the limit, consider $w_\infty(x_3, y) := \sqrt{12}x_3 \int_{-\frac{1}{2}}^{y_1} (\frac{\langle\mu\rangle_{\text{h}}}{\mu(s)} - 1)\mathrm{d}s$ and note that
we have $w_\infty \in \mathcal{H}$ and $\langle\mu\rangle_{\text{h}} = \lim_{\gamma \to \infty} \mathcal{E}_\gamma(w_\infty)$. Combined with the lower bound
$\mathcal{E}_\gamma(w_\infty) \geq \mu_\gamma \geq \langle\mu\rangle_{\text{h}}$, we get $\langle\mu\rangle_{\text{h}} \geq \lim_{\gamma \to \infty} \mu_\gamma \geq \langle\mu\rangle_{\text{h}}$, and thus the claim follows.

Next, we prove $\lim_{\gamma \to 0} \mu_\gamma = \overline{\mu}$. As above, by monotonicity, the limit exists. Let
$w_\gamma \in \mathcal{H}$ be a minimizer of $\mathcal{E}_\gamma$. By (44) we have $\langle\mu\rangle_{\text{h}} \leq \mathcal{E}_\gamma(w_\gamma) \leq \overline{\mu}$, and thus
$\limsup_{\gamma \to 0} \fint_\square |\partial_{y_1} w_\gamma|^2 + |\frac{1}{\gamma}\partial_3 w_\gamma|^2 < \infty$. Hence, (w_γ) is bounded in $\mathcal{H}$ and we
can pass to a subsequence (not relabeled) such that $w_\gamma \rightharpoonup w_0$ weakly in $\mathcal{H}$, where w_0
satisfies $\partial_3 w_0 = 0$. By weak lower semicontinuity of convex functionals and since
$\fint_\square \mu(\sqrt{12}x_3 + \partial_{y_1} w_\gamma)^2 \leq \mathcal{E}_\gamma(w_\gamma) = \mu_\gamma \leq \overline{\mu}$, we conclude

$$\fint_\square \mu(\sqrt{12}x_3 + \partial_{y_1} w_0)^2 \leq \liminf_{\gamma \to 0} \fint_\square \mu(\sqrt{12}x_3 + \partial_{y_1} w_\gamma)^2 \leq \lim_{\gamma \to 0} \mathcal{E}_\gamma(w_\gamma) \leq \overline{\mu}.$$

On the other hand, since $\fint_\square \mu\sqrt{12}x_3\partial_{y_1}w_0 = 0$, we have

$$\fint_\square \mu\big(\sqrt{12}x_3 + \partial_{y_1}w_0\big)^2 = \fint_\square \mu(\sqrt{12}x_3)^2 + \fint_\square \mu(\partial_{y_1}w_0)^2 \geq \overline{\mu}. \quad (113)$$

We conclude that $\lim_{\gamma\to 0}\mu_\gamma = \overline{\mu}$.

Substep 2.4 (Strict monotonicity of μ_γ). It suffices to prove that if μ_γ is not strictly monotone, then μ is constant. For the argument, suppose that μ_γ is not strictly monotone. Since μ_γ is monotone, there exist $\gamma_1 < \gamma_2$ such that $(\gamma_1,\gamma_2) \ni \gamma \mapsto \mu_\gamma$ is constant. Hence $\frac{d}{d\gamma}\mathcal{E}_\gamma(w_\gamma) = 0$ for all $\gamma \in (\gamma_1,\gamma_2)$, where w_γ denotes the minimizer of $\mathcal{E}_\gamma$. By combining the latter with the Euler–Lagrange equation for w_γ, i.e.,

$$\fint_\square \mu\Big((\sqrt{12}x_3 + \partial_{y_1}w_\gamma)\partial_{y_1}\eta + \frac{1}{\gamma^2}\partial_3 w_\gamma \partial_3 \eta\Big) = 0 \quad \text{for all } \eta \in \mathcal{H}, \quad (114)$$

we find that $-2\gamma^{-3}\fint_\square \mu(\partial_3 w_\gamma)^2 = 0$. Hence, w_γ is independent of x_3, and thus $\mathcal{E}_\gamma(w_\gamma) = \overline{\mu} + \fint_\square \mu(\partial_{y_1}w_\gamma)^2$. Since w_γ minimizes $\mathcal{E}_\gamma$, we conclude that $w_\gamma = 0$ and thus (114) reduces to $\fint_\square \mu(\sqrt{12}x_3)\partial_{y_1}\eta = 0$, which especially holds for test-functions of the form $\eta(x_3,y_1) = x_3\tilde{\eta}(y_1)$. We thus conclude that $\mu = \fint_\omega \mu$ a.e. in $\square$ and the claim follows.

Step 3 (Evaluation of effective prestrain)
From Proposition 2.25 (b) we recall the definition of $\widehat{B} \in \mathbb{R}^3$, which we combine with (111), the identity $\varphi_{G_2} = 0$, and (42). We get

$$\widehat{B}_1 = 2\langle\mu\rangle_h \fint_\square \rho x_3 \mathrm{d}(x_3,y), \quad \widehat{B}_2 = 2\fint_\square \mu\rho x_3 \mathrm{d}(x_3,y), \quad \widehat{B}_3^\gamma = 0.$$

Furthermore, we recall from Proposition 2.25 that $\widehat{B}_{\text{eff}}^\gamma = \widehat{Q}^{-1}\widehat{B}$ and note that we have $\widehat{Q} = \frac{1}{6}\mathrm{diag}(\langle\mu\rangle_h, \overline{\mu}, \mu_\gamma)$ by Step 1 and Step 2. Now, (47) follows from a short calculation. $\qquad\square$

Proof of Lemma 4.5 This follows from Lemma 4.3 and direct computations. $\qquad\square$

Proof of Lemma 5.3 The proof is based on case discrimination depending on the sign of det H.
Step 1 (Case (a) and its logical complement)
By the invariance property (59) and identity (62) we have

$$\text{Case (a)} \Leftrightarrow \underset{a\in\mathcal{G}_{\mathbb{R}^2}^+}{\arg\min}\ \mathcal{E}_{Q,B}(a) \subset \partial\mathcal{G}_{\mathbb{R}^2}^+. \quad (115)$$

Suppose (a). Then the inclusion of $\mathcal{S}_{Q,B}$ claimed in (a) follows from (58). On the other hand, if (a) does not hold, then by (115), $\mathcal{E}_{Q,B}$ admits a local minimizer in the interior of $\mathcal{G}_{\mathbb{R}^2}^+$, and thus there exists $a \in \mathcal{G}_{\mathbb{R}^2}^+ \setminus \partial\mathcal{G}_{\mathbb{R}^2}^+$ such that $\nabla\mathcal{E}_{Q,B}(a) = 0$ and $\nabla^2\mathcal{E}_{Q,B}(a)$ is positive semi-definite. Since $\nabla^2\mathcal{E}_{Q,B} = H$ and $\text{trace}(H) = 2(q_1 + q_2) > 0$ (by

positive definiteness of Q), we have $\det H \geq 0$. Thus, to conclude the trichotomy, it suffices to show

$$\big(\neg(a) \text{ and } \det H > 0\big) \Leftrightarrow (b), \tag{116}$$

$$\big(\neg(a) \text{ and } \det H = 0\big) \Leftrightarrow (c). \tag{117}$$

Step 2 (Case (b) and proof of (116))
Suppose $\det H > 0$. Then $\mathcal{E}_{Q,B}$ is strictly convex and g_* is the unique minimizer of $\mathcal{E}_{Q,B}$ on $\mathbb{R}^2$ as can be seen by checking the identity $\nabla \mathcal{E}_{Q,B}(g_*) = 0$. In view of (115), the equivalence (b) follows. Furthermore, if (b) holds, then $\arg\min_{\mathcal{G}^+_{\mathbb{R}^2}} \mathcal{E}_{Q,B} = \{g_*\}$ and the characterization of $\mathcal{S}_{Q,B}$ claimed in (b) follows from (60).

Step 3 (Case (c) and proof of (117))
Let $\det H = 0$. Since $\text{trace}(H) = 2(q_1 + q_2) > 0$, H is positive semi-definite and thus $\mathcal{E}_{Q,B}$ is convex. Therefore, any critical point of $\mathcal{E}_{Q,B}$ is a minimizer of $\mathcal{E}_{Q,B}$ (in $\mathbb{R}^2$). Furthermore, we have $H = 2(q_1 + q_2)q_* \otimes q_*$.

Now assume that (a) is not valid. Then by the argument of Step 1, $\mathcal{E}_{Q,B}$ admits a critical point $a \in \mathcal{G}^+_{\mathbb{R}^2} \setminus \partial \mathcal{G}^+_{\mathbb{R}^2}$, and thus $0 = \nabla \mathcal{E}_{Q,B}(a) = Ha - 2Ab$. We conclude that $2Ab \in \text{range } H$, and thus (c) holds.

On the other hand, if (c) holds, then $2Ab = (2Ab \cdot q_*)q_*$, and thus $H(s_* q_*) = 2Ab$. Hence, $g_* = s_* q_*$ is a critical point. In fact, every point on the line $\mathcal{L} := \{a \in \mathbb{R}^2 : a \cdot q_* = s_*\}$ is a critical point and thus a minimizer of $\mathcal{E}_{Q,B}$. In order to conclude $\neg(a)$ (and thus the validity of (117)), we only need to show that $\mathcal{L} \cap (\mathcal{G}^+_{\mathbb{R}^2} \setminus \partial \mathcal{G}^+_{\mathbb{R}^2}) \neq \emptyset$. The latter can be seen as follows: We parametrize $\mathcal{L}$ by $\ell : \mathbb{R} \to \mathbb{R}^2, \ell(t) := s_* q_* + t(-q_{*,2}, q_{*,1})$ and consider the function $\varphi(t) := (s_* q_{*,1} - tq_{*,2})(s_* q_{*,2} + tq_{*,1})$. By construction we have $\ell(t) \in \mathcal{G}^+_{\mathbb{R}^2} \setminus \partial \mathcal{G}^+_{\mathbb{R}^2}$ if and only if $\varphi(t) > 0$. It is easy to see that φ is concave. We claim that

$$\varphi(0) = s_*^2 q_{*,1} q_{*,2} > 0. \tag{118}$$

Indeed, combining (57) with the identity $0 = \det H = 4q_1 q_2 - (q_{12} + 2q_3)^2$ yields $q_{12} + q_3 > 0$ and thus $2q_2(q_{12} + 2q_3) > 0$. In view of the definition of q_* and the property $s_*^2 > 0$ (which follows from $b \neq 0$), we obtain (118). Since φ is concave and continuous, we conclude from (118) that $\{t \in \mathbb{R} : \varphi(t) \geq 0\}$ is an interval with non-empty interior, and thus $\mathcal{L} \cap \mathcal{G}^+_{\mathbb{R}^2} \setminus \partial \mathcal{G}^+_{\mathbb{R}^2} \neq \emptyset$ follows. This completes the argument for (116). Furthermore, the above argument proves the characterization of $\mathcal{S}_{Q,B}$ stated in (c). □

7.8 Shape Programming: Proofs of Lemma 6.2, Corollary 6.3, Lemma 6.7, and Theorem 6.6

Proof of Lemma 6.2 For convenience set $\square := \square_\Lambda$ and $\widetilde{\square} := \square_{\widetilde{\Lambda}}$.

Step 1 (Reduction using linearity)
We first note that the map

$$\Phi : \mathbf{H}_{\widetilde{\Lambda}} \to \mathbf{H}_\Lambda, \qquad \Phi(\tilde{F}) := F, \qquad \text{where } F(x_3, y) := \widehat{T}^\top \tilde{F}(x_3, Ty)\widehat{T},$$

is an isometric isomorphism. In particular, for all $\tilde{F}, \tilde{G} \in \mathbf{H}_{\tilde{\Lambda}}$ we have

$$\fint_{\tilde{\square}} \tilde{Q}(x_3, y, \tilde{F}) = \fint_{\square} Q(x_3, y, \Phi(\tilde{F})), \qquad \fint_{\tilde{\square}} \tilde{\mathbb{L}}\tilde{F} : \tilde{G} = \fint_{\square} \mathbb{L}\Phi(\tilde{F}) : \Phi(\tilde{G}).$$

Furthermore, the map

$$H_\gamma^1(\square_\Lambda; \mathbb{R}^3) \to H_\gamma^1(\square_{\tilde{\Lambda}}; \mathbb{R}^3), \qquad \varphi \mapsto \tilde{\varphi}, \qquad \tilde{\varphi}(x_3, y) = \widehat{T}^{-\top}\varphi(x_3, T^{-1}y),$$

defines an isomorphism satisfying $\Phi\big(\mathrm{sym}\,\nabla_\gamma\tilde{\varphi}\big) = \mathrm{sym}\,\nabla_\gamma\varphi$. With help of this identity it is easy to check that $\Phi(\mathbf{H}_{\mathrm{rel},\tilde{\Lambda}}^\gamma) = \mathbf{H}_{\mathrm{rel},\Lambda}^\gamma$ and $\Phi(\mathbf{H}_{\tilde{\Lambda}}^\gamma) = \mathbf{H}_\Lambda^\gamma$.

Step 2 (Reduction using projections)
We claim that

$$\Phi(P_{\tilde{\Lambda}}^\gamma \tilde{B}) = P_\Lambda^\gamma B. \tag{119}$$

Indeed, by the definition of $\tilde{B}$ and the properties of Φ, we have for all $F \in \mathbf{H}_\Lambda^\gamma$,

$$\fint_{\square} \mathbb{L}\big(\Phi(P_{\tilde{\Lambda}}^\gamma(\mathrm{sym}\,\tilde{B}) - \mathrm{sym}\,B) : F = \fint_{\tilde{\square}} \tilde{\mathbb{L}}\big(P_{\tilde{\Lambda}}^\gamma(\mathrm{sym}\,\tilde{B}) - \mathrm{sym}\,\tilde{B}\big) : \Phi^{-1}(F) = 0,$$

where the last identity holds, since $\Phi^{-1}(F) \in \mathbf{H}_{\tilde{\Lambda}}^\gamma$ and because $P_{\tilde{\Lambda}}^\gamma$ is the orthogonal projection onto $\mathbf{H}_{\tilde{\Lambda}}^\gamma$.

Step 3 (Conclusion)
Let $\tilde{G} \in \mathbb{R}_{\mathrm{sym}}^{2\times 2}$. Then by Step 1,

$$\begin{aligned}
\tilde{Q}_{\mathrm{hom}}^\gamma(\tilde{G}) &= \inf_{\tilde{\chi}\in\mathbf{H}_{\mathrm{rel},\tilde{\Lambda}}^\gamma} \fint_{\tilde{\square}} \tilde{Q}(x_3, y, \iota(x_3\tilde{G}) + \tilde{\chi}) = \inf_{\tilde{\chi}\in\mathbf{H}_{\mathrm{rel},\tilde{\Lambda}}^\gamma} \fint_{\square} Q\big(x_3, y, \Phi(\iota(x_3\tilde{G}) + \tilde{\chi})\big) \\
&= \inf_{\chi\in\mathbf{H}_{\mathrm{rel},\Lambda}^\gamma} \fint_{\square} Q\big(x_3, y, \iota(x_3 T^\top \tilde{G} T) + \chi\big) = Q_{\mathrm{hom}}^\gamma(T^\top \tilde{G} T),
\end{aligned}$$

as claimed. Similarly,

$$\begin{aligned}
&\tilde{Q}_{\mathrm{hom}}^\gamma(\tilde{G} - \tilde{B}_{\mathrm{eff}}^\gamma) + \fint_{\tilde{\square}} \tilde{Q}(x_3, y, (I - P_{\tilde{\Lambda}}^\gamma)(\mathrm{sym}\,\tilde{B})) \\
&= \inf_{\tilde{\chi}\in\mathbf{H}_{\mathrm{rel},\tilde{\Lambda}}^\gamma} \fint_{\tilde{\square}} \tilde{Q}(x_3, y, \iota(x_3\tilde{G}) + \tilde{\chi} - \tilde{B}) = \inf_{\chi\in\mathbf{H}_{\mathrm{rel},\Lambda}^\gamma} \fint_{\square} Q\big(x_3, y, \iota(x_3 T^\top \tilde{G} T) + \chi - B\big) \\
&= Q_{\mathrm{hom}}^\gamma(T^\top \tilde{G} T - B_{\mathrm{eff}}^\gamma) + \fint_{\square} Q(x_3, y, (I - P_\Lambda^\gamma)(\mathrm{sym}\,B)).
\end{aligned}$$

From (119) and the properties of Φ, we deduce that on both sides the second integrals are equal, and thus

$$\tilde{Q}_{\mathrm{hom}}^\gamma(\tilde{G} - \tilde{B}_{\mathrm{eff}}^\gamma) = Q_{\mathrm{hom}}^\gamma(T^\top \tilde{G} T - B_{\mathrm{eff}}^\gamma).$$

Since this is true for arbitrary $\tilde{G} \in \mathbb{R}^{2 \times 2}_{\text{sym}}$, we conclude that $\tilde{B}^{\gamma}_{\text{eff}} = T^{-\top} B^{\gamma}_{\text{eff}} T^{-1}$ as claimed. $\qquad\square$

Proof of Corollary 6.3 Note that for all $G \in \mathbb{R}^{3 \times 3}$ we have by frame indifference

$$W(R, \kappa; x_3, y, I_{3 \times 3} + G) = \bar{W}(\kappa; x_3, R^\top y, I_{3 \times 3} + R^\top G R).$$

Thus, the quadratic forms associated with $W(R, \kappa; \cdot)$ and $\bar{W}(\kappa; \cdot)$ transform as in Lemma 6.2, that is,

$$Q(R, \kappa; x_3, y, G) = \bar{Q}(\kappa; x_3, R^\top y, R^\top G R).$$

With help of Lemma 6.2 it is straightforward to check the claims of the corollary. $\quad\square$

Proof of Lemma 6.7 *Step 1* (Proof of (a))
W.l.o.g. we may assume $\int_S v_n = 0$. From (70) we get

$$\frac{\alpha}{2} \int_S |\mathbb{I}_{v_n}|^2 \leq \mathcal{I}_n(v_n) + \alpha \|B_n\|^2_{L^2(S)},$$

and thus we have $\|\mathbb{I}_{v_n}\|^2_{L^2(S)} < \infty$. Since $|\mathbb{I}_{v_n}|^2 = |\nabla'\nabla' v_n|^2$, the Poincaré–Wirtinger inequality implies that $\limsup_{n \to \infty} \|v_n\|_{H^2(S;\mathbb{R}^3)} < \infty$. Therefore, we may pass to a subsequence that weakly converges in $H^2(S; \mathbb{R}^3)$ to some limit v. Since $H^2_{\text{iso}}(S; \mathbb{R}^3)$ is weakly closed, we conclude that $v \in H^2_{\text{iso}}(S; \mathbb{R}^3)$.

Step 2 (Proof of (b))
We first note that the construction of a recovery sequence (v_n) for $v \in H^2_{\text{iso}}(S; \mathbb{R}^3)$ is trivial, since we just may consider the constant sequence $v_n = v$. To prove the lower bound part of Γ-convergence, consider a sequence $(v_n) \subset H^2_{\text{iso}}(S; \mathbb{R}^3)$ that weakly converges in H^2 to some $v_\infty \in H^2(S; \mathbb{R}^3)$. We need to show that

$$\liminf_{n \to \infty} \mathcal{I}_n(v_n) \geq \mathcal{I}_\infty(v_\infty).$$

For the argument set $F_n := \mathbb{I}_{v_n} - B_n$ (for $n \in \mathbb{N} \cup \{\infty\}$) and note that we have

$$F_n \rightharpoonup F_\infty \qquad \text{weakly in } L^2. \tag{120}$$

By expanding the square and by positivity of Q_n, we have

$$\int_S Q_n(x', F_n) = \int_S Q_n(x', F_\infty) + Q_n(x', F_n - F_\infty) + \mathbb{L}_n(x')F_\infty : (F_n - F_\infty)$$

$$\geq \int_S Q_n(x', F_\infty) + \mathbb{L}_n(x')F_\infty : (F_n - F_\infty).$$

Thanks to the convergence of Q_n we have $\int_S Q_n(x', F_\infty) \to \int_S Q_\infty(x', F_\infty) = \mathcal{I}_\infty(v_\infty)$. Moreover, the assumption on Q_n implies that $\mathbb{L}_n(x')F_\infty \to \mathbb{L}_\infty(x')F_\infty$ strongly in $L^2(S)$. Together with (120) this yields $\int_S \mathbb{L}_n(x')F_\infty : (F_n - F_\infty) \to 0$.

Step 3 (Proof of (c))

Standard arguments from the theory of Γ-convergence imply that we have $v_n \rightharpoonup v_\infty$ weakly in H^2 (up to extraction of a subsequence) where $v_\infty \in H^2_{\text{iso}}(S; \mathbb{R}^3)$ is a minimizer of $\mathcal{I}^\gamma_{\text{hom},\infty}$. In the following we explain how to upgrade this to $v_n \to v_\infty$ strongly in H^2. Note that it suffices to show

$$\|\mathbb{I}_{v_n} - \mathbb{I}_{v_\infty}\|_{L^2(S)} \to 0. \tag{121}$$

Indeed, thanks to the identity $|\mathbb{I}_{v_n}|^2 = |\nabla'\nabla' v_n|^2$, (121) implies $\|\nabla'\nabla' v_n\|_{L^2(S)} \to \|\nabla'\nabla' v\|_{L^2(S)}$, and thus $\nabla'\nabla' v_n \to \nabla'\nabla' v$ strongly in L^2. To see (121) we argue that

$$\int_S Q_n(x', \mathbb{I}_{v_n} - \mathbb{I}_{v_\infty}) \to 0.$$

The latter can be seen as follows: By adding and subtracting B_n, and by expanding the square, we get

$$\int_S Q_n(x', \mathbb{I}_{v_n} - \mathbb{I}_{v_\infty})$$
$$= \int_S Q_n(x', \mathbb{I}_{v_n} - B_n) - \int_S Q_n(x', \mathbb{I}_{v_\infty} - B_n) + 2\int_S \mathbb{L}_n(x')(\mathbb{I}_{v_\infty} - B_n) : (\mathbb{I}_{v_\infty} - \mathbb{I}_{v_n}).$$

Since (v_n) is a sequence of minimizers, and since v_∞ is a minimizer of the Γ-limit, we have $\int_S Q_n(x', \mathbb{I}_{v_n} - B_n) \to \int_S Q_\infty(x', \mathbb{I}_{v_\infty} - B_\infty)$. Similarly, the second term $\int_S Q_n(\mathbb{I}_{v_\infty} - B_n)$ converges to the same limit, since Q_n and B_n converge by assumption. It remains to show that the last term converges to 0. This is the case, since $\mathbb{L}_n(\mathbb{I}_{v_\infty} - B_n)$ strongly converges in L^2, and $\mathbb{I}_{v_n} \rightharpoonup \mathbb{I}_{v_\infty}$ weakly in L^2. $\qquad\square$

Proof of Theorem 6.6 *Step 1* (Approximation of $\mathbb{I}_*$)

We claim that there exist sequences $(\kappa_n) \subset L^2(S)$ and $(R_n) \subset L^2(S; SO(2))$ such that

$$\kappa_n(R_n e_1 \otimes R_n e_1) \to \mathbb{I}_* \text{ strongly in } L^2,$$
$$(\kappa_n), (R_n) \text{ strongly converge in } L^2,$$

and for each $n \in \mathbb{N}$, the functions κ_n, R_n are piecewise constant functions subject to a partition of S (up to a null-set) into finitely many open, mutually disjoint sets; (in fact, the argument below yields a specific partition of S into equally sized lattice-squares contained in S and a remaining set close to the boundary of S). We prove this claim in two steps. In the first step, we establish the representation $\mathbb{I}_* = \kappa(Re_1 \otimes Re_1)$ with $\kappa \in L^2(S)$ and $R : S \to SO(2)$ measurable. In the second step, we approximate κ and R by functions $\kappa_n : S \to \mathbb{R}$ and $R_n : S \to SO(2)$ that are piecewise constant subordinate to a finite partition of S. The approximation κ_n can be easily obtained, e.g., by an L^2-projection of κ onto the piecewise constant functions. On the other hand, the construction of R_n is a bit more delicate, since the target manifold $SO(2)$ is a non-convex subset of $\mathbb{R}^{2\times2}$. Therefore, in the first step we additionally show that the R

in the representation of $\mathbb{I}_*$ can be chosen to be locally Lipschitz. For the construction of (κ_n, R_n) it is convenient to consider a dyadic decomposition of S: Below, we denote by $\mathcal{Q}_{\mathrm{dyadic}} := \{2^{-n}(\mathbb{Z}^2 + [-\frac{1}{2}, \frac{1}{2})^2) : n \in \mathbb{N}\}$ the set of dyadic squares in $\mathbb{R}^2$, and by $x_\square \in 2^{-n}\mathbb{Z}^2$, $n \in \mathbb{N}$, the center point of the cube $\square := x_\square + 2^{-n}[-\frac{1}{2}, \frac{1}{2})^2 \in \mathcal{Q}_{\mathrm{dyadic}}$.

Substep 1.1. (Representation of $\mathbb{I}_*$). We claim that there exist $\kappa \in L^2(S)$, $R : S \to$ SO(2) measurable, and a partition $\{\square\}_{\square \in \mathcal{Q}}$ of S into (at most countably many) dyadic, mutually disjoint squares $\square \in \mathcal{Q} \subset \mathcal{Q}_{\mathrm{dyadic}}$ such that

$$\mathbb{I}_* = \kappa(Re_1 \otimes Re_1) \text{ almost everywhere in } S, \tag{122}$$

and for all $\square \in \mathcal{Q}$ the restriction $R|_\square$ is Lipschitz with

$$\mathrm{Lip}(R|_\square) \le C \, \mathrm{dist}(\square, \mathbb{R}^2 \setminus S)^{-1}, \tag{123}$$

for a universal constant C. For the argument let $\mathcal{Q}$ denote a dyadic Whitney covering, that is, $\mathcal{Q}$ is a countable family of mutually disjoint, dyadic squares of the form $\square \in 2^{-n}(\mathbb{Z}^2 + [-\frac{1}{2}, \frac{1}{2})^2)$, $n \in \mathbb{N}$, such that

$$S = \bigcup_{\square \in \mathcal{Q}} \square, \quad \forall \square \in \mathcal{Q} : \frac{1}{30}\mathrm{dist}(\square, \mathbb{R}^2 \setminus S) \le \mathrm{diam}(\square) \le \frac{1}{10}\mathrm{dist}(\square, \mathbb{R}^2 \setminus S).$$

Let $\square \in \mathcal{Q}$. By construction there exists a ball B such that $\square \subset B \subset 2B \subset S$. Thus, we may apply (Neukamm and Olbermann 2015, Lemma 8) to obtain a Lipschitz field $\xi : \square \to S^1$ such that $\mathbb{I}_*(x') \in \mathrm{span}(\xi(x') \otimes \xi(x'))$ for a.e. $x' \in \square$, and $\mathrm{Lip}(\xi) \le \frac{2}{\mathrm{diam}(\square)}$. Since $\mathrm{SO}(2) \ni R \mapsto Re_1 \in S^1$ is a diffeomorphism, we find a Lipschitz field $R : \square \to \mathrm{SO}(2)$ such that $\xi = Re_1$ and $\mathrm{Lip}(R) \le C \, \mathrm{dist}(\square, \mathbb{R}^2 \setminus S)^{-1}$. The representation (122) (on $\square$) then follows by setting $\kappa := \mathbb{I}_* : (Re_1 \otimes Re_1)$. Since this can be done for all $\square \in \mathcal{Q}$, the claim follows.

Substep 1.2. (Conclusion). We only explain the construction of (R_n), since the "linear" construction of κ_n is easier. Here comes the argument: For $n \in \mathbb{N}$ set $S_n := \bigcup\{\square : \square \in \mathcal{Q} \text{ with } \mathrm{diam}(\square) \ge 2^{-n}\}$. By construction, this is a finite union of squares in $\mathcal{Q}$ and we have $S_n \uparrow S$ for $n \to \infty$. We partition S_n into (finer) dyadic squares with diameter 2^{-2n}. To that end set $\mathcal{Q}_n := \{\square \in \mathcal{Q}_{\mathrm{dyadic}} : \mathrm{diam}(\square) = 2^{-2n} \text{ and } \square \subseteq S_n\}$. We now define the piecewise constant approximation $R_n : S \to \mathrm{SO}(2)$ as

$$R_n(x') := \begin{cases} R(x_\square) & \text{if } x' \in \square \text{ for some } \square \in \mathcal{Q}_n, \\ I_{2\times 2} & \text{else.} \end{cases}$$

(Recall that $x_\square$ denotes the center point of $\square$). We claim that $R_n(x') \to R(x)$ for all $x' \in S$ (and thus strongly in L^2 by the dominated convergence theorem). For the argument let $x' \in S_n$ and choose $n \in \mathbb{N}$ large enough such that $x' \in S_n$. Then there exists $\square \in \mathcal{Q}_n$ with $x' \in \square$ and $\square' \in \mathcal{Q}$ with $\square \subset \square'$ and $\mathrm{diam}(\square') \ge 2^{-n}$. Hence,

by (123)

$$|R_n(x') - R(x')| = |R(x_\square) - R(x')| \leq \mathrm{diam}(\square)\,\mathrm{Lip}(\kappa|_{\square'}) \leq C2^{-2n}2^n,$$

and thus $R_n(x') \to R(x')$ for $n \to \infty$.

Step 2 (Definition of a sequence of structured composites and its limit)
For $n \in \mathbb{N}$ we define, as in Corollary 6.3,

$$W_n(x, y, F) := \bar{W}(\kappa_n(x'); x_3, R_n(x')^\top y, F\widehat{R}_n(x')),$$
$$B_n(x, y) := \widehat{R}_n(x')\bar{B}(\kappa_n(x'); x_3, R_n(x')^\top y)\widehat{R}_n^\top(x'),$$

and note that (W_n, B_n) is a structured composite. (We remark that (W_n, B_n) is Borel measurable, since $(\bar{W}, \bar{B})$ is measurable and (κ_n, R_n) is piecewise constant subordinate to a finite partition of S into measurable sets). By Theorem 2.8, the functionals $\mathcal{I}_n^h$: $H^1(\Omega; \mathbb{R}^3) \to [0, \infty]$,

$$\mathcal{I}_n^h(v) := \frac{1}{h^2}\int_\Omega W_n(x, \tfrac{x'}{\varepsilon(h)}, \nabla_h v(x)(I_{3\times 3} - hB_n(x, \tfrac{x'}{\varepsilon(h)})))\mathrm{d}x.$$

Γ-converge for $h \to 0$ to a functional of the form $\mathcal{I}_{\mathrm{hom},n}^\gamma(\cdot) + \mathcal{I}_{\mathrm{res}}^\gamma(B_n)$ with

$$\mathcal{I}_{\mathrm{hom},n}^\gamma(v) = \begin{cases} \int_S Q_{\mathrm{hom},n}^\gamma(x', \mathrm{II}_v - B_{\mathrm{eff},n}^\gamma(x'))\mathrm{d}x' & \text{for } v \in H_{\mathrm{iso}}^2(S; \mathbb{R}^3), \\ \infty & \text{else.} \end{cases}$$

Since (W_n, B_n) is defined by locally rotating the building block $(\bar{W}, \bar{B})$, we deduce with help of Corollary 6.3 that

$$Q_{\mathrm{hom},n}^\gamma(x', G) = Q_{\mathrm{hom}}^\gamma(\kappa_n(x'); R_n(x')^\top G R_n(x')),$$
$$B_{\mathrm{hom},n}^\gamma(x') = R_n(x')\bar{B}_{\mathrm{eff}}^\gamma(\kappa_n(x'))R_n(x')^\top.$$

Furthermore, from the pointwise convergence of (κ_n, R_n) we infer that for a.e. $x' \in S$ and $G \in \mathbb{R}_{\mathrm{sym}}^{2\times 2}$ we have

$$Q_{\mathrm{hom},n}^\gamma(x', G) \to Q_{\mathrm{hom}}^\gamma(x', G) := Q_{\mathrm{hom}}^\gamma(\kappa(x'); R(x')^\top G R(x')),$$
$$B_{\mathrm{eff},n}^\gamma(x') \to B_{\mathrm{eff}}^\gamma(x') := R(x')\bar{B}_{\mathrm{eff}}^\gamma(\kappa(x'))R(x')^\top,$$

as $n \to \infty$. Hence, Lemma 6.7 implies that $\mathcal{I}_{\mathrm{hom},n}^\gamma$ Γ-converges for $n \to \infty$ to the functional

$$\mathcal{I}_{\mathrm{hom}}^\gamma(v) = \int_S Q_{\mathrm{hom}}^\gamma(x', \mathrm{II}_v(x') - B_{\mathrm{eff}}^\gamma(x'))\mathrm{d}x'.$$

In view of the definition of $(Q_{\mathrm{hom}}^\gamma, B_{\mathrm{eff}}^\gamma)$ and the identity $\mathrm{II}_* = \kappa(Re_1 \otimes Re_1)$, the algebraic minimization problem $\mathbb{R}_{\mathrm{sym}}^{2\times 2} \ni G \mapsto Q_{\mathrm{hom}}^\gamma(x', G - B_{\mathrm{eff}}^\gamma(x'))$ subject to $\det G = 0$ is uniquely minimized by $G = \mathrm{II}_*(x')$ for a.e. $x' \in S$. We thus conclude

that the minimizer of $\mathcal{I}^\gamma_{\mathrm{hom}}$ is unique in the sense that any minimizer $v_* \in H^2_{\mathrm{iso}}(S; \mathbb{R}^3)$ of $\mathcal{I}^\gamma_{\mathrm{hom}}$ satisfies

$$\mathbb{II}_{v_*} = \mathbb{II}_* \text{ a.e. in } S. \tag{124}$$

Step 3 (Convergence of minimizers as $n \to \infty$)
We consider

$$\Delta_n := \sup\{\|\mathbb{II}_{v_*} - \mathbb{II}_*\|_{L^2(S)} \, : \, v_* \in \arg\min \mathcal{I}^\gamma_{\mathrm{hom},n}\},$$

and claim that $\lim\limits_{n\to\infty} \Delta_n = 0$. For the argument, we choose $v_n \in \arg\min \mathcal{I}^\gamma_{\mathrm{hom},n}$ with $\fint_S v_n = 0$ such that

$$\Delta_n \le \|\mathbb{II}_{v_n} - \mathbb{II}_*\|_{L^2(S)} + \frac{1}{n}. \tag{125}$$

By passing to a subsequence (not relabeled) we may assume that $\limsup\limits_{n\to\infty} \Delta_n = \lim\limits_{n\to\infty} \Delta_n$ and that $v_n \rightharpoonup v_\infty$ weakly in $H^2(S; \mathbb{R}^3)$ for some $v_\infty \in H^2_{\mathrm{iso}}(S; \mathbb{R}^3)$. An application of Lemma 6.7 shows that $v_\infty \in \arg\min \mathcal{I}^\gamma_{\mathrm{hom}}$, and thus $\mathbb{II}_{v_\infty} = \mathbb{II}_*$ in view of (124). Moreover, the lemma implies that $v_n \to v_\infty$ strongly in $H^2(S; \mathbb{R}^3)$, and thus we conclude that $\mathbb{II}_{v_n}) \to \mathbb{II}_{v_\infty} = \mathbb{II}_*$ strongly in $L^2(S)$, which in combination with (125) implies $\Delta_n \to 0$.

Step 4 (Conclusion)
By Step 3 we may choose n large enough such that

$$\sup\{\|\mathbb{II}_{v_*} - \mathbb{II}_*\|_{L^2(S)} \, : \, v_* \in \arg\min \mathcal{I}^\gamma_{\mathrm{hom},n}\} \le \delta. \tag{126}$$

We claim that (W_n, B_n) is the sought after finitely structured composite. Indeed, if $(v_h) \subset H^1(\Omega; \mathbb{R}^3)$ is an almost minimizing sequence with $\fint_\Omega v_h = 0$, then Theorem 2.8 (a) implies that from any subsequence we can extract a subsequence that converges in the sense of (10) to a limit $v_* \in H^2_{\mathrm{iso}}(S; \mathbb{R}^3)$. Since $\mathcal{I}^h_n \to \mathcal{I}^\gamma_{\mathrm{hom},n} + \mathcal{I}^\gamma_{\mathrm{res}}(B_n)$ in the sense of Γ-convergence, we conclude that v_* is a minimizer of the limiting energy and thus of $\mathcal{I}^\gamma_{\mathrm{hom},n}$. Finally, $\|\mathbb{II}_v - \mathbb{II}_*\|_{L^2(S)} \le \delta$ follows from (126). $\qquad\square$

Data Availability Statement Data sharing not applicable to this article as no datasets were generated or analyzed during the current study.

8 Appendix

8.1 Spaces of Λ-Periodic Functions

In this section we introduce various function spaces for periodic functions. Unless stated otherwise, in this section, Λ denotes a matrix in $\mathbb{R}^{2\times 2}$ such that $\Lambda^\top \Lambda > 0$. The column–vectors of Λ generate a Bravais lattice and we consider functions that are periodic w.r.t. this lattice. From Definition 2.4 (i) we recall that $u : \mathbb{R}^2 \to \mathbb{R}$ is called Λ-periodic, if $u(y + \tau) = u(y)$ for all $\tau \in \Lambda\mathbb{Z}^2$ and almost every $y \in \mathbb{R}^2$. We associate with Λ the parallelogram $Y_\Lambda := \Lambda[-\frac{1}{2}, \frac{1}{2})^2$. It represents the *reference cell of Λ-periodicity*. We denote by

$$C(\Lambda) := \{u \in C(\mathbb{R}^2) \ : \ u \text{ is } \Lambda\text{-periodic.}\},$$

the space of continuous, Λ-periodic functions; it is a Banach space when endowed with the norm $\|u\|_{L^\infty(Y_\Lambda)}$. We denote by

$$L^p(\Lambda) := \{u \in L^p_{\mathrm{loc}}(\mathbb{R}^2) \ : \ u \text{ is } \Lambda\text{-periodic.}\},$$

the space of Λ-periodic L^p-functions; it is a Banach space when endowed with the norm of $L^p(Y_\Lambda)$. We denote by

$$H^1(\Lambda) := \{u \in H^1_{\mathrm{loc}}(\mathbb{R}^2) \ : \ u \text{ is } \Lambda\text{-periodic.,}\}$$

the space of Λ-periodic H^1-functions; it is a Hilbert space when endowed with the norm of $H^1(Y_\Lambda)$.

In this paper, we simultaneously have to deal with L^2-functions that are periodic w.r.t. different lattices. Therefore, for the analysis, it is convenient to introduce the common superspace

$$L^2_{\mathrm{uloc}}(\mathbb{R}^2) := \{u \in L^2_{\mathrm{loc}}(\mathbb{R}^2) \ : \ \|u\|_{L^2_{\mathrm{uloc}}} < \infty\},$$
$$\|u\|_{L^2_{\mathrm{uloc}}} := \sup_{z \in \mathbb{R}^2} \|u(\cdot + z)\|_{L^2((-\frac{1}{2}, \frac{1}{2})^2)}, \tag{127}$$

which is a Banach space. We note that $L^2(\Lambda)$ is a closed subspace of $L^2_{\mathrm{uloc}}(\mathbb{R}^2)$. In particular, given a family $\{\Lambda_j\}_{j \in J} \subset \mathbb{R}^{2\times 2}$ satisfying (5), then there exists a constant C only depending on C_Λ of (5), such that for all $j \in J$ and $u \in L^2(\Lambda_j)$ we have

$$\frac{1}{C}\|u\|_{L^2(\Lambda_j)} \leq \|u\|_{L^2_{\mathrm{uloc}}} \leq C\|u\|_{L^2(\Lambda_j)}.$$

8.2 Two-Scale Convergence for Grained Structures

In this section discuss the notion of two-scale convergence *for grained microstructures* introduced in Definition 3.1. It is a slight variant of the notion introduced in

Neukamm (2010). Throughout the section we suppose that $\{\Lambda_j\}_{j \in J}$ and $\{S_j\}_{j \in J}$ are as in Assumption 2.4, and $h \mapsto \varepsilon(h)$ satisfies Assumption 2.1. The notion of two-scale convergence of Definition 3.1 is tailored made to keep track of locally periodic structures that frequently appear in this paper. In particular, within this notion, sequences of the form

$$\varphi_h(x) := \varphi(x, \tfrac{x'}{\varepsilon(h)}),$$

strongly two-scale converge to φ, if the function $\varphi(x, y)$ (next to integrability properties) is *locally periodic* in the sense of (6).

Note that the elastic tensor $\mathbb{L}$ associated with Q in Assumption 2.5 and the prestrain tensor B of Assumption 2.5 (iii) satisfy this periodicity assumption. In the single grain case (when the lattice of periodicity is everywhere the same in S, i.e. $\Lambda_j = \Lambda$), the two-scale limit of a sequence in L^2 is given by a function in $L^2(\Omega; L^2(\Lambda))$. In the multiple grain case, the lattice of periodicity changes from grain to grain, and thus the family of spaces $L^2(\Lambda_j) \subset L^2_{\text{uloc}}(\mathbb{R}^2)$, $j \in J$, needs to be considered.

A simple, yet useful, observation is that a sequence $(u_h) \subset L^2(\Omega)$ two-scale converges in the sense of Definition 3.1, if and only if for all $j \in J$ the restrictions $u_h|_{S_j}$ two-scale converge in the *usual* sense:

Lemma 8.1 *Let (u_h) be a sequence in $L^2(\Omega)$ and $u \in L^2(\Omega; L^2_{\text{uloc}}(\mathbb{R}^2))$. The following are equivalent*

(a) $u_h \overset{2}{\rightharpoonup} u$ *weakly two-scale in L^2 (in the sense of* Definition 3.1).
(b) *For all $j \in J$ we have $u|_{S_j \times (-\frac{1}{2}, \frac{1}{2}) \times \mathbb{R}^2} = u_j$ where $u_j \in L^2(S_j \times (-\frac{1}{2}, \frac{1}{2}); L^2(\Lambda_j))$ is the weak two-scale limit of $u_{h,j} := u_h|_{S_j \times (-\frac{1}{2}, \frac{1}{2})}$ in the usual sense, that is, (u_j) is bounded in $L^2(S_j \times (-\frac{1}{2}, \frac{1}{2}))$ and*

$$\int_{S_j \times (-\frac{1}{2}, \frac{1}{2})} u_{h,j}(x)\varphi(x, \tfrac{x'}{\varepsilon(h)})\mathrm{d}x \to \int_{S_j} \fint_{\square_{\Lambda_j}} u_j(x, y)\varphi(x, y)\mathrm{d}(x_3, y)\mathrm{d}x', \tag{128}$$

for all $\varphi \in C_c^\infty(S_j \times (-\frac{1}{2}, \frac{1}{2}); C(\Lambda_j))$.

With help of this lemma we can lift various properties of two-scale convergence (in the usual sense) to the variant introduced in Definition 3.1:

Lemma 8.2 *(a) (Compactness). Let $(u_h) \subset L^2(\Omega)$ be a bounded sequence. Then there exists a subsequence and $u \in L^2(\Omega; L^2_{\text{uloc}}(\mathbb{R}^2))$ satisfying (6) such that $u_h \overset{2}{\rightharpoonup} u$ weakly two-scale in L^2.*
(b) *(Lower semicontinuity of the norm). Let $(u_h) \subseteq L^2(\Omega)$ weakly two-scale converge to u. Then*

$$\liminf_{h \to 0} \int_\Omega |u_h|^2 \mathrm{d}x \geq \sum_{j \in J} \int_{S_j} \fint_{\square_{\Lambda_j}} |u|^2 \mathrm{d}(x_3, y)\mathrm{d}x_3.$$

(c) (Strong times weak). Let $(u_h) \subseteq L^2(\Omega)$ and $u \in L^2(\Omega; L^2_{\mathrm{uloc}}(\mathbb{R}^2))$. Then $u_h \xrightarrow{2} u$ strongly two-scale, if and only if

$$\int_\Omega u_h(x)\varphi_h(x)\mathrm{d}x \to \sum_{j\in J}\int_{S_j}\fint_{\square_{\Lambda_j}} u(x,y)\varphi(x,y)\mathrm{d}(x_3,y)\mathrm{d}x_3$$

for all weakly two-scale converging sequences $(\varphi_h) \subset L^2(\Omega)$ with limit φ.

(d) (Approximation of two-scale limits). Let $u \in L^2(\Omega; L^2_{\mathrm{uloc}}(\mathbb{R}^2))$ satisfy (6). Then there exists a sequence $(u_h) \subset C_c^\infty(\Omega)$ such that $u_h \xrightarrow{2} u$ strongly two-scale in L^2.

For the proof we refer to Neukamm (2010, 2012), where the single-grain case (i.e., $\Lambda_j = I_{2\times 2}$) is discussed. The extension to the above setting is obvious and left to the reader.

In the context of dimension reduction we are especially interested in two-scale limits of sequences of scaled gradients $\nabla_h u_h$ of displacements $(u_h) \subset H^1(\Omega; \mathbb{R}^3)$. As we shall see, a two-scale limit in L^2 of such a sequence is a vector field $F \in L^2(\Omega; L^2_{\mathrm{uloc}}(\mathbb{R}^2); \mathbb{R}^{3\times 3})$ that satisfies (6) and that can be represented with a help of potential φ in the sense that

$$F = \nabla_\gamma \varphi, \qquad \nabla_\gamma = \left(\nabla_y, \frac{1}{\gamma}\partial_3\right).$$

For the precise statement we need to introduce the Banach space

$$H^1_{\gamma,\mathrm{uloc}} := \left\{ u \in H^1_{\mathrm{loc}}\left(\left(-\tfrac{1}{2}, \tfrac{1}{2}\right) \times \mathbb{R}^2; \mathbb{R}^3\right) : \|u\|_{H^1_{\gamma,\mathrm{uloc}}} < \infty \right\},$$

$$\|u\|^2_{H^1_{\gamma,\mathrm{uloc}}} := \sup_{z\in\mathbb{R}^2}\int_{\left(-\frac{1}{2},\frac{1}{2}\right)^3} |u(x_3, y+z)|^2 + |\nabla_\gamma u(x_3, y+z)|^2 \mathrm{d}(x_3, y), \quad (129)$$

and the subspace of Λ_j-periodic functions,

$$H^1_\gamma(\square_{\Lambda_j}; \mathbb{R}^3) := H^1_{\gamma,\mathrm{uloc}} \cap L^2\left(\left(-\tfrac{1}{2}, \tfrac{1}{2}\right); L^2(\Lambda_j; \mathbb{R}^3)\right),$$

$$\|u\|^2_{H^1_\gamma(\square_{\Lambda_j})} := \fint_{\square_{\Lambda_j}} |u|^2 + |\nabla_\gamma u|^2 \mathrm{d}(x_3, y). \quad (130)$$

Note that $H^1_\gamma(\square_{\Lambda_j})$ is a closed subspace of $H^1_{\gamma,\mathrm{uloc}}\left(\left(-\tfrac{1}{2}, \tfrac{1}{2}\right) \times \mathbb{R}^2\right)$, and we have

$$\frac{1}{C}\|\cdot\|_{H^1_\gamma(\square_{\Lambda_j})} \le \|\cdot\|_{H^1_{\gamma,\mathrm{uloc}}} \le C\|\cdot\|_{H^1_\gamma(\square_{\Lambda_j})}, \quad (131)$$

for some $C = C(\gamma, C_\Lambda)$.

Proposition 8.3 (Two-scale limit of scaled gradients)

(a) *Let $(u_h) \subset H^1(\Omega; \mathbb{R}^3)$ be a sequence and suppose that $(\nabla_h u_h) \subseteq L^2(\Omega; \mathbb{R}^{3\times 3})$ is bounded. Then there exists $u \in H^1(S; \mathbb{R}^3)$ and $\varphi \in L^2(S; H^1_{\gamma,\mathrm{uloc}})$ that satisfies* (6) *such that*

$$\nabla_h u_h \overset{2}{\rightharpoonup} (\nabla' u, 0) + \nabla_\gamma \varphi \quad \text{weakly two-scale in } L^2.$$

(b) *Let $\varphi \in L^2(S; H^1_{\gamma,\mathrm{uloc}})$ satisfy* (6). *Then there exists a sequence $(\varphi_h) \subset C_c^\infty(\Omega; \mathbb{R}^3)$ such that*

$$\nabla_h \varphi_h \overset{2}{\longrightarrow} \nabla_\gamma \varphi \quad \text{strongly two-scale in } L^2,$$

and

$$\lim_{h\to 0} \sqrt{h}(\|\varphi_h\|_{L^\infty(\Omega)} + \|\nabla_h \varphi_h\|_{L^\infty(\Omega)}) = 0.$$

Proof With help of Lemma 8.1 the argument of (Neukamm 2010, Section 6.3) easily extends to the case of grained two-scale convergence, see also (Neukamm 2012). $\quad\square$

Lemma 8.4 ((Lower semi-)continuity of convex functionals) *Let Q be as in* Assumption 2.5 *and let $G \in L^2(\Omega; L^2_{\mathrm{uloc}}(\mathbb{R}^2; \mathbb{R}^{3\times 3}))$. Then:*

(a) *Let $(G_h) \subset L^2(\Omega; \mathbb{R}^{3\times 3})$ be a sequence that weakly two-scale converges to G. Then*

$$\liminf_{h\to 0} \int_\Omega Q(x, \tfrac{x'}{\varepsilon(h)}, G_h(x)) \mathrm{d}x \geq \sum_{j\in J} \int_{S_j} \fint_{\square_{\Lambda_j}} Q(x, y, G(x, y)) \mathrm{d}(x_3, y) \mathrm{d}x'.$$

(b) *Let $(G_h) \subset L^2(\Omega; \mathbb{R}^{3\times 3})$ be a sequence that strongly two-scale converges to G. Then*

$$\lim_{h\to 0} \int_\Omega Q(x, \tfrac{x'}{\varepsilon(h)}, G_h(x)) \mathrm{d}x = \sum_{j\in J} \int_{S_j} \fint_{\square_{\Lambda_j}} Q(x, y, G(x, y)) \mathrm{d}(x_3, y) \mathrm{d}x'.$$

Proof With help of Lemma 8.1 the argument of (Neukamm 2010, Section 3.2) easily extends to the case of grained two-scale convergence. $\quad\square$

Lemma 8.5 (Korn's inequality for scaled gradient) *Let $\gamma \in (0, \infty)$ and $\bar{C} > 0$. Then there exists a constant $C = C(\gamma, \bar{C})$ such that for all $\Lambda \in \mathbb{R}^{2\times 2}$ with $\frac{1}{\bar{C}} \leq \Lambda^\top \Lambda \leq \bar{C}$ the following Korn's inequality holds: For all $\varphi \in H^1_\gamma(\square_\Lambda; \mathbb{R}^3)$, we have*

$$\fint_{\square_\Lambda} |\nabla_\gamma \varphi|^2 \leq C \fint_{\square_\Lambda} |\operatorname{sym} \nabla_\gamma \varphi|^2. \tag{132}$$

Proof In the following we write $\lesssim$ if $\leq$ holds up to a multiplicative constant only depending on γ and $\bar{C}$. We consider the scaled function

$$\tilde{\varphi}(x_3, y) := \frac{1}{\gamma}\varphi(x_3, \gamma y), \quad \tilde{\Lambda} := \frac{1}{\gamma}\Lambda, \quad \tilde{Y} := Y_{\tilde{\Lambda}}.$$

Then $\tilde{\varphi} \in H^1_\gamma((-\frac{1}{2}, \frac{1}{2}) \times \tilde{\Lambda}; \mathbb{R}^3)$ and $\nabla \tilde{\varphi}(x_3, y) = \nabla_\gamma \varphi(x_3, \gamma y)$, and thus (132) is equivalent to

$$\fint_{(-\frac{1}{2}, \frac{1}{2}) \times Y_{\tilde{\Lambda}}} |\nabla \tilde{\varphi}|^2 \leq C \fint_{(-\frac{1}{2}, \frac{1}{2}) \times Y_{\tilde{\Lambda}}} |\operatorname{sym} \nabla \tilde{\varphi}|^2. \tag{133}$$

Thus, it suffices to prove (133) for all $\tilde{\varphi} \in H^1_\gamma((-\frac{1}{2}, \frac{1}{2}) \times \tilde{\Lambda}; \mathbb{R}^3)$. In order to see that the constant can be chosen only depending on γ and $\bar{C}$, we first note that there exists two concentric cubes $Q_i := \ell_i[-\frac{1}{2}, \frac{1}{2})^2$ such that

$$Q_1 \subset \tilde{Y} \subset Q_2 \quad \text{and} \quad \tilde{C} := \frac{|Q_2|}{|Q_1|} \lesssim 1.$$

Thus, we have

$$\fint_{(-\frac{1}{2}, \frac{1}{2}) \times \tilde{Y}} |F|^2 \lesssim \fint_{(-\frac{1}{2}, \frac{1}{2}) \times Q_2} |F|^2, \tag{134}$$

for all $F \in L^2((-\frac{1}{2}, \frac{1}{2}) \times Q_2; \mathbb{R}^{3\times3})$. Furthermore, by exploiting $\tilde{\Lambda}$-periodicity, we see that

$$\fint_{(-\frac{1}{2}, \frac{1}{2}) \times 2Q_2} |F|^2 \lesssim \fint_{(-\frac{1}{2}, \frac{1}{2}) \times \tilde{Y}} |F|^2 \tag{135}$$

for all $\tilde{\Lambda}$-periodic functions $F \in L^2((-\frac{1}{2}, \frac{1}{2}) \times \tilde{\Lambda}; \mathbb{R}^{3\times3})$.

By the standard Korn's inequality there exists $K \in \mathbb{R}^{3\times3}_{\text{skw}}$ such that

$$\fint_{(-\frac{1}{2}, \frac{1}{2}) \times 2Q_2} |\nabla \psi - K|^2 \lesssim \fint_{(-\frac{1}{2}, \frac{1}{2}) \times 2Q_2} |\operatorname{sym} \nabla \psi|^2, \tag{136}$$

for all $\psi \in H^1((-\frac{1}{2}, \frac{1}{2}) \times 2Q_2; \mathbb{R}^3)$. In particular, we may apply this estimate to the scaled function $\tilde{\varphi}$. Combined with (134) and (135) we get

$$\fint_{(-\frac{1}{2}, \frac{1}{2}) \times \tilde{Y}} |\nabla \tilde{\varphi} - K|^2 \lesssim \fint_{(-\frac{1}{2}, \frac{1}{2}) \times 2Q_2} |\nabla \tilde{\varphi} - K|^2 \lesssim \fint_{(-\frac{1}{2}, \frac{1}{2}) \times 2Q_2} |\operatorname{sym} \nabla \tilde{\varphi}|^2$$

$$\lesssim \fint_{(-\frac{1}{2}, \frac{1}{2}) \times \tilde{Y}} |\operatorname{sym} \nabla \tilde{\varphi}|^2.$$

In order to conclude (133), we need to estimate $|K|$. To that end let $\tilde{\Lambda}_1$ and $\tilde{\Lambda}_2$ denote the first and second column vector of $\tilde{\Lambda}$, respectively. Consider

$$u(x_3, y) := \tilde{\varphi}(x_3, y) - K \begin{pmatrix} y \\ x_3 \end{pmatrix}.$$

Then, by $\tilde{\Lambda}$-periodicity of $\tilde{\varphi}$, we have for a.e. $(x_3, y) \in (-\frac{1}{2}, \frac{1}{2}) \times \mathbb{R}^2$,

$$K \begin{pmatrix} \tilde{\Lambda}_i \\ 0 \end{pmatrix} = u(x_3, y + \tilde{\Lambda}_i) - u(x_3, y) = \int_0^1 \nabla' u(x_3, y + s\tilde{\Lambda}_i) \cdot \tilde{\Lambda}_i \, ds.$$

Taking the square, integration w.r.t. y, and Jensen's inequality yield

$$|K \begin{pmatrix} \tilde{\Lambda}_i \\ 0 \end{pmatrix}|^2 \leq |\tilde{\Lambda}_i|^2 \int_0^1 \fint_{(-\frac{1}{2},\frac{1}{2}) \times Q_2} |\nabla' u(x_3, y + s\Lambda_i)|^2 \mathrm{d}y \mathrm{d}x_3 \mathrm{d}s$$

$$\lesssim \fint_{(-\frac{1}{2},\frac{1}{2}) \times 2Q_2} |\nabla u(x_3, y)|^2 \mathrm{d}y \mathrm{d}x_3,$$

where for the last estimate, we used that $y + s\Lambda_i \in 2Q_2$ for all $y \in Q_2$ and $s \in (0, 1)$. Hence, combined with (136) and the definition of u, we get

$$\sum_{i=1,2} |K \begin{pmatrix} \tilde{\Lambda}_i \\ 0 \end{pmatrix}|^2 \lesssim \fint_{(-\frac{1}{2},\frac{1}{2}) \times 2Q_2} |\nabla\tilde{\varphi} - K|^2 \lesssim \fint_{(-\frac{1}{2},\frac{1}{2}) \times \tilde{Y}} |\operatorname{sym} \nabla\tilde{\varphi}|^2.$$

Moreover, by skew symmetry, we have $|K|^2 \lesssim \sum_{i=1,2} |K \begin{pmatrix} \tilde{\Lambda}_i \\ 0 \end{pmatrix}|^2$, and thus,

$$\fint_{(-\frac{1}{2},\frac{1}{2}) \times \tilde{Y}} |\nabla\tilde{\varphi}|^2 \lesssim |K|^2 + \fint_{(-\frac{1}{2},\frac{1}{2}) \times \tilde{Y}} |\nabla\tilde{\varphi} - K|^2 \lesssim \fint_{(-\frac{1}{2},\frac{1}{2}) \times \tilde{Y}} |\operatorname{sym} \nabla\tilde{\varphi}|^2.$$

$\square$

References

Agostiniani, V., DeSimone, A.: Dimension reduction via Γ-convergence for soft active materials. Meccanica **52**(14), 3457–3470 (2017)

Agostiniani, V., DeSimone, A.: Rigorous derivation of active plate models for thin sheets of nematic elastomers. Math. Mech. Solids **25**(10), 1804–1830 (2020)

Agostiniani, V., DeSimone, A., Koumatos, K.: Shape programming for narrow ribbons of nematic elastomers. J. Elast. **127**(1), 1–24 (2017)

Allaire, G.: Homogenization and two-scale convergence. SIAM J. Math. Anal. **23**(6), 1482–1518 (1992)

Bartels, S.: Approximation of large bending isometries with discrete Kirchhoff triangles. SIAM J. Numer. Anal. **51**(1), 516–525 (2013)

Bartels, S.: Finite element approximation of large bending isometries. Numer. Math. **124**(3), 415–440 (2013)

Bartels, S., Bonito, A., Nochetto, R.H.: Bilayer plates: Model reduction, Γ-convergent finite element approximation, and discrete gradient flow. Commun. Pure Appl. Math. **70**(3), 547–589 (2017)

Bartels, S., Griehl, M., Neukamm, S., Padilla-Garza, D., Palus, C.: A nonlinear bending theory for nematic LCE plates (2022). Preprint arXiv:2203.04010

Bauer, R., Neukamm, S., Schäffner, M.: Derivation of a homogenized bending-torsion theory for rods with micro-heterogeneous prestrain. J. Elast. **141**(1), 109–145 (2020)

Bhattacharya, K., Lewicka, M., Schäffner, M.: Plates with incompatible prestrain. Arch. Ration. Mech. Anal. **221**(1), 143–181 (2016)

Blatt, M., Burchardt, A., Dedner, A., Engwer, Ch., Fahlke, J., Flemisch, B., Gersbacher, Ch., Gräser, C., Gruber, F., Grüninger, Ch., Kempf, D., Klöfkorn, R., Malkmus, T., Müthing, S., Nolte, M., Piatkowski, M., Sander, O.: The distributed and unified numerics environment, version 2.4. Arch. Numer. Softw. **4**(100), 13–29 (2016). https://doi.org/10.11588/ans.2016.100.26526 ISSN 2197-8263

Bonito, A., Guignard, D., Nochetto, R., Yang, S.: Numerical analysis of the LDG method for large deformations of prestrained plates. Preprint arXiv:2106.13877 (2021a)

Bonito, A., Nochetto, R.H., Ntogkas, D.: DG approach to large bending plate deformations with isometry constraint. Math. Models Methods Appl. Sci. **31**(01), 133–175 (2021)

Bonito, A., Guignard, D., Nochetto, R.H., Yang, S.: LDG approximation of large deformations of prestrained plates. J. Comput. Phys. **448**, 110719 (2022)

Bukal, M., Velčić, I.: On the simultaneous homogenization and dimension reduction in elasticity and locality of Γ-closure. Calc. Var. Partial. Differ. Equ. **56**(3), 59 (2017)

Cherdantsev, M., Cherednichenko, K.: Bending of thin periodic plates. Calc. Var. Partial. Differ. Equ. **54**(4), 4079–4117 (2015)

Ciarlet, P.G., Larsonneur, F.: On the recovery of a surface with prescribed first and second fundamental forms. Journal de mathématiques pures et appliquées **81**(2), 167–185 (2002)

de Delgado, M.B., Schmidt, B.: Energy minimising configurations of pre-strained multilayers. J. Elast. **140**(2), 303–335 (2020)

de Benito Delgado, M., Schmidt, B.: A hierarchy of multilayered plate models. ESAIM Control Optim. Calc. Var. **27**, S16 (2021)

Eckart, C.: The thermodynamics of irreversible processes: iii: relativistic theory of the simple fluid. Phys. Rev. **58**(10), 919 (1940)

Flory, P.J., Rehner, J., Jr.: Statistical mechanics of cross-linked polymer networks i: rubberlike elasticity. J. Chem. Phys. **11**(11), 512–520 (1943)

Friesecke, G., James, R.D., Müller, S.: A theorem on geometric rigidity and the derivation of nonlinear plate theory from three-dimensional elasticity. Commun. Pure Appl. Math. J. Issued Courant Inst. Math. Sci. **55**(11), 1461–1506 (2002)

Friesecke, G., James, R.D., Müller, S.: A hierarchy of plate models derived from nonlinear elasticity by gamma-convergence. Arch. Ration. Mech. Anal. **180**(2), 183–236 (2006)

Ge, H.Q., Qi, J., Dunn, M.L.: Active materials by four-dimension printing. Appl. Phys. Lett. **103**(13), 131901 (2013)

Gibiansky, L.V., Torquato, S.: Thermal expansion of isotropic multiphase composites and polycrystals. J. Mech. Phys. Solids **45**(7), 1223–1252 (1997)

Gloria, A., Neukamm, S.: Commutability of homogenization and linearization at identity in finite elasticity and applications. Annales de l'IHP Analyse non linéaire **28**(6), 941–964 (2011)

Hornung, P.: Approximation of flat w 2, 2 isometric immersions by smooth ones. Arch. Ration. Mech. Anal. **199**(3), 1015–1067 (2011)

Hornung, P., Neukamm, S., Velčić, I.: Derivation of a homogenized nonlinear plate theory from 3d elasticity. Calc. Var. Partial. Differ. Equ. **51**(3–4), 677–699 (2014)

Hornung, P., Pawelczyk, M., Velčić, I.: Stochastic homogenization of the bending plate model. J. Math. Anal. Appl. **458**(2), 1236–1273 (2018)

Ionov, L.: Biomimetic hydrogel-based actuating systems. Adv. Funct. Mater. **23**(36), 4555–4570 (2013)

Klein, Y., Efrati, E., Sharon, E.: Shaping of elastic sheets by prescription of non-euclidean metrics. Science **315**(5815), 1116–1120 (2007)

Kröner, E.: Allgemeine kontinuumstheorie der versetzungen und eigenspannungen. Arch. Ration. Mech. Anal. **4**(1), 273 (1959)

Lee, E.H.: Elastic-plastic deformation at finite strains. J. Appl. Mech. **36**(1), 1 (1969)

Lewicka, M.: Quantitative immersability of riemann metrics and the infinite hierarchy of prestrained shell models. Arch. Ration. Mech. Anal. **236**(3), 1677–1707 (2020)

Lewicka, M., Lučić, D.: Dimension reduction for thin films with transversally varying prestrain: oscillatory and nonoscillatory cases. Commun. Pure Appl. Math. **73**(9), 1880–1932 (2020)

Lewicka, M., Pakzad, M.R.: Scaling laws for non-euclidean plates and the $W^{2,2}$ isometric immersions of Riemannian metrics. ESAIM Control Optim. Calc. Var. **17**(4), 1158–1173 (2011)

Lewicka, M., Pakzad, M.R.: Convex integration for the Monge-Ampère equation in two dimensions. Anal. PDE **10**(3), 695–727 (2017)

Lewicka, M., Mahadevan, L., Pakzad, M.R.: The Föppl-von Kármán equations for plates with incompatible strains. Proc. R. Soc. A Math. Phys. Eng. Sci. **467**(2126), 402–426 (2010a)

Lewicka, M., Mora, M.G., Pakzad, M.R.: Shell theories arising as low energy γ-limit of 3d nonlinear elasticity. Annali della Scuola Normale Superiore di Pisa-Classe di Scienze **9**(2), 253–295 (2010b)

Lewicka, M., Mora, M.G., Pakzad, M.R.: The matching property of infinitesimal isometries on elliptic surfaces and elasticity of thin shells. Arch. Ration. Mech. Anal. **200**(3), 1023–1050 (2011)

Lewicka, M., Raoult, A., Ricciotti, D.: Plates with incompatible prestrain of high order. Annales de l'Institut Henri Poincaré C, Analyse non linéaire **34**(7), 1883–1912 (2017)

Mohan, P., Yip, N.K., Yu, T.: Minimal energy configurations of bilayer plates as a polynomial optimization problem. Nonlinear Anal. 113034 (2022)

Müller, S., Neukamm, S.: On the commutability of homogenization and linearization in finite elasticity. Arch. Ration. Mech. Anal. **201**(2), 465–500 (2011)

Neukamm, S.: Homogenization, linearization and dimension reduction in elasticity with variational methods. PhD thesis, Technische Universität München (2010)

Neukamm, S.: Rigorous derivation of a homogenized bending-torsion theory for inextensible rods from three-dimensional elasticity. Arch. Ration. Mech. Anal. **206**(2), 645–706 (2012)

Neukamm, S., Olbermann, H.: Homogenization of the nonlinear bending theory for plates. Calc. Var. Partial. Differ. Equ. **53**(3–4), 719–753 (2015)

Neukamm, S., Velčić, I.: Derivation of a homogenized von-karman plate theory from 3d nonlinear elasticity. Math. Models Methods Appl. Sci. **23**(14), 2701–2748 (2013)

Nguetseng, G.: A general convergence result for a functional related to the theory of homogenization. SIAM J. Math. Anal. **20**(3), 608–623 (1989)

Padilla-Garza, D.: Dimension reduction through gamma convergence for general prestrained thin elastic sheets. Calc. Var. Partial. Differ. Equ. **61**(5), 1–40 (2022)

Pakzad, M.R.: On the sobolev space of isometric immersions. J. Differ. Geom. **66**(1), 47–69 (2004)

Plucinsky, P., Kowalski, B.A., White, T.J., Bhattacharya, K.: Patterning nonisometric origami in nematic elastomer sheets. Soft Matter **14**(16), 3127–3134 (2018a)

Plucinsky, P., Lemm, M., Bhattacharya, K.: Actuation of thin nematic elastomer sheets with controlled heterogeneity. Arch. Ration. Mech. Anal. **227**(1), 149–214 (2018b)

Rumpf, M., Simon, S., Smoch, C.: Finite element approximation of large-scale isometric deformations of parametrized surfaces. Preprint arXiv:2110.13604 (2021)

Sander, O.: DUNE: The Distributed and Unified Numerics Environment. Lecture Notes in Computational Science and Engineering. Springer (2020). ISBN 9783030597023

Schmidt, B.: Minimal energy configurations of strained multi-layers. Calc. Var. Partial. Differ. Equ. **30**(4), 477–497 (2007)

Schmidt, B.: Plate theory for stressed heterogeneous multilayers of finite bending energy. Journal de Mathématiques Pures et Appliquées **88**(1), 107–122 (2007)

Sigmund, O., Torquato, S.: Design of materials with extreme thermal expansion using a three-phase topology optimization method. J. Mech. Phys. Solids **45**(6), 1037–1067 (1997)

Tanaka, T., Fillmore, D.J.: Kinetics of swelling of gels. J. Chem. Phys. **70**(3), 1214–1218 (1979)

van Manen, T., Janbaz, S., Zadpoor, A.A.: Programming the shape-shifting of flat soft matter. Mater. Today **21**(2), 144–163 (2018)

Velčić, I.: On the derivation of homogenized bending plate model. Calc. Var. Partial. Differ. Equ. **53**(3), 561–586 (2015)

Visintin, A.: Two-scale convergence of some integral functionals. Calc. Var. Partial. Differ. Equ. **29**(2), 239–265 (2007)

Vujošević, L., Lubarda, V.A.: Finite-strain thermoelasticity based on multiplicative decomposition of deformation gradient. Theoret. Appl. Mech. **28–29**, 379–399 (2002)

Ware, T.H., McConney, M.E., Wie, J.J., Tondiglia, V.P., White, T.J.: Voxelated liquid crystal elastomers. Science **347**(6225), 982–984 (2015)

Warner, M., Terentjev, E.M.: Liquid Crystal Elastomers, vol. 120. Oxford University Press (2007)